A combined forecasting and packing model to optimize decision-making under uncertainty in transportation logistics: an application to air cargo revenue management

A case study for Air France KLM Martinair Cargo

Iordanis Tseremoglou

TU Delft

A combined forecasting and packing model to optimize decision-making under uncertainty in transportation logistics: an application to air cargo revenue management

A case study for Air France KLM Martinair Cargo

by

Iordanis Tseremoglou

to obtain the degree of Master of Science
at the Delft University of Technology,
to be defended publicly on Tuesday August 11, 2020 at 09:00 AM.

Student number:	4779843	
Project duration:	November 6, 2019 – June 19, 2020	
Thesis committee:	Dr. B. F. Lopes dos Santos,	TU Delft, Chair
	Dr. A. Bombelli,	TU Delft, Supervisor
	Dr. O. A. Sharpanskykh,	TU Delft, Examiner
	Dr. D. Ragni,	TU Delft, External Examiner

An electronic version of this thesis is available at http://repository.tudelft.nl/.

TU Delft

Preface

This thesis, which I proudly present, is the final milestone of my MSc Degree in Aerospace Engineering. It focuses in optimizing decision-making under uncertainty in the air cargo supply chain, an area rather complex and unexplored at the same time. The challenging and innovative nature of the project provided me with the right motivation, while the feeling of accomplishment kept my spirit up during the difficult period of the COVID-19 quarantine measures.

In this nine-month exciting journey of exploration and research I was lucky to work with a group of people, who have been a source of support and inspiration. First and foremost, I would like to express my gratitude to my daily supervisor, Alessandro Bombelli for his support and guidance during this project. He was always there to provide me with insightful remarks and advice on the successful completion of such a large and demanding project. Secondly, I would like to express my sincere thanks to Bruno Lopes dos Santos for his critical questions and remarks during the milestone meetings of the project. Next, a big thanks to Hans Zwitzer and Luuk Heling for giving me the opportunity to conduct my thesis in Air France KLM Martinair Cargo and provided me with valuable insights on the industrial aspects of the project. Last but not least, I would like to thank all the other KLM employees who were always willing to help when necessary.

Iordanis Tseremoglou
Delft, July 2020

Contents

List of Figures

List of Abbreviations

3D-MHKP	Three-Dimensional Multiple Heterogeneous Knapsack Problem
AFKLMP	Air France KLM Martinair Cargo
ANN	Artificial Neural Network
ARIMA	Autoregression Integrated Moving Average
ARMA	AutoRegression Moving Average
BPP	Bin Packing Problem
BRKGA	Biased Random Key Genetic Algorithm
CART	Classification and Regression Trees
CCOPT	Chance Constrained Optimization
CG	Center of Gravity
CVaR	Conditional Value-at-Risk
EPs	Extreme Points
GA	Genetic Algorithm
IATA	International Air Transport Association
KP	Knapsack Problem
LDP	Lower Deck Pallet
LSTM	Long Short-Term Memory
MA	Moving Averages
MAE	Mean Absolute Error
MAPE	Mean Aboslute Percentage Error
MBSBPP	Multiple Bin Size Bin Packing Problem
MF	Merit Function
MILP	Mixed Integer Linear Programming
MLP	Multi-Layer Perceptron
PICP	Prediction Interval Coverage Probability
RF	Random Forests
RF	Relax-and-Fix
RKGA	Random Key Genetic Algorithm
RM	Revenue Management
RNN	Recurrent Neural Network

SA	Simulated Annealing
SAA	Sample Average Approximation
SCb	Shipment Contribution
SES	Single Exponential Smoothing
SKP	Single Knapsack Problem
SVR	Support Vector Regression
TS	Tabu Search
ULD	Unit Load Devices
VaR	Value-at-Risk

Introduction

During the last decades, the demand for safer and fastest transportation of goods has driven a rapid growth in the domain of air cargo transportation. As a result, airlines are facing an increasing thrust to manage air cargo operations efficiently by developing optimal decision-making tools encapsulated in the revenue management disciplines. In fact, the optimal management of aircraft capacity and loading of cargo into containers has become a key aspect of the revenue manager decision-making process, as small improvements to the former procedure can result in savings of millions annually.

For the revenue manager to make an informed decision on whether to accept or reject a booking, two elements must be known : the exact shipment dimensions and the available aircraft and cargo capacity. However, the planning phase takes place several days before the actual values of these elements are known, which introduces the need for forecasting models. These forecasting models, as their name suggests, provide revenue management with predictions of shipment dimensions and aircraft capacity days in advance. Under the assumption of a perfect forecasting model being 100% accurate, these values could be fed directly to a palletization model, which would address the optimal assignment of goods into containers so that the highest utilization of available space is reached.

Unfortunately, there is no forecasting model that is 100% accurate, meaning that there would always be an uncertainty in the outcome of the forecasting model. This uncertainty is something that cannot be overseen by the revenue manager. On the contrary, it poses risks that can severely affect the loading strategy obtained through the palletization model. These risks can be translated to accepting goods that cannot be loaded onto the aircraft, or rejecting goods even though there is still sufficient capacity left. As it has become evident, the revenue manager must be aware of these risks and should have the ability to control them.

This research will address the aforementioned steps of the decision process by contributing to the development of a combined forecasting and stochastic packing model that will tackle the uncertainty of the forecast and provide revenue managers with a tool that will facilitate the accept-or-reject decision. This defines the framework for the research that will be conducted below.

We will investigate the use of this model in the context of Air France-KLM-Martinair Cargo (AFKLMP) with focus on single flight legs with passenger aircraft. Moreover, we will evaluate the impact of the developed model over a set of flights using real booking data provided by AFKLMP.

This thesis report is organized as follows : In Part I, the scientific paper is presented, where the formulation of the developed model is described in details, along with the relevant results of testing and validating the model on four case studies with real booking data. Part II contains the relevant Literature Study that supports the research. More specifically, the research objective and questions are defined and the distinct elements of the air cargo load planning problem addressed in this work are scrutinized. Moreover, an exhaustive overview of state-of-the-art forecasting and packing models that provide the theoretical grounds upon which this work will be conducted is presented. Finally, in Part III, the experiments conducted to select the optimal design approach for the three dimensional packing model are presented. Two design approaches were considered, and their efficiency was evaluated and compared against real booking data of four case studies.

I

Scientific Paper

A combined forecasting and packing model to optimize decision-making under uncertainty in transportation logistics: an application to air cargo revenue management

Iordanis Tseremoglou,* Alessandro Bombelli,† Bruno F. Santos, ‡

Delft University of Technology, Delft, The Netherlands

Abstract

In transportation logistics, Revenue Management departments are in charge of accepting or rejecting incoming booking requests. The overarching goal is to accept as many requests as possible, hence maximizing revenue, while limiting overbooking to ensure timely deliveries. In this paper, we present a novel combined forecasting and optimization model to assist the air cargo Revenue Management department of an airline. Using historical data from a partner airline, the forecasting block predicts the available cargo space in passenger aircraft (with a Long Short Term Memory network) and shipment dimensions (with a Multi-Layer Perceptron network), that are generally unknown at the time of the booking. On top of predicted values, probability distributions are also computed to be used as input for the optimization block. A Knapsack Problem is solved sequentially, using a heuristic based on the Extreme Points method, anytime a booking is received. A loading strategy of shipments, whose dimensions are computed using the aforementioned distributions and a user-defined confidence interval, into Unit Load Devices is determined, and the incoming booking is accepted if no other booking is offloaded in the process. The effectiveness, efficacy, and robustness of the model are tested on four case studies based on real booking data provided by partner airline.

1 Introduction

During the recent years, globalization has significantly fostered the growth of international air trade. Although goods transported by air correspond to only 1% of the overall transported volume, the percentage spikes to 35% if value is used as a parameter. This percentage translates to a value of US $ 5.5 trillion and annual revenues of US $ 50 billions for the IATA members [IATA, 2019].

Air cargo can be transported either in full freighter aircraft or passenger aircraft, through special pallets or containers called Unit Load Devices (ULDs). ULDs have specific shapes and sizes in order to fit into designated positions in the belly space of an aircraft. Full freighter aircraft are dedicated to cargo transportation and have a fixed and large capacity. On the other hand, in passenger aircraft, passenger baggage have priority over cargo, meaning that cargo capacity is more limited and subject to uncertainty. In both aircraft types, cargo capacity is split into capacity reserved for long-term contracts (allotments) and capacity available for sale during the booking period (short-term capacity).

The utilization of cargo capacity in a way that maximizes profit constitutes the overall objective of the air cargo load planning problem faced by the airlines, as defined by [Brandt and Nickel, 2018]. In general, the air cargo load planning problem involves many stakeholders inside an airline, such as the Revenue Management (RM), Handling and Operations Department. In this paper though, it will be addressed in the context of RM, and in particular, we will focus on short-term capacity management for passenger aircraft.

To achieve the former objective, a revenue manager has to make an informed decision on whether to accept or reject an incoming booking request. An incoming booking request may consist of one or multiple shipments, which may be of the same or different size. In daily air cargo practice, this decision is based mostly on the experience of the revenue manager and the skills of the palletization workers rather than on automated systems. In fact, the support of decision-making in the air cargo domain is far less digitized in comparison with the passenger systems [Wada et al., 2017]. This is mostly due to the fact that the air cargo supply chain possesses more complex industry characteristics than passenger systems [Kasilingam, 1996]. One fundamental difference is the fact that, while a passenger seat is a one-dimensional problem, in the case of cargo there is substantial variability due to volume, weight and shape of the shipment. In addition, when considering passenger aircraft,

*Msc Student, Air Transport and Operations, Faculty of Aerospace Engineering, Delft University of Technology
†Lecturer, Air Transport and Operations, Faculty of Aerosopace Engineering, Delft University of Technology
‡Assistant Professor,Air Transport and Operations, Faculty of Aerospace Engineering, Delft University of Technology

available cargo capacity is not fixed but stochastic, as it depends on several factors such as payload, belly space and the expected passenger baggage for this specific flight. Some airlines, as our partner airline, do not even require shippers to provide shipment dimensions when submitting a request, but only volume, weight, and other pieces of information. Hence, the true shipment dimensions are not always known when operational planning is performed, but their realized values are learnt shortly before the shipment is loaded onto the aircraft. For example, consider that case of a shipment with volume of $2m^3$ which could be represented by i) $1 \times 1 \times 2m$ or ii) $0.5 \times 2 \times 2m$. The difference in the two shapes can severely impact the ULD loading strategy.

The above complexities can be summarized in the form of two nested challenges that the revenue manager must resolve when receiving a new booking request. The outer challenge consists of forecasting the shipment dimensions and the available aircraft capacity. The inner challenge is a packing problem, i.e., based on the results of the forecasting phase, the optimal ULD configuration in combination with the optimal palletization of shipments into the ULDs should be determined. The model presented in this paper tackles both challenges. Although the model is shown here in the context of an air cargo application, we believe its applicability extends to other fields, such as the shipping or the rail industry.

In the literature, the development of forecasting models specifically intended for air cargo applications, is a rather unexplored area. In general, forecasting can be performed using statistical or machine learning models. The focus of this work is on machine learning models and Deep Neural Networks (DNNs) in particular. More specifically, shipment dimensions will be predicted through a multi-layer feed forward network, also called Multi-Layer Perceptron (MLP), using as inputs the volume and shipments' booking information. Forecasting of the available cargo capacity would be performed per flight and per aircraft type using Long Short Term Memory (LSTM) networks.

Most machine learning modes are treated as deterministic functions and do not capture uncertainty. However, in operating environments such as the RM department of an organization, it is considered of vital importance to quantify the confidence level of the predictions of the model. Towards this end, a probabilistic view of the models output offers the required confidence bounds for data analysis and optimization. Therefore, since this research is conducted under the revenue management perspective, it is considered essential to use probability distributions instead of point estimates as inputs to the packing model, in order to protect the revenue manager from any uncertainty in the outputs of the forecasting models.

The packing model will have a dual functionality. First, it will load in the aircraft compartment a set of weakly heterogeneous containers, or ULDs, such that the utilization of the predicted aircraft capacity is maximized. This problem is the Classic (One-Dimensional) Knapsack Problem (1D-KP), according to the typology by [Wascher et al., 2007]. Secondly, it will load a set of strongly heterogeneous shipments into the previously defined set of weakly heterogeneous ULDs, such that the maximum number of shipments is loaded. This type of combinatorial optimization problem falls into the category of three-dimensional Multiple Heterogeneous Knapsack Problem (3D-MHKP) in accordance with the typology defined by [Wascher et al., 2007]. However, the fact that the Knapsack Problem is NP-Hard, in combination with the requirement that the model should serve as a decision support tool in a quasi real-time environment, introduces the need for a heuristic. The goal of the heuristic is to calculate a good feasible packing solution within a very short computational time. Readers are referred to [Brandt and Nickel, 2018] for an extensive review of packing models with heuristics that have been developed during the recent years.

The majority of the literature addressing the Knapsack Problem in the air cargo context, assumes that the aircraft capacity or shipment dimensions are deterministic and known with certainty. However, for the reasons previously explained, such a hypothesis is unlikely to be observed in daily air cargo practice. Therefore we propose a new stochastic packing model that will take into account this uncertainty by integrating, in the form of probabilistic (chance) constraints, the distribution of the predicted values, as determined by the forecasting model(s). The main input of the model is a confidence level, which defines a trade-off between increasing load factor and ensuring the loading strategy is robust between predicted and actual shipment dimensions.

All the above make the contribution of this paper twofold. First, it is the first work that tackles all the phases of the RM decision-making process, namely the cargo capacity and shipment dimensions forecast, the optimal ULD configuration and the palletization of shipments inside the ULDs. Secondly, this combined model is further enriched with chance constraints, so that the revenue manager can decide to adopt either a high risk gain or a more conservative approach.

We will investigate the use of this model in the context of a major airline with focus on single flight legs with passenger aircraft. Moreover, we will evaluate the impact of the developed model over a set of flights using real booking data provided by our partner airline.

The rest of the paper is organized as follows. In Sec. 2, the definition of the problem along with the methodology and the relevant academic literature is presented. Section 3 describes into detail the developed forecasting models and their performance. Section 4 provides the implementation details of the stochastic 1D-KP and 3D-MHKP models. The combined forecasting and stochastic packing model is presented in Sec. 5 along with application examples which shed light into the efficiency of the proposed model. Finally, Sec. 6 provides conclusions and recommendations for future work.

2 Problem Statement and Methodology

The problem we are addressing can be summarized as follows : Let us a consider a specific (flight, aircraft type, departure date) triplet, unknown cargo capacity, a set of shipments and a set of ULDs. Shipments are assumed to be cuboid boxes, each with unknown length, width, height, and known weight. The overall objective is to maximize the number of loaded shipments compatibly with a user-defined confidence level.

2.1 Forecasting Problem

The forecasting block of our proposed framework consists of predicting the aircraft cargo capacity and the shipment dimensions. Predicting cargo capacity is treated as a time series forecasting problem, since we use the airline's historical capacity values to generate the future values. On the other hand, predicting shipment dimensions falls under the broader category of feature prediction problems, and more specifically, it can be categorized as a regression problem.

In recent years, machine learning methods have become increasingly popular for building predictive data analytics models that address both of the aforementioned problems. With the emergence of the age of "Big Data", the huge amount and the complexity of available data has led to the development of Deep Neural Networks (DNNs), i.e., neural networks with more than one hidden layer. According to [Le Roux and Bengio, 2010], DNNs can provide better approximations to nonlinear functions than the models with a single hidden layer. The quintessential example of DNNs is the Multi-Layer Perceptron (MLP), which is a multi-layer feedforward neural network with more than one hidden layers. The fact that a large amount of high-dimensional booking data is used in this research to predict shipment dimensions, make MLP an ideal tool towards this purpose.

Moreover, a very promising variation of DNNs, and Recurrent Neural Networks (RNNs) in particular, that handles the time series forecasting problem are the Long Short-Term Memory networks (LSTMs) developed by [Hochreiter and Schmidhuber, 1997]. LSTMs have been found to perform exceptionally well for a long-time horizon forecasting problem and capture the long-term dependencies of non-linear data [Sagheer and Kotb, 2019], as the historical flight data that are used in this work. The detailed implementation and structure of both forecasting models is provided in Sec. 3.

However, how much trust can be attributed in a forecast has a profound impact on the decision-making process of a revenue manager. Under this aspect, it is considered of vital importance to quantify the uncertainty of the predictions, which shapes one of the side-goals of this work. The methodology followed to estimate the uncertainty of the developed models and build the corresponding prediction distributions is partly driven by the work of [Zhu and Laptev, 2017].

More specifically, our goal is to quantify the uncertainty of the models' prediction $\hat{y}^* = f^{\hat{W}}(x^*)$, where $f^{\hat{W}}(\cdot)$ is the neural network(s), $\hat{W}$ are the fitted parameters and x^* is the sample data. In other words, we aim to construct a probability distribution $\sim N(\bar{y^*}, \sigma^2)$ where, $\bar{y^*}$ is the mean predicted value and σ^2 is the model's variance. Using this distribution, a corresponding prediction interval will be formed as follows:

$$[\bar{y^*} - z_{\alpha/2}\sigma,\ \bar{y^*} + z_{\alpha/2}\sigma] \tag{1}$$

where $z_{\alpha/2}$ is the upper $\alpha/2$ quantile of the standard Normal distribution. This prediction interval can further assist the revenue managers in the choice of the confidence level that is deemed appropriate for the airline.

The Bayesian probability theory, and in particular, the Bayesian Neural Networks (BNNs), provides us with the required framework to construct the probability distribution of the prediction and the corresponding prediction interval. In BNNs, a prior distribution, such as $W \sim N(0, I)$ is used to define the network's weight. Given a set of N inputs $X = \{x_1.....x_N\}$ and corresponding outputs $Y = \{y_1.....y_N\}$, the model aims to find the optimal posterior distribution $P(W|X, Y)$, also known as Bayesian inference. Bayesian inference is the key to estimate the model's uncertainty. In this work, we approximate Bayesian inference using the recently developed Monte Carlo (MC) dropout technique by [Gal, 2016]. Dropout involves dropping a random subset of neurons after each hidden layer with probability p. Hence, the model's output can be viewed as randomly generated sample from the posterior predictive distribution.

The developed algorithm works as follows : for a fitted neural network $f^{\hat{W}}(\cdot)$, a specific input x^*, and for M iterations, hidden units of the neural network are dropped with probability p. A set of $\{\hat{y_1^*}, ...\hat{y_M^*}\}$ predictions is obtained, which define the empirical distribution of the model's output for the specific input x^*. The predictive mean, $\bar{y^*}$, equals:

$$\bar{y^*} = \frac{1}{M}\sum_{i=1}^{M}\hat{y_i^*} \tag{2}$$

The model's uncertainty is captured by the model's variance. Since this model is designed from a RM perspective, a more conservative approach will be followed. Specifically, the uncertainty of the model is not defined

solely by the variance $\sigma^2_{\hat{y^*}}$ of the empirical distribution of $\hat{y^*}$. On the contrary, we incorporate in the model's variance an additional source of uncertainty which accounts for the model misspecification, namely the residual standard error σ^2_{res} observed during the training phase. The residual standard error measures how well every predicted value $\{\hat{y_1}, ..., \hat{y_N}\}$ approximates the corresponding real value $\{y_1, ...y_N\}$. This approach aims at ensuring that the corresponding prediction interval will contain, for the majority of cases, the real actual value(s) of the shipment dimension(s). Hence, the total variance of the model is formulated as follows :

$$\sigma^2 = \sigma^2_{\hat{y^*}} + \sigma^2_{res} \tag{3}$$

The final algorithm along with the mathematical formulation is presented in Algorithm 1.

Algorithm 1 Calculation of model's uncertainty and prediction interval

Input Sample data x^*, neural network $f(\cdot)$, dropout probability p, number of observations N, number of iterations M
for $i = 1$ to M **do**
  $\boldsymbol{y_i^*} = \textbf{MC Dropout}(f(x^*), p)$
end for
// Predicted mean
$\boldsymbol{\bar{y^*}} = \frac{1}{M}\sum_{i=1}^{M} y_i^*$
18
// Variance of empirical distribution y^*
$\boldsymbol{\sigma^2_{\hat{y^*}}} = \frac{1}{M}\sum_{i=1}^{M}(\hat{y_i^*} - \bar{y^*})^2$
// Residual standard error
$\boldsymbol{\sigma^2_{res}} = \frac{1}{N-1}\sum_{i=1}^{N}(\hat{y_i} - y_i)^2$
// Total variance
$\boldsymbol{\sigma^2} = \sigma^2_{\hat{y^*}} + \sigma^2_{res}$
return $\bar{y^*}, \sigma$
Output Prediction interval

2.2 Packing Problem

The developed packing model determines the ULD configuration along with the palletization strategy that maximizes the number of shipments loaded consistently with a user-defined confidence interval. This problem belongs to the broader category of KP with chance constraints.

A generic formulation of a stochastic KP that incorporates the 1D-KP and the 3D-MHKP models can be described as follows : Given a knapsack with volume capacity V and set of $N = \{1....n\}$ items, each of them having profit p_i and a volume distribution whose mean is $\tilde{v_i}$, the objective is to determine the subset of items that maximize the profit subject to volume capacity restrictions. The corresponding mathematical notation is as follows:

$$\textbf{maximize} \quad \sum_{i=1}^{n} p_i x_i \tag{4a}$$

$$\text{subject to :} \quad \mathbb{P}(\sum_{i=1}^{n} \tilde{v_i} x_i \leq V) \geq \alpha \tag{4b}$$

where x_i is a binary variable, taking unitary value when item i is loaded in the knapsack. Furthermore, in case $\tilde{v_i} \sim N(\bar{v_i}, \sigma^2_{v_i})$, constraint (4b) can be reformulated as follows:

$$\sum_{i=1}^{n} \bar{v_i} x_i + \Phi^{-1}(\alpha) \cdot \sqrt{\sum_{i=1}^{n} \sigma_i^2 x_i} \leq V \tag{5}$$

where $\Phi^{-1}(\cdot)$ is the inverse CDF of the normal distribution $N(0, 1)$ It is noted that $x_i^2 = x_i$ since x_i is binary. While a detailed formulation of the chance constrained 1D-KP and 3D-MHKP will be provided in Sec. 4, a preliminary formulation is provided in the following.

As stated previously, ULDs come into different shapes and sizes and they are loaded into specific positions in the compartment of the aircraft, equipped with latches. Readers are referred to [Brandt and Nickel, 2018] for an overview of the most popular ULD types. The floor latches can be rearranged, offering the airlines a

range of different ULD configurations corresponding to the specific cargo capacity. The airline selects the ULD configuration that accommodates the highest amount of shipments for this specific flight. For example, an airline might decide to use one large ULD instead of two small ULDs to accommodate large shipments received for this specific flight.

In this work, we address the former procedure as follows: Based on the predicted cargo capacity distribution, we determine the possible alternative ULD configurations through the stochastic 1D-KP model, within a user-defined confidence level. Then, the ULD configuration that accommodates the highest amount of shipments should be selected. Towards this end, having as inputs the predicted shipment dimensions distributions, the stochastic 3D-MHKP is solved for every ULD configuration defined by the 1D-KP model and the configuration that maximizes the number of shipments loaded is selected.

In addition to the basic geometry constraints requiring the shipment to lie entirely within the ULD and not to overlap with other shipments, some additional constraints are considered. More specifically, 1) shipments may be rotated into six different orientations, 2) they must be stable and 3) the weight capacity of the container must be respected. For the purposes of this work, all the aforementioned constraints, with the exception of weight capacity, are modified to chance constraints, to account for the uncertainty in the predicted shipment dimensions. Moreover, the following assumptions are applied:

- Only single flight legs are considered, meaning that requirements that dictate the positioning of specific shipments inside the ULD to facilitate the offloading - loading procedures in multiple flight legs are not addressed.
- Weight and balance restrictions are not considered, i.e., weight distribution of shipments inside the ULDs is not part of the proposed model.

Given our modeling approach, each shipment is characterized by length $l_i \sim N(\bar{l_i}, \sigma^2_{l_i})$, width $w_i \sim N(\bar{w_i}, \sigma^2_{w_i})$ and height $h_i \sim N(\bar{h_i}, \sigma^2_{h_i})$, that are computed by the forecasting block. In addition, each shipment can be placed inside a ULD using up to six possible orientations. This number is lower for shipments containing fragile or non-turnable items, as described in [Junqueira et al., 2012], [Paquay et al., 2014] and [Paquay et al., 2017].

Load stability ensures that shipments are loaded in a stable manner, and that they will not fall onto the container floor during loading or transport, resulting in cargo damage or handling personnel injuries. This can be achieved by requiring either full shipment base support, as implemented in [Goncalves and Resende, 2012] and [Paquay et al., 2018], or partial base support, as in [Techanitisawad and Tangwiwatwong, 2004] and [Fuellerer et al., 2010]. In the context of this work, load stability will be addressed by enforcing the four vertices of each shipment base to be fully supported, either by the floor of the container or by the top face of other shipments.

Each ULD j has length L_j, width W_j and height H_j and weight capacity WC_j. The ULD can be represented as a 3D coordinate system, the origin (0,0,0) of which lies on the back bottom left vertex of the ULD. The length, width and height of the ULD lie on the x, y and z-axis respectively. ULDs are parallelepipeds that may have one or several cuts on their corners in order to fit in the aircraft fuselage. For the purposes of this work, the considered ULDs would be either Lower Deck Pallets (LDPs) or LD-3 containers, which have a cut in their lower left corner (see Figure 1). This specific cut can be modelled, in a similar manner as in [Paquay et al., 2018], by the linear equation $z = -\frac{b}{a}x + b$, where $a = 40cm$ and $b = 51cm$ according to LD-3 specifications. The considered ULDs are the same ULDs that our partner airline is using. It is noted that more cuts can be added accordingly to account for more ULD types, or this feature can be dropped completely if this model is used for other transportation methods other than air transportation.

(a) Lower Deck Pallet (LDP)

(b) LD-3 container

Figure 1: Considered ULDs (images from www.searates.com)

The weight of the shipments loaded on a ULD may not exceed the weight capacity WC_j of the specific ULD. This type of constraint is known as weight capacity constraint, and readers are referred to [Dereli and Das, 2010], [Paquay et al., 2014] and [Paquay et al., 2017] for indicative examples.

Shipments are positioned inside the ULD using the Extreme Point (EP) heuristic, designed by [Crainic et al., 2008] to address the Bin Packing Problem for a set of identical bins. Most recently, the same technique has been used by [Paquay et al., 2018] to develop a fast constructive heuristic for the three-dimensional Multiple Bin Size Bin Packing Problem (MBSBPP). The basic idea of the EPs is that shipments are placed with their left-back-down corner on existing EPs of a specific partial packing strategy, and in the process new potential EPs are generated that can accommodate future shipments. This concept would be extended to take into account the two types of the considered ULDs, namely the LDP and the LD-3 container, as well as the orientation, stability and weight capacity constraints. The generation of EPs is further explained in Sec. 4.2.

The conceptual design of the combined model proposed in this work is summarized in Figure 2.

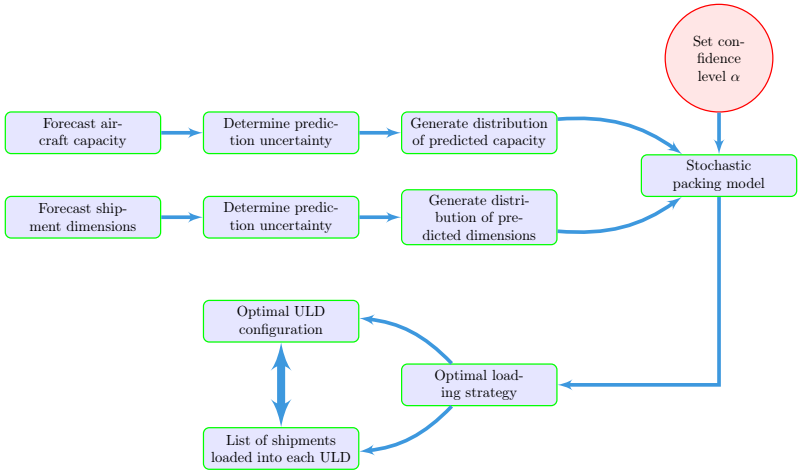

Figure 2: Conceptual design of the proposed revenue management model

3 Forecasting models

3.1 Cargo Capacity Forecasting Model

A LSTM network is used to predict the cargo capacity. The model input is based on cargo capacity data for the period 2010-2019, provided by the partner airline. The exact approach selecting the inputs for the model is presented in Figure 3.

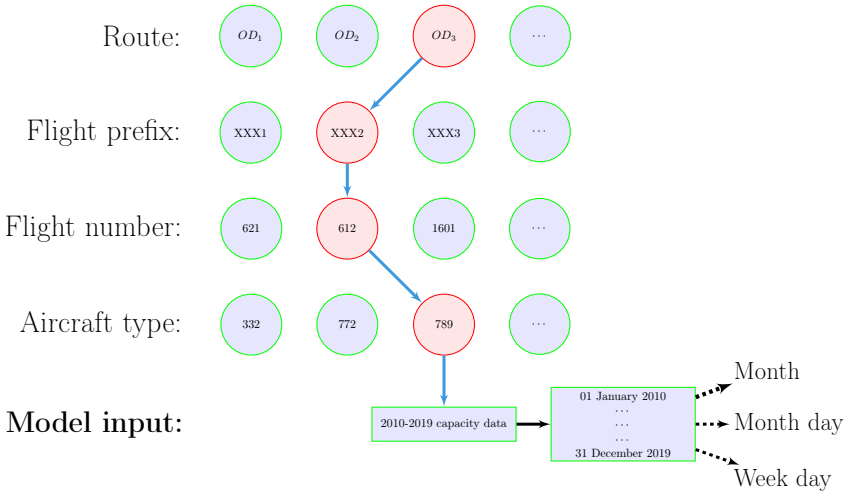

Figure 3: Input selection approach for the LSTM network.

From each specific data entry we extract the corresponding month, day of the month and weekday. Together with the palletized cargo capacity, this is the input for the LSTM network. It is highlighted that the palletized

cargo capacity refers to the capacity corresponding solely to the volume of the loaded ULDs and not the total belly capacity of the aircraft. In general, each ULD cannot be placed in any position in the aircraft compartment, but rather, there are speficic positions equipped with latches and rollers. Using the palletized cargo capacity instead of the generic belly capacity, allows us to apply the 1D-KP model, for determining the optimal ULD configuration(s), directly on the predicted values, without having to compensate for the spacing between the ULDs, due to position requirements. The palletized cargo capacity would be referred simply as cargo capacity hereinafter.

More specifically, at each step, the LSTM network is given the history of the cargo capacity of the sixty previous date entries and predicts the cargo capacity for the sixty first date entry. The timelag of sixty date entries has been determined by trial and error as the optimal timelag. By repeating the same procedure over multiple steps, the model learns to predict a sequence of future values, the range of which depends on the desired forecasting horizon.

3.1.1 LSTM architecture and performance metrics

During the training phase of the LSTM, we used Grid Search to determine the optimal hyperparameters. The resulting LSTM architecture as defined by the optimal hyperparameters is presented in Table 1.

Hyperparameters	**Values**
Number of hidden layers	3
Number of neurons per layer	50
Optimizer	Adam
Dropout probability	0.2
Number of epochs	50
Batch size	20
Loss function	Mean Squared Error

Table 1: Optimal Hyperparameters of LSTM network

To assess the performance of the LSTM network, the following performance indicators are used:

$$MAPE = \frac{1}{N}\sum_{i=1}^{N}\left|\frac{y_i - \hat{y_i}}{y_i}\right| \times 100$$

$$MAE = \frac{1}{N}\sum_{i=1}^{N}|y_i - \hat{y_i}|$$

where N is the number of observations, y_i is the true value for the palletized cargo capacity and $\hat{y_i}$ the predicted value. In addition, since a probability distribution is also computed, we introduce the Prediction Interval Coverage Probability (PICP) metric. PICP identifies the number of occurrences where an interval contains the actual value of the prediction and can be written as:

$$PICP_{l(x),u(x)} = \frac{1}{N}\sum_{i=1}^{N} h_i \qquad \text{where} \quad h_i = \begin{cases} 1 & \text{if } l(x_i) \leq y_i \leq u(x_i) \\ 0 & \text{otherwise} \end{cases} \tag{6}$$

where $l(x_i)$ and $u(x_i)$ are respectively the upper and lower bound of the prediction interval for observation i.

3.1.2 Results

Training and testing of the neural network is performed on a laptop computer with Intel i5 9300, 16GB RAM and NVIDIA 1660Ti GPU. The performance of the model was checked against the cargo capacity data of several flights and the results are summarized in Appendix A. Here, results for four flights are shown as representative of the overall model. The exact flight details are omitted for confidentiality reasons. The corresponding datasets are split into training and testing set, with a proportion of 75% training and 25% testing. The last 25% of the training set is withheld for validation.

The relation between the real cargo capacity and the predicted cargo capacity is presented in Figure 4 while the corresponding boxplots are depicted in Figure 5.

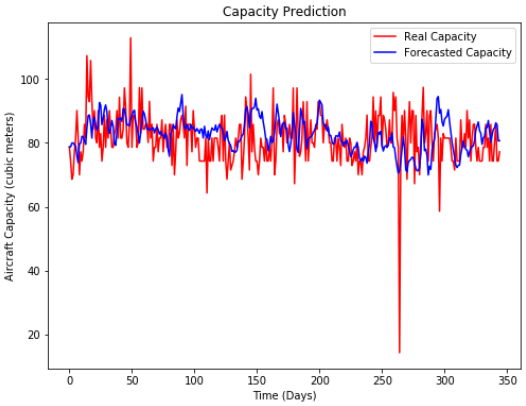

(a) Flight #1-Aircraft Type A330-300

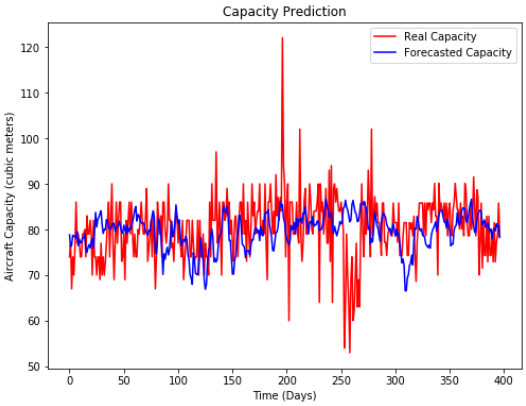

(b) Flight #2-Aircraft Type B777-200

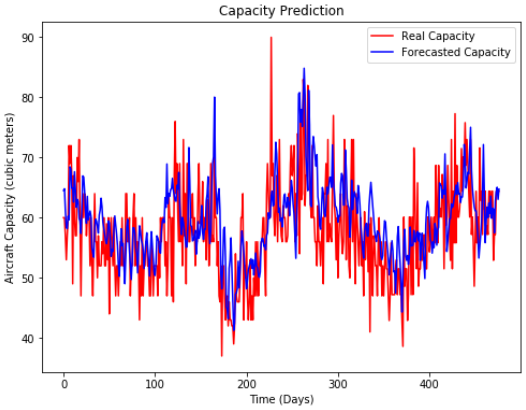

(c) Flight #3-Aircraft Type B767-300

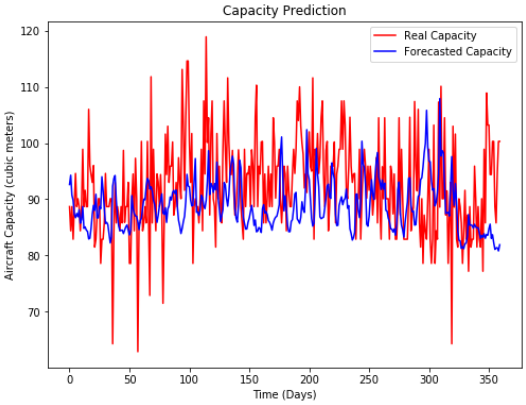

(d) Flight #4-Aircraft Type A330-200

Figure 4: Predicted cargo capacity vs real cargo capacity

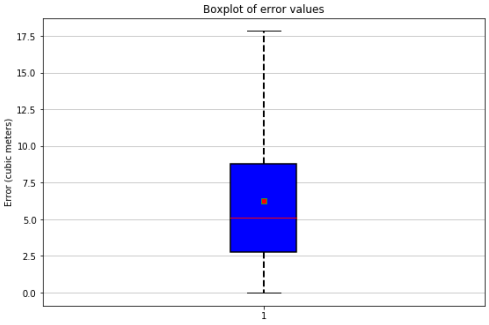

(a) Boxplot flight #1

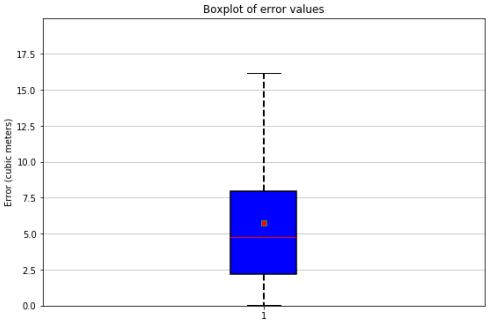

(b) Boxplot flight #2

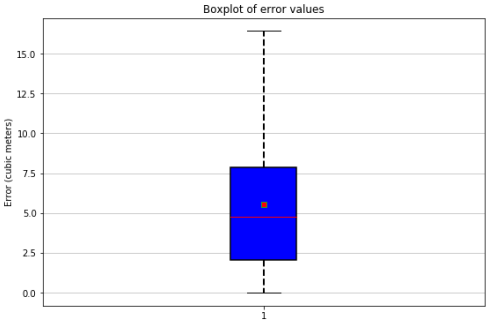

(c) Boxplot flight #3

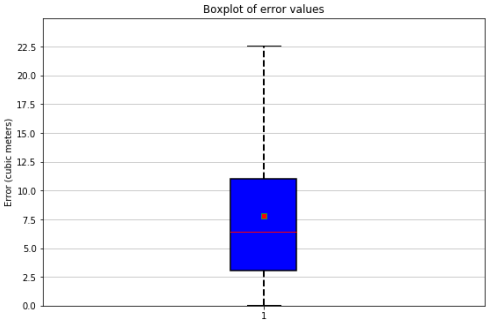

(d) Boxplot flight #4

Figure 5: Boxplots for predicted cargo capacity

Furthermore, the performance metrics for each flights along with the corresponding training time are presented in Table 2. It can be observed that the forecasting model achieves high accuracy, with MAE remaining below 7.82 m^3 in the considered flights.

Flight #	**MAPE**	**MAE** (m^3)	**Training time** (min)
Flight #1	9.14%	6.23	8
Flight #2	7.59%	5.72	9
Flight #3	14.41%	5.56	11
Flight #4	8.63%	7.82	24

Table 2: Performance indicators for cargo capacity.

In order to determine the probability distribution of the predicted capacity values, the fitted LSTM network was run over 1,000 iterations using the MC dropout technique. In each iteration, hidden units were dropped with probability $p = 0.2$. The resulting distributions were tested for normality through the Shapiro-Wilk test. The null hypothesis of the Shapiro-Wilk test is that the data are normally distributed. When the p-value is less than .05, the null hypothesis is rejected and it can be concluded that the data do not follow the normal distribution. The results of the Shapiro-Wilks test for each flight over the probability distributions are presented in Table 3.

Flight #	**Normally distributed predictions(%)**
Flight# 1	96.8%
Flight #2	95.9%
Flight #3	94.9%
Flight #4	96.5%

Table 3: Normally distributed predictions (%).

From the results it can be concluded that normality assumption is verified for the vast majority of the generated distributions, a fact that supports the adoption of the normality assumption for the predicted cargo capacity.

Finally, for each probability distribution, a 95% prediction interval is constructed by running the algorithm presented in Sec. 2. Based on the constructed prediction interval, we calculate the PICP for the predicted values per flight, which is presented in Table 4. The achieved high values of the PICP indicate that the true value of cargo capacity is included, for the majority of cases, in the generated distribution of the predicted cargo capacity.

Flight #	**PICP**
Flight 1	99.5%
Flight 2	99.2%
Flight 3	94.1%
Flight 4	91.1%

Table 4: Prediction Interval Coverage Probability (PICP).

3.2 Shipment Dimensions Forecasting Model

The distribution of predicted shipment dimensions is generated using a MLP network. The model inputs are based on booking information provided by customers of the partner airline. These booking information is contained in a dataset spanning from January 2019 until December 2019. Each row of the dataset corresponds to a specific shipment and includes relevant information such as the booking origin, the booking destination, the reference number of the customer, the volume of the shipment and the type of the shipment, etc. For the purposes of this work, and driven partly by the similar study of [Koch, 2019], the input nodes of the neural network consist of 1) the Booking Origin 2) the Booking Destination 3) the Product Code 4) the Commodity Code and 5) the Shipment Volume.

The model has three outputs, namely the length, width and height of the shipment. It is noted that the dimensions of the shipments were not always included in the dataset, since it is not a mandatory piece of information to be provided by the customers. Since all three dimensions are needed to test and train the model, only bookings having dimensions information were considered.

3.2.1 Data preparation and pre-processing

In the considered dataset, booking entries that had missing values in one of the aforementioned fields where excluded from the subsequent training and testing of the model. This resulted in a total of almost 1,150,000 entries. In order for the model to be efficient in terms of computational resources and time, a representative sample of 500,000 shipment entries was chosen, by ensuring that every shipment feature was represented with the same percentage as in the original dataset.

For shipments where rotations were allowed in all three axis, dimensions were re-arranged considering length as the longest dimension, followed by width and height. Differently from other fields, where length or width have an unambiguous definition, we decided to follow the common convention that defines length as the longest dimension of a box. For shipments that could not be rotated in the height dimension, only length and width were re-arranged using the same logic. Additionally, z-score was used to assess and remove outlier values in either three dimensions. Finally, in order to provide the reader with an impression of the order of magnitude of shipment dimensions, the resulting empirical distribution of the length, width and height for the final list of shipments are presented in Figure 6. It is noted that these distributions are very similar to the ones derived by [Brandt and Nickel, 2018], a fact which verifies the representativeness of the chosen sample.

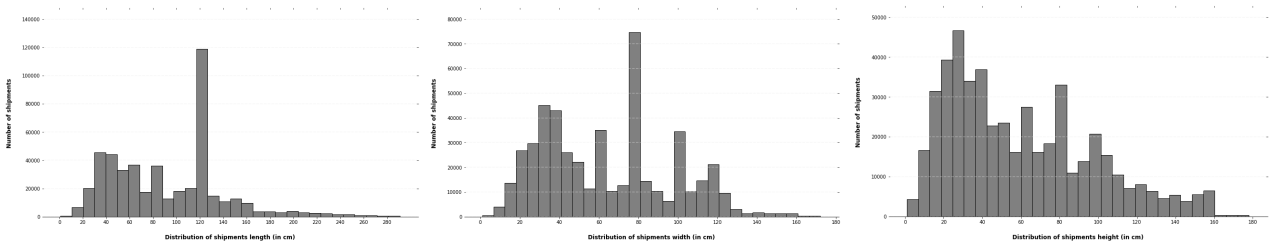

(a) Length (b) Width (c) Height

Figure 6: Distribution of considered shipment dimensions

Consistently with the cargo capacity analysis, the dataset is split into training and test set, with a proportion of 75% training and 25% testing. The last 25% of the training set is withheld for validation.

3.2.2 MLP architecture and performance metrics

In the training phase of the neural network, we used Grid search to infer the optimal selection of the hyperparameters. The resulting MLP architecture along with the optimal hyperparamaters are presented in Figure 7.

Hyperparameters	Values
Number of hidden layers	2
Number of neurons per layer	600
Optimizer	Adam
Dropout probability	0.2
Number of epochs	100
Batch size	20
Loss function	Mean Absolute Error

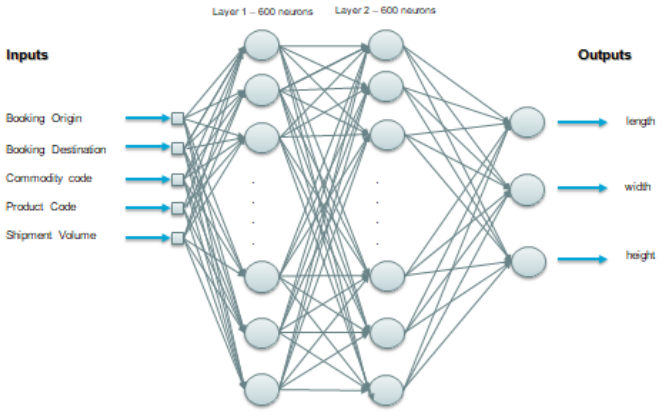

Figure 7: MLP architecture

To evaluate the performance of the MLP, the same performance metrics that were applied to the LSTM network are used.

3.2.3 Results

Training and testing of the neural network was carried using the same laptop previously described. The training time was 6 hours and 32 minutes. Figure 8 presents the model's performance in terms of MAE and MAPE per dimension, along with the corresponding Boxplots for MAE. As it is evident, for 75% of the predictions, the MAE is below 13.5, 9 and 11 cm for length, width and height accordingly.

Dimensions	MAPE	MAE (cm)
Length	13.9%	12.9
Width	13.1%	6.5
Height	19.8%	8.8

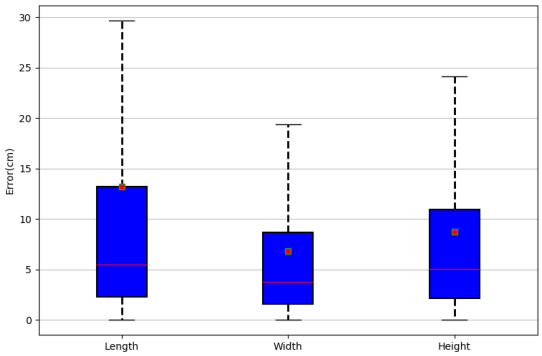

Figure 8: MLP performance metrics

In order to generate the probability distributions for the predicted values and build the prediction interval, we run 1,000 iterations of the fitted network using the MC dropout technique. To determine whether the resulting distributions can be approximated with a normal distribution, we applied once more the Shapiro-Wilk tests. The results of running the Shapiro-Wilks test over a total of 97,450 generated probability distributions are presented in Table 5:

Dimensions	Normally distributed predictions(%)
Length	75.2%
Width	70.1%
Height	69.9%

Table 5: Normally distributed predictions (%).

The results demonstrate that normality assumption is reasonable for the obtained distributions. To further fortify this assumption, QQ plots were created for the distributions that did not pass the Shapiro-Wilk test. Some characteristic examples with the corresponding histograms are provided in Figure 9. As it is evident, no major deviations from the normal distribution are observed. Overall, there is valid evidence which support the normality assumption.

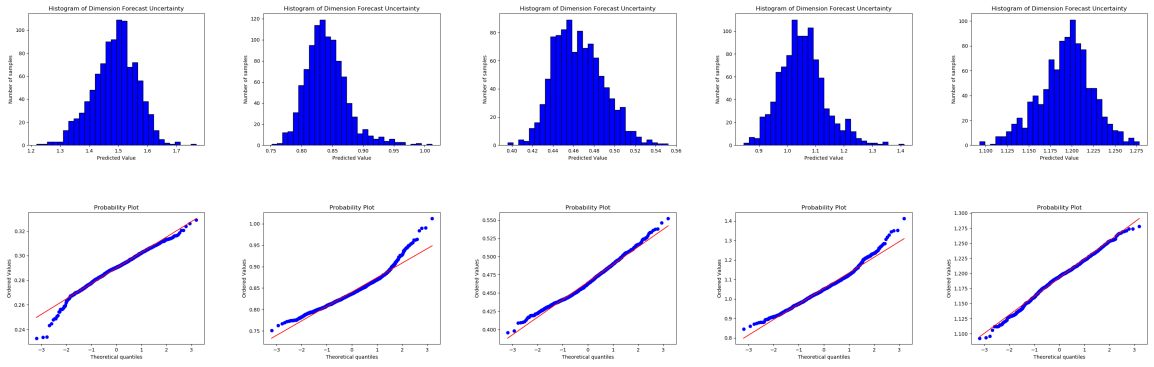

Figure 9: Histograms and QQ plots for the predicted dimensions distributions

For each probability distribution, a 95% prediction interval is established according to the algorithm presented in Sec. 2. Based on the constructed prediction intervals, we calculate the PICP for each dimension. The results are presented in Table 6. In accordance with the capacity forecasting model, high values of PICP were achieved, providing the revenue manager with the confidence that the true value of the corresponding shipment dimension is captured in the generated distribution of the predicted values in the majority of cases.

Dimensions	PICP
Length	95.1%
Width	98.6%
Height	95.2%

Table 6: Prediction Interval Coverage Probability (PICP).

4 Packing Models

4.1 One - Dimensional Knapsack Problem with chance constraints

Given the predicted palletized aircaft capacity $V_{cc} \sim N(\bar{V_{cc}}, \sigma^2_{V_{cc}})$ and an unlimited set of n LD-3 containers and k LDPs with volume $V_{LD-3} = 4\ m^3$ and $V_{LDP} = 10\ m^3$ respectively, the stochastic 1D-KP can be formulated as follows:

$$\max \quad \mathcal{J} = n \cdot V_{LD-3} + k \cdot V_{LDP} \tag{7a}$$

s.t.

$$\mathbb{P}(n \cdot V_{LD-3} + k \cdot V_{LDP} \leq \tilde{V_{cc}}) \geq \alpha, \tag{7b}$$

$$n, k \quad \in \mathbb{Z}^+ \tag{7c}$$

Taking into account, as proven in section 3, that $\tilde{V_{cc}}$ is Gaussian, Equation 7b becomes:

$$\bar{V_{cc}} + \Phi^{-1} \cdot (1 - \alpha) \cdot \sigma_{V_{cc}} - n \cdot V_{LD-3} - k \cdot V_{LDP} \leq 0 \tag{8}$$

where $\Phi^{-1}(\cdot)$ is the inverse CDF of normal distribution $\sim N(0, 1)$ and α is the desired confidence level. The optimal solution of this problem may be achieved with different combinations of the decision variables n and k. Each combination of the decision variables corresponds to a ULD configuration. Moreover, and since the ultimate goal is to maximize the number of shipments loaded, we choose to take into account the first sub-optimal solution of the problem (and the corresponding ULD configuration(s)). The reason behind this choice becomes evident if we consider the following example: Let us assume, for reasons of simplicity, that the predicted cargo capacity is $V_{cc} = 12\ m^3$ and we have a shipment with dimensions $3 \times 2 \times 1.5\ m$. The optimal solution of the 1D-KP corresponds to three LD-3 containers (i.e., $3 \cdot 4 = 12\ m^3$). However, this specific shipment exceeds the dimensions of an LD-3 container and hence, it is offloaded. On the other hand, the first sub-optimal solution of the 1D-KP is $10\ m^3$ which corresponds to one LDP. The LDP can accommodate this shipment and thus, this the optimal configuration for the complete packing problem, even though it is not the optimal solution of the 1D-KP. The former becomes more obvious during the validation of the model in Sec. 5.1.

4.2 Three-Dimensional Multiple Heterogeneous Knapsack Problem with chance constraints

In general, packing problems, and in particular the ones considering more than one dimension, are considered to be combinatorial optimization problems that are Non-Deterministic Polynomial-time Hard (NP-Hard) to solve. To address this NP-Hardness, several heuristics have been developed. Although heuristics are not always guaranteed to find the optimal solution, their low computational time when solving large instances of NP-Hard problems, makes them an efficient strategy that can be used to find a satisfactory feasible solution. Since the developed tool aims to provide the revenue manager with an answer within minutes, we resort to the EP heuristic algorithm developed by [Crainic et al., 2008] to solve the 3D-MHKP. However, readers are referred to Appendix B for the exact formulation of the stochastic 3D-MHKP.

The EP algorithm of [Crainic et al., 2008] addressed the Single Size Bin Packing Problem for items with known dimensions and that could not be rotated or overlap. This algorithm has proven to be fast enough to address the real time requirements of the proposed revenue management model, and, thus, it forms the backbone of our model as well. The algorithm is further extended to account for the stochasticity of shipment dimensions as well as additional constraints considered in the 3D-MHKP.

The input for the packing algorithm is, apart from the predetermined ULD configurations, a list of shipments $\mathbf{P} = (p_{1m}, p_{2m}, ...p_{nm})$ corresponding to a specific flight. Each shipment p_{im} may be composed of m multiple individual part shipments, that must be delivered together. Moreover, every (part) shipment p_{im} is characterized by length $l_{im} \sim N(\bar{l_{im}}, \sigma^2_{l_i})$, width $w_{im} \sim N(\bar{w_{im}}, \sigma^2_{w_{im}})$, height $h_{im} \sim N(\bar{h_{im}}, \sigma^2_{h_{im}})$ (as determined by the forecasting model), volume V_{im} and weight W_{im}. Unless differently specified, each shipment can be positioned inside a ULD according to one of the six rotations shown in Figure 10. The allowable rotations are modeled

using the binary parameters l_{im}^{+}, w_{im}^{+} and h_{im}^{+}. If a parameter is unitary, the associated dimension can be aligned with the vertical side of ULD.

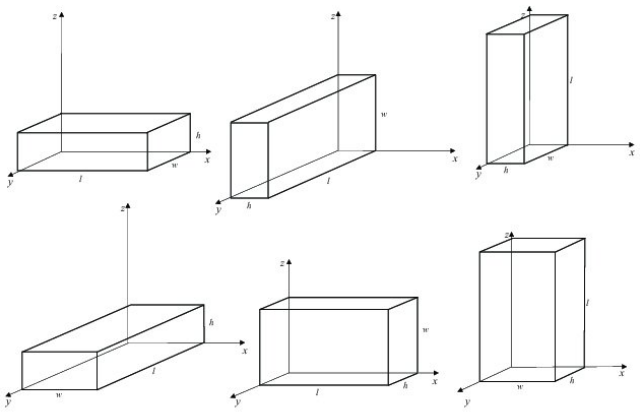

Figure 10: Shipment possible orientations [Jozefowska et al., 2018]

The location of a shipment inside the ULD is selected based on a global list containing all the EPs in all the ULDs. After a shipment is placed with its back-bottom-left vertex on the selected EP (x_i, y_i, z_i), a new set of EPs is generated, that correspond to potential positions for future packings and appended to the global list. The EPs generation process is summarized in 11(a). It is noted that an EP is projected only in case it can be supported either by an underlying shipment, the ULD's floor, or the ULD's cut as depicted in figure 11(b).

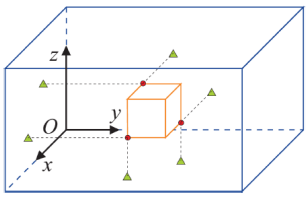

(a) EPs generation example-triangle represent the potential LPs [Baldi et al., 2012]

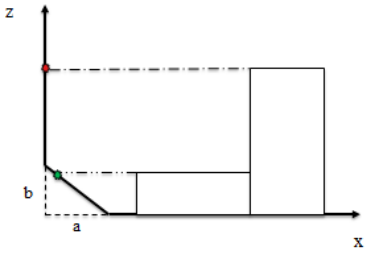

(b) EPs valid and non-valid EPs example in LD-3 container - only the green projection is usable

Figure 11: EPs generation process

When the considered ULD is empty, the shipment is placed in position $(0, 0, 0)$ for LDPs or $(0, a, 0)$ for LD-3 containers. In all other cases, a subset of candidate EPs from the global list are evaluated as potential locations of the shipment p_{im}, following an approach inspired by [Crainic et al., 2008]. This approach is based on the development of a merit function that maximizes the utilization of the EP Residual Space (RS). The RS quantifies the free volume around an EP and consists of three components, RS_x, RS_y, RS_z. Each component captures the distance between the EP and the wall of the container or the nearest shipment along the corresponding axis. Every time a shipment is placed into the container, the RS of all EPs is updated (see Figure 12).

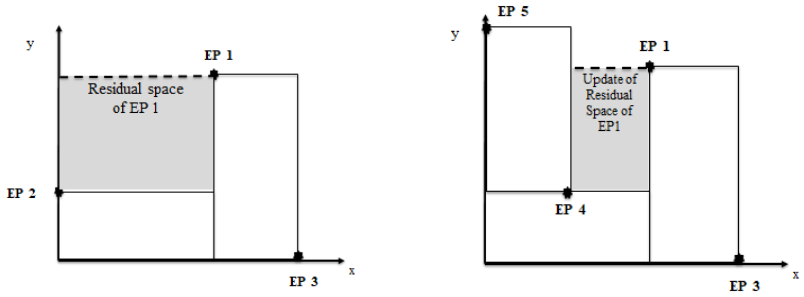

Figure 12: Example of residual space update

The merit function developed in this work is further extended to take into account the allowable rotations of the shipment as well as the stochasticity of the predicted dimensions. More specifically, our suggested merit function places the shipment in the EP and in the allowable orientation that minimizes the difference between the RS component and the corresponding shipment dimension along the relevant axis. In other words, for every EP, it is chosen the allowable shipment orientation that minimizes the corresponding RS and it can be written as follows:

$$MF = (RS_x - l_{im} r_{iab}) + (RS_y - w_{im} r_{iab}) + (RS_z - z_{im} r_{iab}) \tag{9}$$

where r_{iab} is a rotation binary variable introduced to model the six possible orientations of the shipment p_{im}, taking the value of 1 if side a of shipment is aligned with side b of the ULD. Moreover, since l_{im}, w_{im}, h_{im} are not deterministic but follow a Gaussian probability distribution, the merit function can be modified as follows:

$$\begin{aligned} MF = & \left(RS_x - \sum_{b=1}^{3} \bar{l_{im}} r_{i1b} - \Phi^{-1}(a) \sqrt{\sum_{b=1}^{3} \sigma^2_{l_{im}} r_{i1b}} \right) \\ & + \left(RS_y - \sum_{b=1}^{3} \bar{w_{im}} r_{i2b} - \Phi^{-1}(a) \sqrt{\sum_{b=1}^{3} \sigma^2_{w_{im}} r_{i2b}} \right) \\ & + \left(RS_z - \sum_{b=1}^{3} \bar{h_{im}} r_{i3b} - \Phi^{-1}(a) \sqrt{\sum_{b=1}^{3} \sigma^2_{h_{im}} r_{i3b}} \right) \end{aligned} \tag{10}$$

where $\Phi^{-1}(\cdot)$ is the inverse CDF of $N(0,1)$ and α is the desired confidence level. By taking into account the fact that only one of the three rotation variables for every dimension can take a unitary value each time the merit function is calculated, Equation 10 can be simplified as:

$$\begin{aligned} MF = & \left(RS_x - \sum_{b=1}^{3} \bar{l_{im}} r_{i1b} - \Phi^{-1}(a) \sum_{b=1}^{3} \sigma_{l_{im}} r_{i1b} \right) \\ & + \left(RS_y - \sum_{b=1}^{3} \bar{w_{im}} r_{i2b} - \Phi^{-1}(a) \sum_{b=1}^{3} \sigma_{w_{im}} r_{i2b} \right) \\ & + \left(RS_z - \sum_{b=1}^{3} \bar{h_{im}} r_{i3b} - \Phi^{-1}(a) \sum_{b=1}^{3} \sigma_{h_{im}} r_{i3b} \right) \end{aligned} \tag{11}$$

After the merit function for all the EPs is calculated, the EPs with negative RS components are removed, in order to ensure that the placed shipment would not overlap with any of the previously packed shipments. The remaining EPs are sorted in terms of ascending values of the corresponding merit function and form the list with the candidate EPs. These candidate EPs are evaluated as potential positions of the shipment p_{im} based on the following constraints:

1. The corresponding ULD dimensions must be respected, i.e., a shipment must lie within the corresponding ULD boundaries.
2. The corresponding ULD weight capacity must be respected.
3. Load stability must be ensured, i.e., all four vertices of the shipment must be supported either by an underlying shipment, or by the ULD's floor.
4. In case of part shipments, when a part of the shipment is not loaded, then all the parts should be offloaded.

These constraints are verified against the shipment characteristics using the same formulation as in [Paquay et al., 2017], adjusted to account for the stochasticity in the predicted shipment dimensions. Specifically, constraints (1) and (3) need to be modified to chance constraints as they incorporate the probability distributions of the predicted shipment dimensions. Readers are referred to Appendix B for the exact mathematical formulation of the aforementioned constraints. Algorithm 2 presents the framework of the proposed packing heuristic applied to a single ULD and a list of shipments with no part shipments ($m = 1$ for all shipments).

Algorithm 2 Heuristic Packing Method.

Input List of shipments to be loaded **P** with dimensions $l_i \sim N(\bar{l_i}, \sigma^2_{l_i})$, width $w_i \sim N(\bar{w_i}, \sigma^2_{w_i})$, height $h_i \sim N(\bar{h_i}, \sigma^2_{h_i})$ and weight W_i.

$WeightCapacityRespected(W_i)$: function returning **true** if weight of shipments loaded do not exceed weight capacity of the ULD.

$CanBeSupported(l_i, w_i, h_i, \alpha)$: function returning **true** if all four vertices of shipment p_i are supported by underlying shipment or the ULD's floor within a specified confidence level α.

$ULDBoundsRespected(l_i, w_i, h_i, \alpha)$: function returning **true** if the packed shipment p_i lies within the boundaries of the ULD within the specified confidence level α.

$EPProjectionSupported(l_i, w_i, h_i, \alpha)$: function returning **true** if the projected EP is supported either by an underlying box or by the ULD's floor within the specified confidence level α.

Set List of loaded shipment $\mathbf{L_p} \leftarrow \emptyset$
Set List of Extreme Points $\mathbf{EP_L} \leftarrow \emptyset$
Set Weight of shipments loaded $\mathbf{W_L} = 0$
Set List of Residual Space values $\mathbf{RS} \leftarrow \emptyset$
for all $\mathbf{p_i} \in \mathbf{P}$ **do**
  Set List of Candidate Extreme Points $\mathbf{EP_{Cand}} \leftarrow \emptyset$
  for all $RSvalues \in \mathbf{RS}$ **do**
    Compute $RSvalues$ components for every allowable rotation of shipment p_i
  end for
  Remove RS instances with negative $RSvalues$ components
  Compute corresponding Merit Functions
  Order Merit Functions by ascending order along with the associated **EPs** and shipment orientations
  Set $\mathbf{EP_{Cand}} \leftarrow$ **EPs**
  for $\mathbf{EP} \in \mathbf{EP_{Cand}}$ **do**
    if $WeightCapacityRespected$ **and** $ULDBoundsRespected$ **and** $CanBeSupported$ **then**
      Set $\mathbf{L_p} \leftarrow \mathbf{L_p} \cup \mathbf{p_i}$
      Compute $newEP$ projections as in Figure 11(a)
      if corresponding $EPProjectionSupported$ **then**
        Set $\mathbf{EP_L}' \leftarrow \mathbf{EP_L}' \cup newEP$
      end if
      Set $\mathbf{EP_L} \leftarrow \mathbf{EP_L} \cup \mathbf{EP_L}'$
      Update Residual Space List $\mathbf{RS}'$ as in Figure 12
      Set $\mathbf{RS} \leftarrow \mathbf{RS}'$
      Set $\mathbf{W_L} = \mathbf{W_L} + \mathbf{W_i}$
      break
    end if
  end for
end for
Output List of loaded shipments $\mathbf{L_p}$

5 Design of the combined forecasting and stochastic packing model

Given the objective of this paper, we now analyze more into details how the different modeling blocks can be used in real operations. Specifically, let us consider a 14-days time frame before the departure of the flight of interest. This choice is consistent with the operations of the partner airline, that starts accepting bookings 14 days before departure. At the beginning of the time frame, no bookings for this flight have been received. Until one day before departure, revenue managers receive shipment booking requests and must decide whether to accept them or not. As one could easily imagine, this task is fairly simple at the beginning of the time frame, when available cargo capacity is still high but becomes rather challenging as the day of departure approaches and the available capacity decreases. To tackle this challenge, the forecasting and the packing models previously developed were combined into a single framework that guides the decision making process, as demonstrated in Figure 13.

The first step of the proposed framework consists of generating the distribution of the predicted cargo

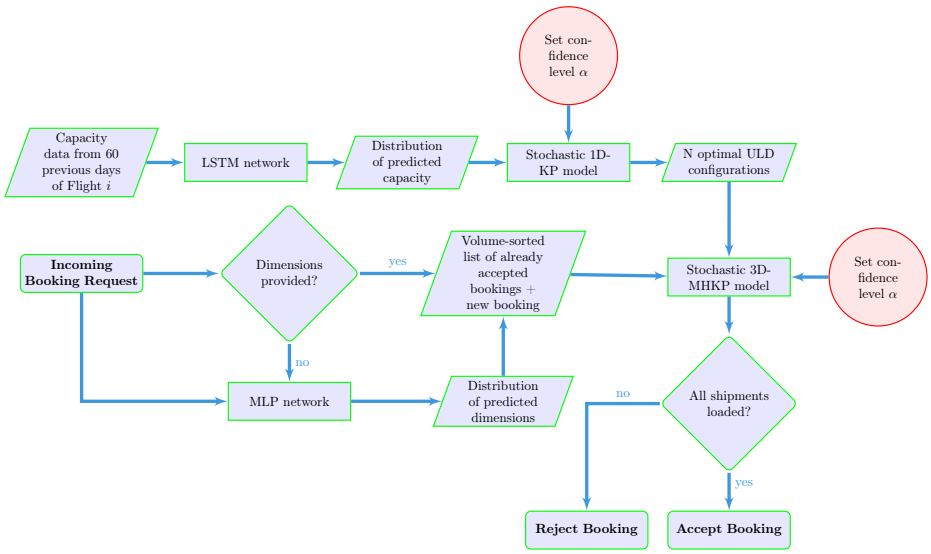

Figure 13: Flowchart of decision making process

capacity for the specific flight, $\tilde{V_{cc}} \sim (\bar{V_{cc}}, \sigma^2_{V_{cc}})$ with the LSTM network developed in Sec. 3.1. Then, the 1D-KP described in Sec. 4.1 is run, within a specific confidence level defined by the revenue manager, in order to determine the available optimal ULD configuration(s).

Every time a booking request with unspecified dimensions is received, the features of the booking described in section 3.2 are passed to the MLP network, and the distribution of the predicted shipment dimensions $l_{im} \sim N(\bar{l_{im}}, \sigma^2_{l_i})$, $w_{im} \sim N(\bar{w_{im}}, \sigma^2_{w_{im}})$, $h_{im} \sim N(\bar{h_{im}}, \sigma^2_{h_{im}})$ is generated. Afterwards, the candidate shipment along with the already accepted shipments (if any) are sorted by non-increasing values of their volume and fed to the 3D-MHKP model developed in Sec. 4.2. In general, placing large shipments is difficult, especially when it happens at the latest stages of the loading procedure. We address this difficulty by considering the largest shipments for loading first.

The 3D-MHKP model is solved for all the ULD configurations that have been defined by the 1D-KP model within a specific confidence level. More specifically, for every ULD of the determined ULD configuration(s), the 3D-MHKP is solved sequentially, i.e the EP heuristic is applied to the first ULD until no more shipments can be accommodated and the offloaded shipments (if any) are considered for placement in the next ULD. The same procedure continues until there are no offloaded shipments or ULDs left. Finally, the ULD configuration that maximizes the number of shipments loaded is selected.The corresponding block diagram can be found in Figure 14.

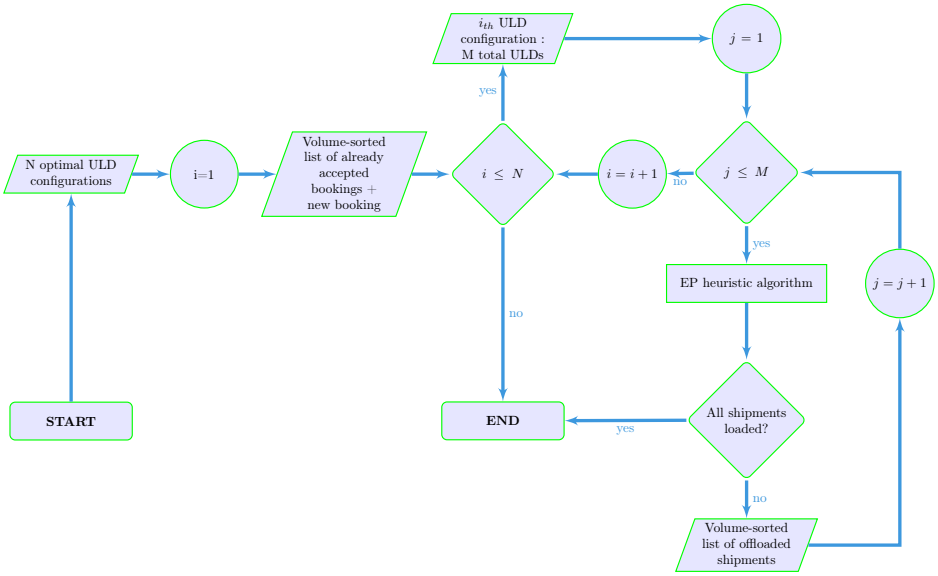

Figure 14: 3D-MHKP model

5.1 Computational Experiments

In this section, we will apply the developed model to four real case scenarios with booking data provided by our partner airline. More specifically, we will consider four sets of booking requests received for four different flights. A booking may consist of multiple individual shipments. Each set of booking requests is sorted by chronological order in order to simulate the revenue management rationale of accepting/rejecting an incoming booking request.

A booking is accepted when the computed loading strategy (ULD configuration + shipments loaded) does not offload any previously accepted bookings. Moreover, in case of bookings consisting of multiple shipments, as explained in Sec. 4.2, if a part of a booking is offloaded, then the whole booking is rejected. If the booking is rejected, the last optimal loading strategy is kept, until a new booking request is received. Using this ordered sequence of bookings, our developed model is run every time a 'new' booking is received and, in case the aforementioned condition is met, the booking is accepted.

A good indicator of the solution quality of our model, apart from the volume of the shipments loaded, is the Acceptance Factor (AF). The AF is defined as the ratio of the volume of the loaded shipments to the volume of all incoming booking requests, i.e., in case we have 10 booking requests and 9 of them are accepted, the achieved AF = 90 %.

Moreover, a metric widely used in daily cargo practice is Shipment Contribution (SCb), i.e., how much a shipment contributes towards the total generated revenue for the specific flight. Even though SCb is not included in the objective function of the proposed stochastic packing model, it is interesting to provide the readers with an order of magnitude of the achieved SCb.

The exact booking data for the considered flights can be found in Appendix C. For bookings that the customer did not provide any dimensions information, the palletization software used by our partner airline assumed that the corresponding volume was filled by $40cm \times 40cm \times 40cm$ cuboid boxes. Since booking data are extremely sensitive, any indication of the considered flight or the original shipper is omitted for confidentiality reasons. The corresponding flight and booking characteristics are summarized in Table 7, whereas in Figure 15-Figure 18, a visual representation of the volume and shipment contribution of each shipment per flight is depicted.

Flight #	**Cargo capacity (m^3)**	**ULD configuration**	**Total. shipments**	**Volume of booking requests (m^3)**	**SCb of booking requests**
Flight #1	74	7 LDPs - 1 LD-3	97	71.232	45,554.81
Flight #2	77	6 LDPs - 3 LD-3	91	72.651	18,413.13
Flight #3	96	8 LDPS - 4 LD-3	122	89.49	55,182.34
Flight #4	78	7 LDPs - 1 LD-3	194	70.480	15,834.80

Table 7: Flight and booking information.

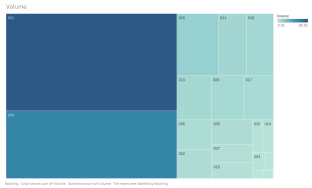

(a) Volume

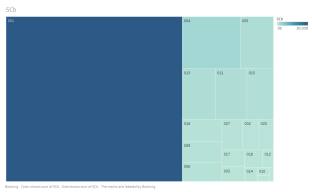

(b) SCb

Figure 15: Flight #1

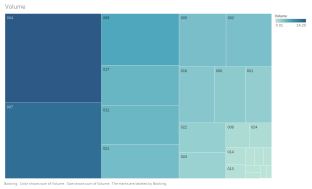

(a) Volume

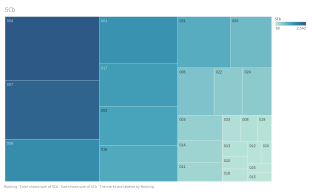

(b) SCb

Figure 16: Flight #2

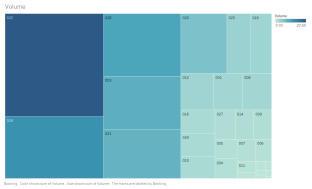

(a) Volume

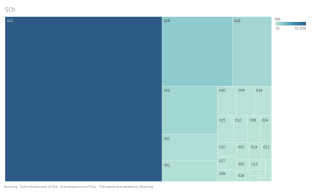

(b) SCb

Figure 17: Flight #3

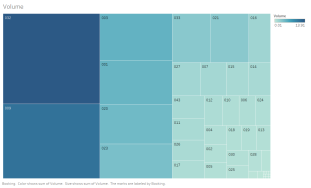

(a) Volume

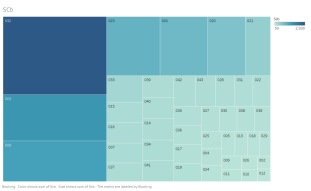

(b) SCb

Figure 18: Flight #4

Before applying the combined forecasting and packing model to the dataset, it is interesting to have an indication of how our developed packing model performs with deterministic inputs, thus excluding the forecasting functionality, in comparison with the partner airline. Isolating the packing model in this phase will clarify the effects of introducing forecasting uncertainty in the subsequent stages of testing the model. The results are summarized in Table 8 - Table 11. Row **Partner Airline** indicates the decision taken by our industrial

partner, whereas row **Packing Model** depicts the decision output of our developed packing model. Used ULD configuration corresponds to the actual ULD configuration used by the airline, whereas the optimal ULD configuration is the ULD configuration determined by the packing model.

It is highlighted that in the examined sets of booking requests, the rejection decisions are associated solely with lack of capacity and not other reasons such as delayed delivery or qualitative rejection. Moreover, when interpreting the results, we have to remember that no weight and balance restrictions are considered and that the model is designed for a single flight. Consequently, any lack of capacity caused in the actual flights by requirements of specific shipments being in the same ULD to facilitate the offloading - loading process in multiple flight legs or by weight and balance restrictions, is not addressed in the current work. The developed packing model utilizes the residual space subject only to the constraints referred in Sec. 4.2.

	Partner Airline	Packing Model
	Used ULD Config. : 7 LDPs - 1LD-3	Optimal ULD Config. : 7 LDPs - 1 LD-3
Booking No.	Loading Decision	
001	Accepted	Accepted
002	Accepted	Accepted
003	Accepted	Accepted
004	Accepted	Accepted
005	Accepted	Accepted
006	Accepted	Accepted
007	Accepted	Accepted
008	Accepted	Accepted
009	Accepted	Rejected
010	Accepted	Accepted
011	Rejected	Accepted
012	Accepted	Accepted
013	Rejected	Accepted
014	Accepted	Accepted
015	Rejected	Accepted
016	Rejected	Accepted
017	Rejected	Accepted
018	Accepted	Accepted
019	Accepted	Accepted
020	Rejected	Accepted
Performance Metrics		
Computational time	N/A	$\leq 5sec$
Volume Loaded	62.226	68.76
Acceptance Factor	83.2%	96.51%
Shipment Contribution	39,008.61	45,233.66

Table 8: Loading decision and performance metrics for flight #1.

	Partner Airline	Packing Model
	Used ULD Config. : 6 LDPs - 4LD-3	Optimal ULD Config. : 7 LDPs - 1 LD-3
Booking No.	Loading Decision	
001	Accepted	Accepted
002	Accepted	Accepted
003	Accepted	Accepted
004	Accepted	Accepted
005	Accepted	Accepted
006	Accepted	Accepted
007	Accepted	Accepted
008	Accepted	Accepted
009	Accepted	Accepted
010	Accepted	Accepted
011	Accepted	Accepted
012	Accepted	Accepted
013	Accepted	Accepted
014	Accepted	Accepted
015	Accepted	Accepted
016	Accepted	Accepted
017	Accepted	Accepted
018	Rejected	Accepted
019	Accepted	Accepted
020	Accepted	Accepted
021	Rejected	Accepted
022	Rejected	Accepted
023	Accepted	Accepted
024	Rejected	Rejected
025	Accepted	Accepted
Performance Metrics		
Computational time	N/A	$\leq 5sec$
Volume Loaded	60.86	71.73
Acceptance Factor	83.7%	98.7%
Shipment Contribution	13,240.13	17,831.9

Table 9: Loading decision and performance metrics for flight #2.

	Partner Airline	Packing Model
	Used ULD Config. : 8 LDPs - 4 LD-3s	Optimal ULD Config. : 9 LDPs - 1 LD-3
Booking No.	Loading Decision	
001	Accepted	Accepted
002	Accepted	Accepted
003	Accepted	Accepted
004	Accepted	Accepted
005	Accepted	Accepted
006	Accepted	Accepted
007	Accepted	Accepted
008	Accepted	Accepted
009	Accepted	Accepted
010	Accepted	Accepted
011	Accepted	Accepted
012	Accepted	Accepted
013	Accepted	Accepted
014	Accepted	Accepted
015	Accepted	Accepted
016	Accepted	Accepted
017	Accepted	Accepted
018	Accepted	Accepted
019	Accepted	Accepted
020	Accepted	Accepted
021	Accepted	Accepted
022	Accepted	Accepted
023	Accepted	Accepted
024	Rejected	Accepted
025	Rejected	Accepted
026	Accepted	Accepted
027	Rejected	Accepted
028	Rejected	Accepted
029	Rejected	Rejected
Performance Metrics		
Computational time	N/A	≤ 7 sec
Volume Loaded	61.53	76.53
Acceptance Factor	68.7%	85.5%
Shipment Contribution	44,647.20	49,290.63

Table 10: Loading decision and performance metrics for flight #3.

In the light of the aforementioned assumptions and as depicted, our proposed packing model provides better results in terms of AF and SCb. The optimal ULD configuration determined by the model is the same as the

	Partner Airline	Packing Model
	Used ULD Config. : 7 LDPs - 2 LD-3	Optimal ULD Config. : 7 LDPs - 2 LD-3
Booking No.	**Loading Decision**	
001	Accepted	Accepted
002	Accepted	Accepted
003	Accepted	Accepted
004	Accepted	Accepted
005	Accepted	Accepted
006	Accepted	Accepted
007	Accepted	Accepted
008	Accepted	Accepted
009	Accepted	Accepted
010	Accepted	Accepted
011	Accepted	Accepted
012	Accepted	Accepted
013	Accepted	Accepted
014	Accepted	Accepted
015	Accepted	Accepted
016	Accepted	Accepted
017	Rejected	Accepted
018	Accepted	Accepted
019	Accepted	Accepted
020	Rejected	Accepted
021	Accepted	Accepted
022	Accepted	Accepted
023	Accepted	Accepted
024	Accepted	Accepted
025	Rejected	Accepted
026	Accepted	Accepted
027	Accepted	Accepted
028	Rejected	Accepted
029	Accepted	Accepted
030	Accepted	Accepted
031	Rejected	Accepted
032	Rejected	Accepted
033	Rejected	Accepted
034	Accepted	Accepted
035	Accepted	Accepted
036	Accepted	Accepted
037	Accepted	Accepted
038	Accepted	Accepted
039	Accepted	Accepted
040	Accepted	Accepted
041	Accepted	Accepted
042	Accepted	Accepted
043	Rejected	Rejected
Performance Metrics		
Computational time	N/A	$\leq$ 89 sec
Volume Loaded	60.58	69.32
Acceptance Factor	85.9%	98.3%
Shipment Contribution	14,122.13	15,606.19

Table 11: Loading decision and performance metrics for flight #4.

ULD configuration used by the airline for flights #1 and #4, while it changes for flights #2 and #3, where our model prefers the option of using one extra LDP instead of three LD-3 containers that the airline used. This choice becomes evident if we examine the bookings that are additionally rejected by our model when using the ULD configuration of the airline, namely booking 018 for flight #2 and booking 028 for flight #3. Due to shipments' big dimensions (booking 018) or the high number of part shipments having relatively big dimensions (booking 028), a configuration yielding one extra LDP instead of three LD-3 containers, even though it corresponds to less total cargo capacity (74 m^3 vs 76 m^3 for flight #2 and 94 m^3 vs 96 m^3 for flight #3), proves to be more suitable for accommodating those shipments with these specific dimensions. This observed result further justifies our design choice mentioned in Sec 4.1, i.e., to take into account both the optimal and the first sub-optimal solution of the 1D-KP model.

Moreover, the efficiency of the model in terms of computational time is highlighted, as it is a necessary requirement for the model to be used in a revenue management environment. It is noted that the upper bound of the computational time corresponds to the time needed for the model to solve the complete set of bookings. For flights #1, #2 and #3 the computational time remains below 7 sec whereas for flight #4 is increased to 89 sec, when considering the complete set of bookings. This sharp increase is attributed to the fact that a total of 194 individual shipments are considered for flight #4, in comparison with 97, 91 and 122 individual shipments for flights #1 and #2 and #3 respectively.

An indicative visualization of the loading strategy implemented for flight #1 is presented in Figure 19.

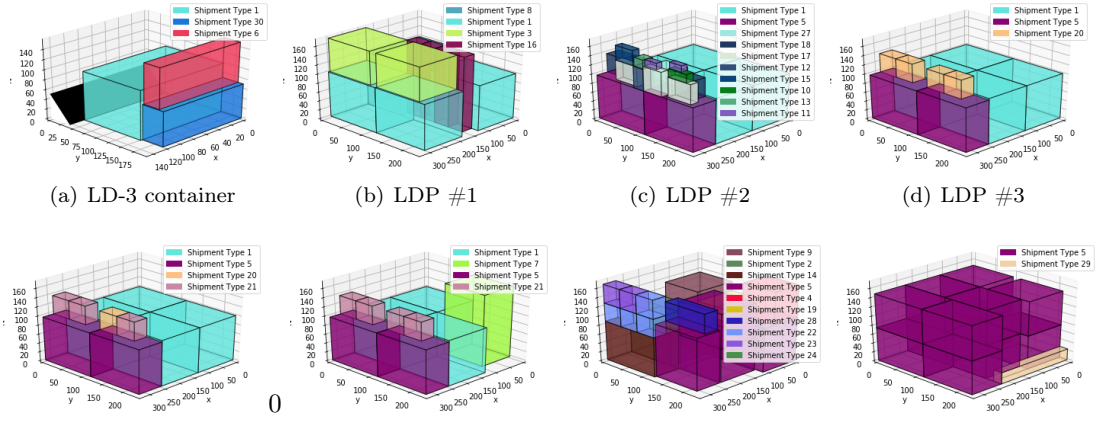

(a) LD-3 container (b) LDP #1 (c) LDP #2 (d) LDP #3

(e) LDP #4 (f) LDP #5 (g) LDP #6 (h) LDP #7

Figure 19: Visualization of loading strategy (flight #1)

5.1.1 Sensitivity analysis for capacity forecast

In this section, an analysis of how variations in the confidence level of the predicted cargo capacity affect the loading performance is presented.

First, we generate the probability distribution of the predicted cargo capacity. Passing as inputs the capacity data of the previous sixty days of the corresponding flight to the LSTM network developed in section 3.1, the predicted capacity distributions were found to be as follows:

- Flight #1 :$V_{cc} \sim N(80.23, 7.4)\ m^3$
- Flight #2 :$V_{cc} \sim N(85.01, 7.1)\ m^3$
- Flight #3 :$V_{cc} \sim N(100.51, 6.3)\ m^3$
- Flight #4 :$V_{cc} \sim N(84.32, 5.2)\ m^3$

Next, the stochastic packing model was run for different confidence levels of the predicted capacity using as inputs the booking dimensions as provided by our partner airline. The results in terms of loaded volume and corresponding shipment contribution for each flight are presented in Figure 20. Moreover, for each confidence level, the corresponding cargo capacity as defined by the stochastic 1D-KP model, along with the determined optimal ULD configuration and the rejected bookings are noted.

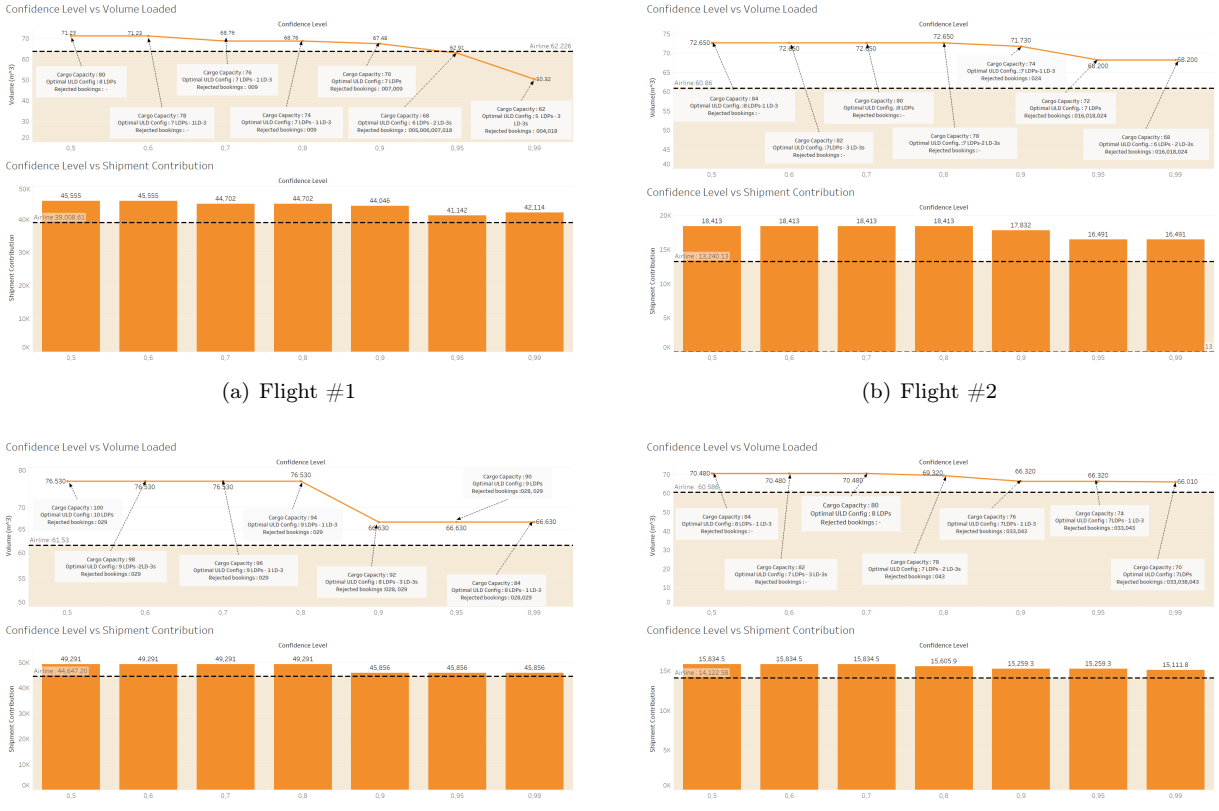

(a) Flight #1

(b) Flight #2

(c) Flight #3

(d) Flight #4

Figure 20: Effect of confidence level on loaded volume and shipment contribution

It is observed that for all four flights choosing a higher confidence level for the capacity forecast results in lower volume of shipments loaded. The former is a direct consequence and validation at the same time of the intended functionality of the combined model, which is to protect the revenue manager from any uncertainty included in the forecast. A more conservative approach means that the revenue manager is less willing to be exposed to cases where the actual capacity of the flight is lower than the predicted and accept bookings that should not have been accepted.

However, with the exception of flight #1 for confidence levels $\alpha = 0.9$ and $\alpha = 0.99$, our combined model results in higher volume of shipments loaded in comparison with our partner airline. Moreover, the sharp decrease that is observed in flight #1 at confidence level $\alpha = 0.99$ is due to the fact that the rejected booking 004 (Figure 15) is a rather bulky shipment with volume $V = 19.5\ m^3$. A similar decrease is observed for flight

#3 at confidence level $\alpha = 0.90$ for the same reason (booking 028). As such, the rejection of this single booking is causing the volume of the loaded shipments to sharply decrease.

Finally, the variation of the corresponding AFs per flight with respect to confidence level is presented in Figure 21, where, as expected, a negative correlation is depicted.

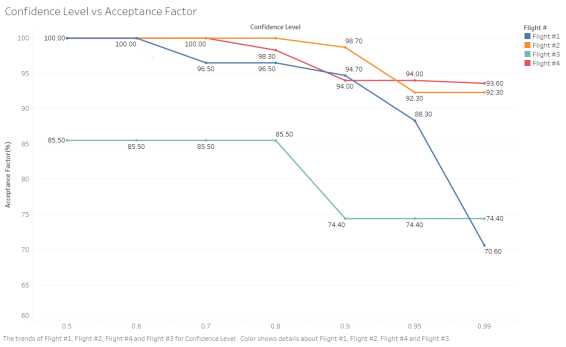

Figure 21: Effect of confidence level in Acceptance Factor

5.1.2 Sensitivity analysis for dimensions forecast

The next step of the sensitivity analysis consists of evaluating how loading performance is affected when changing the confidence interval of the predicted shipment dimensions. The distribution of the predicted shipment dimensions is generated using the MLP model developed in Sec. 3.2. The results of the forecasting model can be found in Appendix D. In order to have a benchmark reference, we choose to use a standard cargo capacity that corresponds to the real capacity of the flights, which can be found in Table 7. However, the optimal ULD configurations will still be determined by packing model.

The stochastic packing model is run for different confidence levels of the predicted shipment dimensions. The results for every flight in terms of loaded volume and shipment contribution along with the optimal ULD configuration can be found in Figure 22.

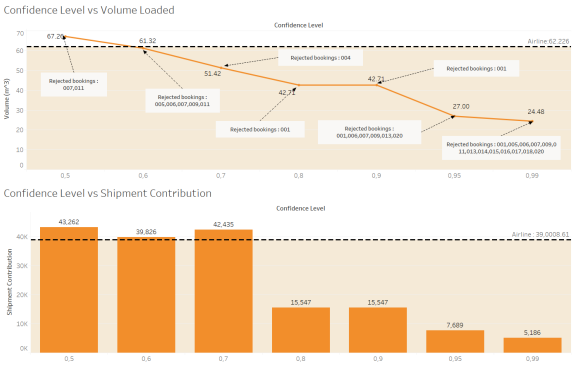

(a) Flight #1: 7 LDPs - 1 LD-3

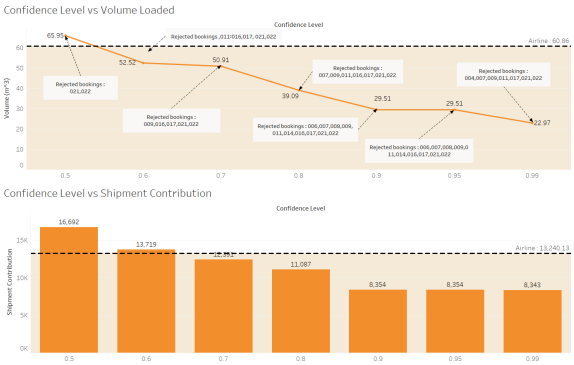

(b) Flight #2 : 7LDPs - 1 LD-3

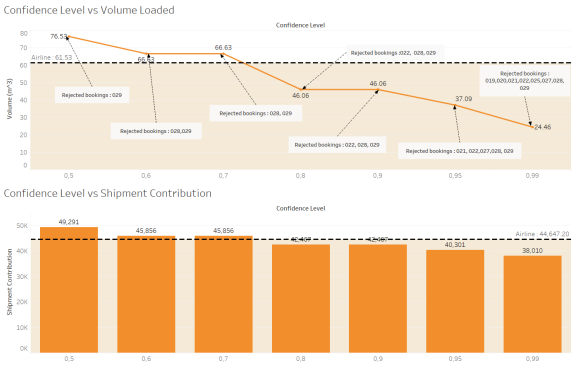

(c) Flight #3 : 9LDPs - 1 LD-3

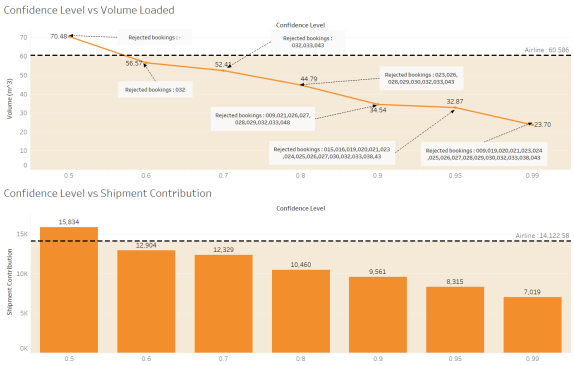

(d) Flight #4 : 7LDPs - 2 LD-3s

Figure 22: Effect of confidence level on loaded volume and shipment contribution

As expected, when increasing the confidence level, the volume of loaded shipments decreases. This pattern can be further justified by looking at Figure 23, where a visualization of the loading strategy for flight #1 and confidence level $\alpha = 0.9$ is presented.

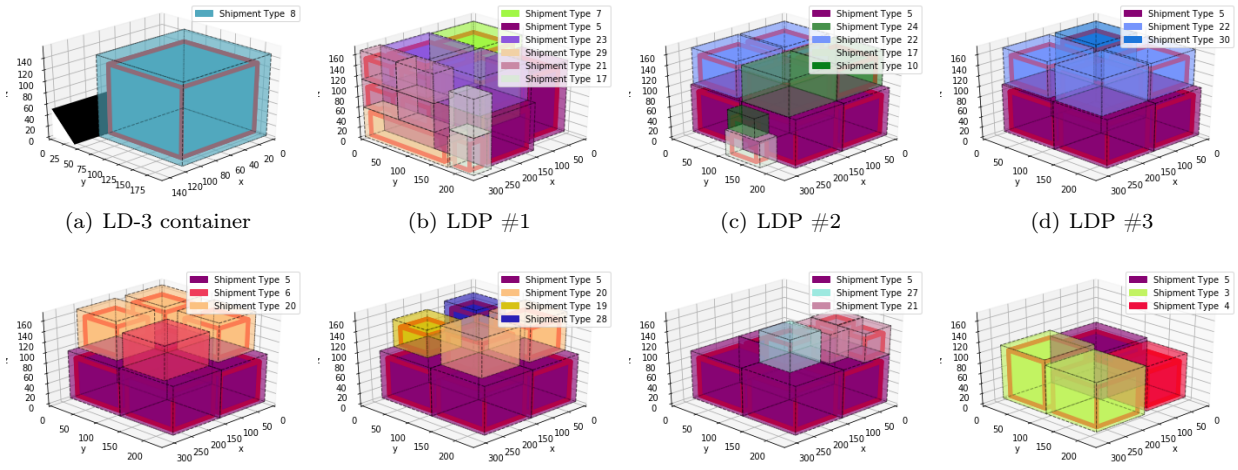

(a) LD-3 container (b) LDP #1 (c) LDP #2 (d) LDP #3

(e) LDP #4 (f) LDP #5 (g) LDP #6 (h) LDP #7

Figure 23: Visualization of loading strategy for confidence level $\alpha = 0.9$ (flight #1)

The solid red lines represent the mean dimension of each shipment, as defined by the forecasting model, whereas the dotted lines represent the worst-case boundaries of the shipments, as defined by the corresponding confidence level and the total standard deviation of the prediction. In other words, increasing the confidence level of the predicted dimensions is translated as considering the worst-case scenario. The worst-case scenario in our case occurs when a shipment appears at the Operations Department of the airline with bigger dimensions that the dimensions predicted by the forecasting model. Hence, increasing the confidence level results in a loading strategy that addresses inflated dimensions, hence protecting the manager from the worst-case scenario, but being more conservative in terms of volume loaded at the same time.

In comparison with our partner airline, our model performs better in terms of loaded volume only for confidence level $\alpha = 0.5$. This can be partly explained by the conservative approach we adopted when estimating the total standard deviation of our predictions in exchange for a higher PICP (Sec. 2.1), yielding $\sigma_{l_i} \approx 16cm$, $\sigma_{w_i} \approx 11cm$ and $\sigma_{h_i} \approx 14cm$ for length, width and height accordingly.

The former is reflected in the higher sensitivity of the Acceptance Factor with respect to confidence level, in comparison with the corresponding behavior for varying confidence levels of the predicted cargo capacity, as illustrated in Figure 24.

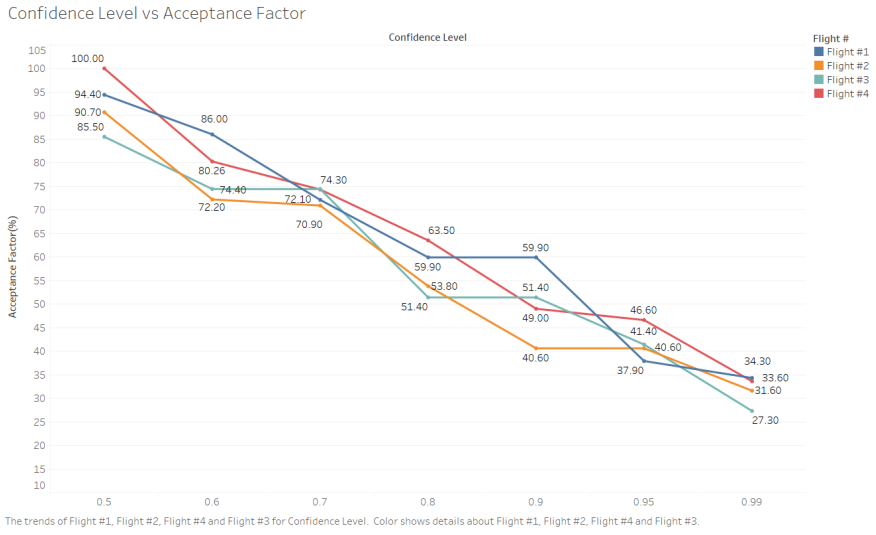

Figure 24: Effect of confidence level on Acceptance Factor

Moreover, for some cases, even though the volume of shipments loaded by the combined model is lower than the volume loaded by the partner airline, the corresponding shipment contribution achieved is higher. This

is explained by the fact that in specific cases, rejecting booking(s) with high volume results in leaving free capacity for accepting a higher number of smaller shipments, which have higher total shipment contribution but less volume than the booking(s) rejected. For example, in flight #1 at confidence level $\alpha = 0.7$, rejecting booking 004, which has a volume of $V = 19.5\ m^3$, results in accepting all the other bookings. As a result, the loaded volume is less than the volume loaded by the partner airline, but the shipment contribution is higher.

However, as previously explained, the results regarding shipment contribution are provided for reference purposes and cannot be directly compared to the partner airline , since the objective of the stochastic packing model is to maximize the volume of shipments loaded. Exploring a loading strategy that maximizes the shipment contribution of shipments loaded is left as recommendation for our future work.

5.1.3 Robustness evaluation of the stochastic packing model

The goal of this section is to evaluate the robustness and reliability of the packing model when the shipment dimensions assume random values taken from the distributions generated by the forecasting model. The reason for not choosing to perform a similar analysis with respect to the predicted cargo capacity is that the model, as shown in Sec. 5.1.1 and Sec. 5.1.2, appears to be less sensitive in the variations of the predicted cargo capacity, due to higher accuracy and less total standard deviation of the capacity forecasting model.

We simulated a total of 1,000 scenarios per flight. For each scenario, the dimension values per booking were randomly drawn from the corresponding distributions defined by the forecasting model and passed as inputs to the stochastic packing model, while the cargo capacity corresponds to the real cargo capacity of the flight. The results in terms of loaded volume and shipment contribution for the considered flights over the 1,000 scenarios are presented in Figure 25 and Figure 26.

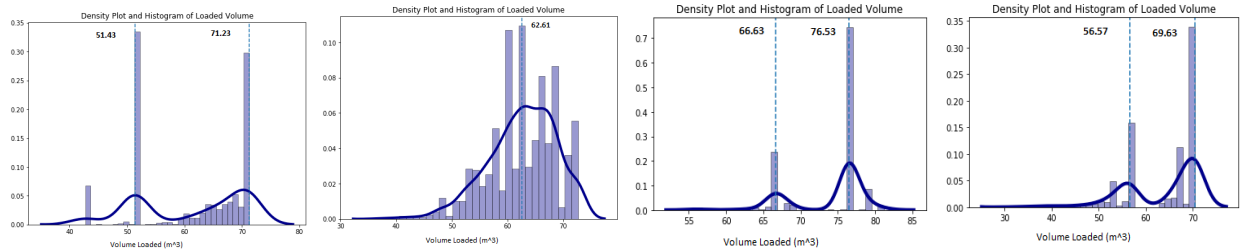

(a) Flight #1 (b) Flight #2 (c) Flight #3 (d) Flight #4

Figure 25: Density Plots of loaded volume

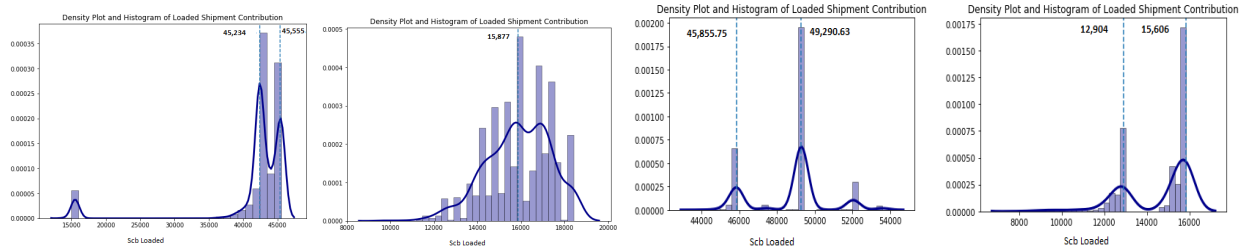

(a) Flight #1 (b) Flight #2 (c) Flight #3 (d) Flight #4

Figure 26: Density Plots of Shipment Contribution

For flights #1, #3 and #4 the amount of volume loaded (and of the corresponding SCb) follows a bimodal distribution, whereas for flight #2 approaches the normal distribution with a mean value of $\bar{V} = 62.61\ m^3$. More specifically, for flight #1, two distinct peaks are appearing at volume values $V = 51.43\ m^3$ and $V = 71.23\ m^3$, for flight #3, peaks are appearing at volume values $V = 66.63\ m^3$ and $V = 76.53\ m^3$, whereas for flight #4 the corresponding peaks are noted at volume values $V = 56.57\ m^3$ and $V = 70.48\ m^3$. This behavior is attributed to the loading (or offloading) decision determined by our combined model for three specific high volume bookings included in these three flights (see Figure 15-Figure 18). In particular, accepting (or rejecting) booking 004 for flight #1, booking 028 for flight #3 and booking 032 for flight #4 corresponds to the difference between the peak values and has a decisive effect on the amount of loaded volume. Moreover, the fact that the bookings considered in flight #2 are more evenly distributed in terms of volume, is reflected to the normal shape of the resulting distribution. In this case, the loaded volume is not so much influenced by the acceptance (or rejection) of a single booking.

To gain further insights on the performance of the model, the Cumulative Distribution Function (CDF) of the loaded volume and corresponding SCb are presented in Figure 27 and Figure 28.

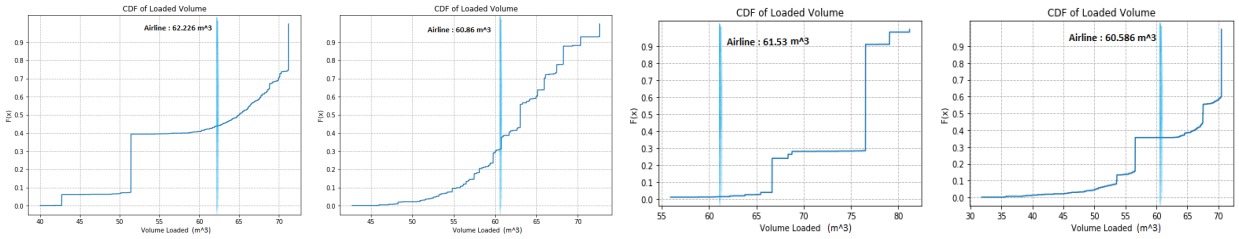

(a) Flight #1 (b) Flight #2 (c) Flight #3 (d) Flight #4

Figure 27: CDFs of loaded volume

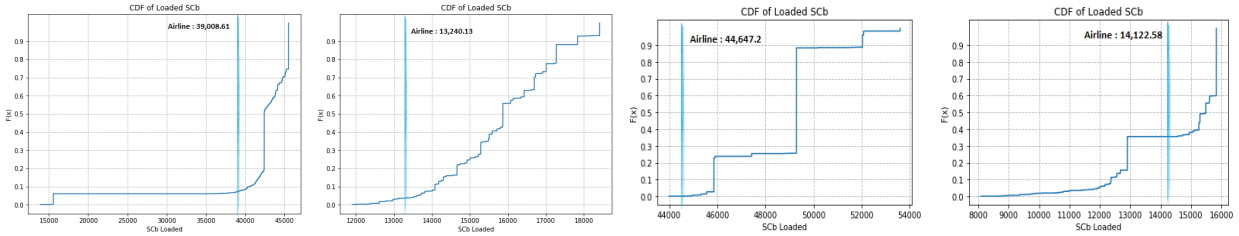

(a) Flight #1 (b) Flight #2 (c) Flight #3 (d) Flight #4

Figure 28: CDFs of Shipment Contribution

As it can be observed, in 90% of the simulated scenarios, our proposed packing model loads more than 50 m^3 of bookings in all four considered flights . Moreover, it outperforms the corresponding volume of bookings accepted by the airline in approximately 55%, 60%, 90% and 65% of the simulated scenarios respectively. Overall, the obtained results emphasize the efficiency and the robustness of the developed model.

6 Conclusions

In this paper, we presented a novel combined forecasting and stochastic packing model, developed adopting the revenue management perspective of cargo department of an airline. In particular, the overarching goal is to facilitate the decision-making process of accepting or rejecting a booking request. Due to its complexity and specificity,this problem has not been addressed deeply in the academic literature and, to our knowledge, there is no work that integrates forecasting and packing features under uncertainty in a single model.

The forecasting functionality of the model consists of generating the probability distribution of the predicted values for cargo capacity and shipment dimensions, and is implemented through a LSTM and MLP network. Both models provided very accurate predictions, while the produced distributions established prediction intervals with high PICP.

The generated distributions are passed as inputs to the stochastic packing model, which has a dual functionality: determine the optimal ULD configuration and the optimal palletization strategy under a specific confidence level. The former is achieved through a stochastic 1D-KP model while the latter through a stochastic 3D-MHKP model. The real-time environment requirement introduces the need for a good feasible solution in a short computational time. On that grounds, the 3D-MHKP model was designed using the EP heuristic. Moreover, to comply with real operational needs, the EP heuristic was enriched with the additional constraints referring to shipment possible orientations, stability, weight capacity of the ULD and complete shipments.

Experimentations have been performed on booking data sets from four real flights provided by our partner airline. First of all, our findings highlight the computational efficiency of the model, as in any case, the computational time did not exceed the 89 s and it remained below 7 s for the three of the four tested flights. Secondly, when using as inputs the shipment dimensions and cargo capacity as provided by our partner airline, in all four cases we achieved an improvement of 9.6%, 17.8%, 24.3% and 14.4% in terms of volume of shipments loaded. Testing the model over more flights to further verify its robustness and reliability is left as part or our future work.

Furthermore, for the four test cases considered, the sensitivity analysis performed for varying confidence levels of predicted cargo capacity and shipment dimensions, showed a negative correlation between confidence

level and volume of shipments loaded, which verifies the anticipated behaviour of the model. The model was found to be more sensitive when varying the confidence level of the predicted shipment dimensions distribution, but this is attributed to our design choice to assume a higher total standard deviation in exchange for a higher PICP. To further verify the efficiency and robustness of our model we simulated 1,000 scenarios per flight. In each scenario, the considered bookings per flight assumed random values from the corresponding distributions produced by the shipment dimensions forecasting model. Our findings highlight that our model obtained better results than our partner airline in terms of loaded volume in 55%, 60%, 90% and 65% of the scenarios.

In addition, the sensitivity analysis for the corresponding SCb revealed that there is not always a negative correlation between this value and the confidence level. The former is explained by the fact that SCb was not included in the objective function and is used only as reference. Related to this, a possible future direction is to include the SCb in the objective function of a two-stage stochastic packing model with recourse. This model would shed light on whether accepting a new booking, even though it offloads previously accepted bookings, can result in a higher total SCb.

Another future research direction is to include weight and balance restrictions and to devise the model so that it can account for multiple flight legs. This is a necessary step towards the development of a model capable of addressing all the needs of an airline cargo department.

References

[Baldi et al., 2012] Baldi, M., Perboli, G., and Tadei, R. (2012). The three dimensional knapsack problem with balancing constraints. *Applied Mathematics and Computation*, 218:9802–9818.

[Brandt and Nickel, 2018] Brandt, F. and Nickel, S. (2018). The air cargo load planning problem - a consolidated problem definition and literature review on related problems. *European Journal of Operational Research*, 275:399–410.

[Crainic et al., 2008] Crainic, T., Preboli, G., and Tadei, R. (2008). Extreme Point-Based heuristics for the Three-Dimensional bin packing. *Inform Journals on Computing*, 20:368–384.

[Dereli and Das, 2010] Dereli, Z. and Das, G. (2010). A hybrid simulated annealing algorithm for solving multi-objective container-loading problems. *Applied Artificial Intelligence*, 23:463–486.

[Fuellerer et al., 2010] Fuellerer, G., Doerner, K., Hartl, R., and Iori, M. (2010). Metaheuristics for vehicle routing problems with three-dimensional loading constraints. *European Journal of Operational Research*, 201:751–759.

[Gal, 2016] Gal, Y. (2016). Uncertainty in Deep Learning. *PhD Thesis University of Cambridge*.

[Goncalves and Resende, 2012] Goncalves, J. and Resende, M. (2012). A parallel multi-population biased random- key genetic algorithm for a container loading problem. *Computers and Operations Research*, 39:179–190.

[Hochreiter and Schmidhuber, 1997] Hochreiter, S. and Schmidhuber, J. (1997). Long short-term memory. *Neural Computation*, 9:1735–80.

[IATA, 2019] IATA (2019). Cargo stategy report. www.iata.org.

[Jozefowska et al., 2018] Jozefowska, J., Pawlak, G., Pesch, E., Morze, M., and Kowalski, D. (2018). Fast truck-packing of 3d boxes. *Engineering Management in Production and Services*, 10:29–40.

[Junqueira et al., 2012] Junqueira, L., Morabito, R., and Yamashita, D. (2012). Three-dimensional container loading models with cargo stability and load bearing constraints. *Computers and Operations Research*, 39:74–85.

[Kasilingam, 1996] Kasilingam, R. (1996). Air cargo revenue management : Characteristics and Complexities. *European Journal of Operations Research*, 96:36–44.

[Koch, 2019] Koch, M. (2019). An Optimisation and Forecast Framework for ULD Packing in the Air Cargo Supply Chain. Master's thesis, TU Delft, Netherlands.

[Le Roux and Bengio, 2010] Le Roux, N. and Bengio, Y. (2010). Deep Belief Networks are Compact Universal Approximators. *Neural Computation*, 8:2192–2207.

[Paquay et al., 2014] Paquay, C., Schyns, M., and Limburg, S. (2014). A mixed integer programming formulation for the three-dimensional bin packing problem deriving from an air cargo application. *International Transactions In Operational Research*, 23:187–213.

[Paquay et al., 2018] Paquay, C., Schyns, M., and Limburg, S. (2018). A tailored two-phase constructive heuristic for the three-dimensional multiple bin size bin packing problem with transportation constraints. *European Journal of Operational Research*, 267:1–12.

[Paquay et al., 2017] Paquay, C., Schyns, M., Limburg, S., and Oliveira, J. (2017). MIP-based constructive heuristics for the three-dimensional Bin Packing Problem with transportation constraints. *International Journal of Production Research*, pages 1–12.

[Sagheer and Kotb, 2019] Sagheer, A. and Kotb, M. (2019). Time series forecasting of petroleum production using deep LSTM recurrent networks. *Neurocomputing*, 323:203–213.

[Techanitisawad and Tangwiwatwong, 2004] Techanitisawad, A. and Tangwiwatwong, P. (2004). A GA-based Heuristic for the Interrelated Container Selection Loading Problems . *Industrial Engineering and Management Systems*, 3:22–37.

[Wada et al., 2017] Wada, M., Delgado, F., and Pagnoncelli, B. (2017). A risk averse approach to the capacity allocation problem in the airline cargo industry. *Journal of the Operations Research Society*, 68:643–651.

[Wascher et al., 2007] Wascher, G., Haußner, H., and Schumann, H. (2007). An improved typology of cutting and packing problem. *European Journal of Operational Research*, 183:1109–1130.

[Zhu and Laptev, 2017] Zhu, L. and Laptev, N. (2017). Deep and Confident prediction for time series at Uber. *Proc. IEEE Int. Conf. Data Min. Workshops*, pages 103–110.

Appendices

A Test results of the LSTM forecasting model

Flight #	**Aircraft type**	**MAPE**	**MAE** (m^3)	**PICP**	**Training time** (min)
Flight #1	A330-300	9.14%	6.23	99.5%	8
Flight #2	B777-200	7.59%	5.72	99.2%	9
Flight #3	B767-300	14.41%	5.56	94.1%	11
Flight #4	A330-200	8.63%	7.82	91.1%	24
Flight #5	B747-400	6.62%	6.18	96.2%	2
Flight #6	B787-9	9.19%	7.81	95.9%	4
Flight #7	B787-9	7.4%	5.5	95.6%	5
Flight #8	B777-200	14.18%	9.8	96.1%	8
Flight #9	A330-200	11.8%	8.66	94.2%	8
Flight #10	B747-400	12.58%	9.88	95.3%	4
Flight #11	A330-300	13.26%	8.9	96.5%	4
Flight #12	B747-400	14.15%	9.44	93.5%	3
Flight #13	B777-200	11.26%	7.32	95.6%	2
Flight #14	A330-200	5.58%	4.97	91.5%	4
Flight #15	B767-300	10.53%	7.14	96.2%	2
Flight #16	B777-200	12.19%	10.01	95.3%	5
Flight #17	A330-200	7.18%	6.12	99.3%	11
Flight #18	A330-300	11.65%	8.53	94.9%	10
Flight #19	A330-200	6.69%	5.44	99.5%	10
Flight #20	B767-300	10.24%	10.47	97.6%	4

Table 12: Validation results of the LSTM forecasting model.

B 3D-MHKP : Mathematical formulation of the model

The stochastic 3D-MHKP formulation is a modification of the 3D Bin Packing model developed by [Paquay et al., 2017], to account for stochasticity in the predicted shipment dimensions. More specifically, the following parameters are considered:

Table 13: Sets for the 3D-MHKP.

Set	Description
P	total number of shipments
N	total number of ULDs

Table 14: Parameters for the 3D-MHKP.

Parameter	Description
V_i	volume of shipment i
W_i	weight of shipment i
V_j	volume capacity of ULD j
WC_j	weight capacity of ULD j
L_j, W_j, H_j	length, width and height of ULD j
$\bar{l_i}, \bar{w_i}, \bar{h_i}$	mean predicted length, width and height of shipment i
$\sigma_{l_i}, \sigma_{w_i}, \sigma_{h_i}$	standard deviation of predicted length, width and height of shipment i
α_j	slope of cut in ULD j
β_j	intercept of cut in ULD j
D_m	maximum length, width or height among ULDs
α	confidence level

Table 15: Decision variables for the 3D-MHKP.

Decision Variable	Type	Description
p_{ij}	binary	unitary if shipment i is loaded to ULD j
q_i	binary	unitary if shipment i is offloaded
r_{iab}	binary	unitary if side a of shipment i is aligned with side b of ULD j
l_i^+, w_i^+, h_i+	binary	unitary if length, width and height of shipment i can be in vertical position
x_{ik}, y_{ik}, z_{ik}	binary	unitary if shipment i is placed on the right, behind or above shipment k respectively
g_i	binary	unitary if shipment i is placed on the ULD's floor
h_{ik}	binary	unitary if shipment k does not have the right height to support shipment i
o_{ik}	binary	unitary if there is no empty intersection between shipments i and k
s_{ik}	binary	unitary if shipment k supports at least one of the vertices of shipment i
n_{ik}^1	binary	unitary if $x_k \geq x_i$
n_{ik}^2	binary	unitary if $y_k \geq y_i$
n_{ik}^3	binary	unitary if $x_k^{'} \geq x_i^{'}$ ($x_k^{'}$ and $x_i^{'}$ are the horizontal positions of the right vertices of shipments k and i respectively
n_{ik}^4	binary	unitary if $y_k^{'} \geq y_i^{'}$ ($y_k^{'}$ and $y_i^{'}$ are the alternative positions of the right vertices of shipments k and i respectively
β_{ik}^l	binary	unitary if vertex l of shipment i is supported by shipment k
γ_i^c	binary	unitary if shipment i is supported by cut c
x_i, y_i, z_i	continuous	horizontal, vertical and lateral position of shipment i

The MILP formulation of the 3D-MHKP is as follows :

$$\max \quad \mathcal{J} = \sum_{i=1}^{P} \sum_{j=1}^{N} p_{ij} V_i \tag{12a}$$

s.t.

$$\sum_{j \in N} p_{ij} + q_i = 1, \qquad \forall i \in \mathbf{P}, \tag{12b}$$

$$r_{ik1} + r_{ik2} + r_{ik3} = 1, \qquad \forall i \in \mathbf{P}, k = [1, 2, 3], \tag{12c}$$

$$r_{i1k} + r_{i2k} + r_{i3k} = 1, \qquad \forall i \in \mathbf{P}, k = [1,2,3], \tag{12d}$$

$$r_{i1k} + r_{i2k} + r_{i3k} = 1, \qquad \forall i \in \mathbf{P}, k = [1,2,3], \tag{12e}$$

$$r_{i31} \leq l_i^+, \qquad \forall i \in \mathbf{P}, \tag{12f}$$

$$r_{i32} \leq w_i^+, \qquad \forall i \in \mathbf{P}, \tag{12g}$$

$$r_{i33} \leq h_i^+, \qquad \forall i \in \mathbf{P}, \tag{12h}$$

$$\sum_{i \in \mathbf{P}} W_i p_{ij} \leq WC_j, \qquad \forall j \in \mathbf{N}, \tag{12i}$$

$$x_i' = x_i + \overline{l_i} r_{11} + \Phi^{-1}(\alpha)\sigma_{l_i} r_{i11} + \overline{h_i} r_{i13} + \Phi^{-1}(\alpha)\sigma_{h_i} r_{i13} + \overline{w_i} r_{i12} + \Phi^{-1}(\alpha)\sigma_{w_i} r_{i12}, \quad \forall i \in \mathbf{P}, \tag{12j}$$

$$y_i' = y_i + \overline{l_i} r_{21} + \Phi^{-1}(\alpha)\sigma_{l_i} r_{i21} + \overline{h_i} r_{i23} + \Phi^{-1}(\alpha)\sigma_{h_i} r_{i23} + \overline{w_i} r_{i22} + \Phi^{-1}(\alpha)\sigma_{w_i} r_{i22}, \quad \forall i \in \mathbf{P}, \tag{12k}$$

$$z_i' = z_i + \overline{l_i} r_{31} + \Phi^{-1}(\alpha)\sigma_{l_i} r_{i31} + \overline{h_i} r_{i33} + \Phi^{-1}(\alpha)\sigma_{h_i} r_{i33} + \overline{w_i} r_{i32} + \Phi^{-1}(\alpha)\sigma_{w_i} r_{i32}, \quad \forall i \in \mathbf{P}, \tag{12l}$$

$$x_i' \leq \sum_{j \in N} L_j p_{ij}, \qquad \forall i \in \mathbf{P}, \tag{12m}$$

$$y_i' \leq \sum_{j \in N} W_j p_{ij}, \qquad \forall i \in \mathbf{P}, \tag{12n}$$

$$z_i' \leq \sum_{j \in N} H_j p_{ij}, \qquad \forall i \in \mathbf{P}, \tag{12o}$$

$$x_{ik} + x_{ki} + y_{ik} + y_{ki} + z_{ik} + z_{ki} \geq (p_{ij} + p_{kj}) - 1 \qquad \forall i,k \in \mathbf{P}, \tag{12p}$$

$$x_k' - x_i - D_m(1 - x_{ik}) \leq 0 \qquad \forall i,k \in \mathbf{P}, \tag{12q}$$

$$x_i - x_k' - D_m(1 - x_{ik}) \leq 1 \qquad \forall i,k \in \mathbf{P}, \tag{12r}$$

$$y_k' - y_i - D_m(1 - y_{ik}) \leq 0 \qquad \forall i,k \in \mathbf{P}, \tag{12s}$$

$$y_i - y_k' - D_m(1 - y_{ik}) \leq 1 \qquad \forall i,k \in \mathbf{P}, \tag{12t}$$

$$z_k' - z_i - D_m(1 - z_{ik}) \leq 0 \qquad \forall i,k \in \mathbf{P}, \tag{12u}$$

$$z_i - z_k' - D_m(1 - z_{ik}) \leq 1 \qquad \forall i,k \in \mathbf{P}, \tag{12v}$$

$$z_i + a_j x_i \geq b_j - M(1 - p_{ij}) \qquad \forall i,k \in \mathbf{P}, \tag{12w}$$

$$\sum_{l=1}^{4} \sum_{k \in \mathbf{P}} \beta_{ik}^l + 2\gamma_c - 4(1 - g_i) \geq 0 \qquad \forall i \in \mathbf{P}, \tag{12x}$$

$$z_i - (1 - g_i) D_m \leq 0 \qquad \forall i \in \mathbf{P}, \tag{12y}$$

$$z_k' - z_i - v_{ik} \leq 0 \qquad \forall i,k \in \mathbf{P}, \tag{12z}$$

$$z_i - z_k' - v_{ik} \leq 0 \qquad \forall i,k \in \mathbf{P}, \tag{12aa}$$

$$z_i - z_k' + v_{ik} - 2D_m(1 - m_{ik}) \leq 0 \qquad \forall i,k \in \mathbf{P}, \tag{12ab}$$

$$z_k' - z_i + v_{ik} - 2D_m m_{ik} \leq 0 \qquad \forall i,k \in \mathbf{P}, \tag{12ac}$$

$$h_{ik} - v_{ik} \leq 0 \qquad \forall i,k \in \mathbf{P}, \tag{12ad}$$

$$v_{ik} - D_m h_{ik} \leq 0, \qquad \forall i,k \in \mathbf{P}, \tag{12ae}$$

$$o_{ik} - x_{ik} - x_{ki} - y_{ik} - y_{ki} \leq 0, \qquad \forall i,k \in \mathbf{P}, \tag{12af}$$

$$2o_{ik} - x_{ik} - x_{ki} - y_{ik} - y_{ki} \geq 0, \qquad \forall i,k \in \mathbf{P}, \tag{12ag}$$

$$1 - o_{ik} - h_{ik} - s_{ik} \leq 0, \qquad \forall i,k \in \mathbf{P}, \tag{12ah}$$

$$h_{ik} + o_{ik} + 2(s_{ik} - 1) \leq 0, \qquad \forall i,k \in \mathbf{P}, \tag{12ai}$$

$$p_{ij} - p_{kj} + s_{ik} - 1 \leq 0, \qquad \forall i,k \in \mathbf{P}, \forall j \in \mathbf{N}, \tag{12aj}$$

$$p_{jk} - p_{ij} + s_{ik} - 1 \leq 0, \qquad \forall i,k \in \mathbf{P}, \forall j \in \mathbf{N}, \tag{12ak}$$

$$\beta_{ik}^l - s_{ik} \leq 0, \qquad \forall i,k \in \mathbf{P}, l = [1,2,3,4], \tag{12al}$$

$$n_{ik}^1 - n_{ik}^2 - 2(1 - \beta^1 ik) \leq 0, \qquad \forall i,k \in \mathbf{P}, \tag{12am}$$

$$n_{ik}^2 - n_{ik}^2 - 2(1 - \beta^2 ik) \leq 0, \qquad \forall i,k \in \mathbf{P}, \tag{12an}$$

$$n_{ik}^3 - n_{ik}^4 - 2(1 - \beta^3 ik) \leq 0, \qquad \forall i,k \in \mathbf{P}, \tag{12ao}$$

$$n^1_{ik} - n^4_{ik} - 2(1 - \beta^4 ik) \leq 0, \qquad \forall i, k \in \mathbf{P}, \qquad (12ap)$$

$$x_k - x_i - n^1_{ik} D_m \leq 0, \qquad \forall i, k \in \mathbf{P}, \qquad (12aq)$$

$$x'_k - x'_i - n^3_{ik} D_m \leq 0, \qquad \forall i, k \in \mathbf{P}, \qquad (12ar)$$

$$y_k - y_i - n^2_{ik} D_m \leq 0, \qquad \forall i, k \in \mathbf{P}, \qquad (12as)$$

$$y'_k - y'_i - n^4_{ik} D_m \leq 0 \qquad \forall i, k \in \mathbf{P}, \qquad (12at)$$

$$z_i + a_j x_i - b_j - (1 - p_{ij})M - (1 - \gamma_c)M \leq 0 \qquad \forall i \in \mathbf{P}, \forall j \in \mathbf{N}, \quad (12au)$$

$$p_{ij} + \gamma_c - a_j - b_j - 1 \leq 0 \qquad \forall i \in \mathbf{P}, \forall j \in \mathbf{N} \quad (12av)$$

Equation 12b ensures that a shipment is either loaded on a ULD or offloaded. Equation 12c-Equation 12e enforce that each side of shipment is aligned with a side of the ULD, whereas Equation 12f - Equation 12h define whether a shipment can be rotated in the corresponding axis. Equation 12i ensures that the weight capacity of the ULD is not exceeded. Equation 12j -Equation 12l define the position of the right vertex of the box, taking into account the uncertainty as captured by the mean and the total standard deviation of the corresponding dimension generated by the shipment dimensions forecasting model. Equation 12m-Equation 12o verify that the ULD boundaries are respected. Equation 12p - Equation 12v prevent overlap between two shipments in all of the three axis, when these shipments are placed within the same ULD. Equation 12w ensures that when a shipment is placed within an LD-3 container, it lies within the boundaries defined by the cut in the left-hand side of the ULD. This constraint can be dropped if there are no cuts in the considered containers or ULDs. Equation 12x verifies that all four vertices of a shipment are supported either by an underlying shipment or an underlying shipment and a ULD cut, if the shipment is not placed on the ULD's floor. Equation 12y defines that when $g_i = 1$,the shipment lies on the ULD's floor. Equation 12z-Equation 12ae define that a shipment k can support shipment i when the vertical position of shipment k equals the vertical position of shipment i. Moreover, shipment k can support shipment i, when the orthogonal projections of both shipments on the XY axis overlap, as defined by Equation 12af -Equation 12ai. Equation 12aj and Equation 12ak ensure that a shipment k can support shipment i if both shipments are placed within the same ULD. Equation 12al verifies that a shipment k supports one of the four vertices of shipment i only when shipment is is supported by shipment k. Equation 12am-Equation 12ap prevents loading of shipments on top of each other when either of the four vertices is not supported. Equation 12aq -Equation 12at force $n^l_{ik} = 0$, when there is overlap on the horizontal axis between shipments i and k, i.e., shipment i cannot be supported by shipment k. Finally Equation 12au and Equation 12av forces $\gamma_c = 1$, when shipment i is supported by ULD's cut.

C Booking Data

Booking No.	Part Shipments	Shipment Type No.	Pieces	L (cm)	W (cm)	H(cm)	Volume (m^3)	Weight (kg)	SC
001	001.1	1	19	125	115	100	1.437	229.3	30,008.25
	001.2	2	2	120	100	100	1.200	441.9	30,008.25
002	N/A	3	2	120	100	70	0.864	124.5	507.42
003	N/A	4	1	80	73	70	0.408	471	348.61
004	N/A	5	24	115	97	74	0.825	91.6	3,119.96
005	005.1	6	1	120	80	30	0.288	297.7	1,799.48
	005.2	7	1	157	99	91	1.414	1462.2	1,799.48
006	N/A	8	1	181	88	113	1.772	600	783.55
007	N/A	9	1	120	80	133	1.276	165	655.19
008	N/A	10	1	41	21	17	0.014	2	55.86
009	009.1	11	2	27	17	13	0.005	1.2	853.21
	009.2	12	1	46	23	34	0.035	7.4	853.21
	009.3	13	1	31	21	18	0.011	2.4	853.21
	009.4	14	2	120	80	87	0.835	172.3	853.21
	009.5	15	1	41	31	21	0.026	5.5	853.21
	009.6	16	4	163	33	33	0.177	36.6	853.21
010	N/A	17	3	52	42	23	0.050	5	106.54
011	N/A	18	3	40	40	40	0.895	425	1,637.8
012	N/A	19	1	120	80	26	0.249	140	187.34
013	N/A	20	5	40	40	40	0.684	100	1,748.67
014	N/A	21	7	40	40	40	0.085	15.57	184.91
015	N/A	22	5	40	40	40	0.478	150	1,398.51
016	N/A	23	2	40	40	40	0.645	150	901.96
017	N/A	24	2	40	40	40	0.46	120	399.4
018	018.1	25	1	134	105	77	1.083	280	321.16
	018.2	26	1	31	31	17	0.016	15	321.16
019	N/A	27	1	50	50	50	0.130	25	77.13
020	020.1	28	1	91	41	41	0.159	58	459.86
	020.2	29	1	230	25	18	0.103	39.3	459.86
	020.3	30	1	122	71	40	0.346	11.5	459.86
Total							**71.232**	**14,630.39**	**45,554.81**

Table 16: Booking data for the examined flight #1.

Booking No.	**Part Shipments**	**Shipment Type No.**	**Pieces**	**L** (cm)	**W** (cm)	**H**(cm)	**Volume** (m^3)	**Weight** (kg)	**SC**
001	001.1	1	1	120	80	59	0.566	295.4	1,568.85
	001.2	2	1	86	55	41	0.1939	101.1	1,568.85
	001.3	3	1	61	36	44	0.096	50.4	1,568.85
	001.4	4	1	45	38	34	0.058	30.3	1,568.65
	001.5	5	1	120	88	52	0.549	286.4	1,568.65
	001.6	6	1	85	55	50	0.233	121.9	1,568.65
	001.7	7	1	82	72	81	0.478	249.4	1,568.65
	001.8	8	1	86	62	56	0.298	155.7	1,568,65
002	N/A	9	7	103	75	73	0.574	295.5	1,287.92
003	N/A	10	1	200	100	100	2.000	398.5	480.07
004	N/A	11	17	113	88	84	0.834	386.7	2,542.14
005	005.1	12	2	120	100	110	1.320	225	892.37
	005.2	13	1	220	50	50	0.550	225	892.37
	005.3	14	1	190	70	70	0.930	225	892.37
006	N/A	15	1	178	102	158	2.868	522	730.69
007	007.1	16	7	120	80	160	1.536	189	2,351.87
	007.2	17	1	120	80	140	1.334	161	2,351.87
008	N/A	18	1	120	80	100	0.960	104	189.20
009	N/A	19	1	230	190	150	6.550	634	1,687.84
010	N/A	20	1	45	45	60	0.121	70	135.62
011	N/A	21	7	103	98	70	0.706	18.57	359.62
012	N/A	22	1	120	50	42	0.252	105	123.14
013	N/A	23	3	50	60	50	0.150	17.9	158.57
014	N/A	24	1	120	85	54	0.550	535	406.18
015	N/A	25	1	60	80	54	0.259	100	88.57
016	016.1	26	2	80	120	130	0.965	400	1,205.74
	016.2	27	2	80	65	130	0.676	310	1,205.74
017	N/A	28	8	40	40	40	0.650	500	1,407.15
018	N/A	29	1	300	34	25	0.255	24	135.48
019	N/A	30	1	102	42	42	0.180	62	158.61
020	N/A	31	1	20	25	20	0.011	25	98.58
021	N/A	32	4	40	40	40	1.100	900	1,140.50
022	N/A	33	4	40	40	40	0.575	231	581.20
023	N/A	34	1	60	40	60	0.144	100	204.88
024	N/A	35	4	150	130	67	0.920	10	581.02
025	N/A	36	1	70	31	54	0.117	32	93.93
Total							**72.651**	**25,199.2**	**18,413.13**

Table 17: Booking data for the examined flight # 2.

Booking No.	**Part Shipments**	**Shipment Type No.**	**Pieces**	**L** (cm)	**W** (cm)	**H**(cm)	**Volume** (m^3)	**Weight** (kg)	**SC**
001	N/A	1	2	120	100	90	1.080	544	1,449.80
002	N/A	2	1	78	53	51	0.210	138	276.68
003	003.1	3	1	153	65	75	0.745	467	32,639.00
	003.2	4	1	153	65	70	0.696	607	32,639.00
	003.3	5	10	153	65	70	0.696	127	32,639.00
004	N/A	6	1	122	102	71	0.883	350	671.76
005	N/A	7	1	135	110	60	0.891	200	189.44
006	006.1	8	1	120	80	73	0.710	256	288.01
	006.2	9	1	29	19	19	0.020	2	288.01
007	007.1	10	1	120	80	86	0.8256	188	60.52
	007.2	11	1	30	16	16	0.007	2	60.52
008	N/A	12	3	120	80	75	0.72	160	410.81
009	N/A	13	1	120	80	110	1.056	180	78.60
010	010.1	14	1	60	80	55	0.264	203	334.86
	010.2	15	1	120	80	55	0.528	203	334.86
	010.3	16	1	120	80	75	0.72	203	334.86
	010.4	17	1	36	36	20	0.025	56	334.86
011	N/A	18	1	120	80	46	0.441	163	218.76
012	N/A	19	1	120	85	80	0.816	122	492.94
013	013.1	20	1	35	28	11	0.017	1.628	114.92
	013.2	21	1	80	60	35	0.168	25.370	114.92
014	N/A	22	1	120	80	115	1.104	160	273.69
015	015.1	23	1	150	5	5	0.003	2.2	72.38
	015.2	24	1	32	22	16	0.011	6.6	72.38
	015.3	25	1	20	10	10	0.002	1.1	72.38
016	016.1	26	1	120	80	56	0.54	154	171.20
	016.2	27	1	80	120	35	0.5376	154	171.20
017	017.1	28	1	58	27	27	0.042	2	74.78
	017.2	29	1	40	40	20	0.032	9	74.78
018	N/A	30	1	52	53	24	0.066	17.5	67.22
019	N/A	31	1	250	120	85	2.550	570	650.98
020	020.1	32	4	127	85	105	1.133	25.2	719.17
	020.2	33	1	120	85	105	1.071	25.2	719.97
021	021.1	34	1	122	102	150	1.866	111	1,866.60
	021.2	35	1	122	102	113	1.679	96	1,866.60
	021.3	36	1	122	102	113	1.406	166	1,866.60
022	N/A	37	20	120	90	80	1.03	200	3388.3
023	N/A	38	4	30	30	25	0.022	6.5	390.44
024	N/A	39	2	40	40	40	0.800	128	390.44
025	N/A	40	5	40	40	40	0.576	91	530.30
026	026.1	41	1	39	29	11	0.020	2.8	65.05
	026.2	42	1	22	17	11	0.01	2.8	65.05
	026.3	43	1	19	17	17	0.01	2.8	65.05
	026.4	44	1	28	28	25	0.02	2.8	65.05
	026.5	45	1	39	24	21	0.02	2.8	65.05
	026.6	46	1	31	30	19	0.002	2.8	65.05
027	N/A	47	1	40	40	40	1.200	170	299.57
028	028.1	48	10	114	87	95	0.94	60	3,434.90
	028.2	49	1	91	61	85	0.47	18	3,434.90
029	N/A	50	18	114	81	75	0.69	600	6,179.50
Total							**89.49**	**17,153.2**	**55,182.34**

Table 18: Booking data for the examined flight # 3.

Booking No.	Part Shipments	Shipment Type No.	Pieces	L (cm)	W (cm)	H(cm)	Volume (m^3)	Weight (kg)	SC
001	001.1	1	2	120	80	130	1.248	294.3	1,023.00
	001.2	2	2	120	80	135	0.193	305.6	1,023.00
002	002.1	3	1	204	40	20	0.574	70	61.62
	002.2	4	1	81	71	59	0.339	58	61.62
	002.3	5	1	72	62	26	0.116	30	61.62
003	003.1	6	2	180	97	89	1.553	120.7	1,739.01
	003.1	7	1	173	102	99	1.746	135.6	1,739.01
	003.2	8	1	99	94	86	0.800	62.7	1,739.01
004	N/A	9	2	65	65	80	0.338	148	122.91
005	N/A	10	1	80	82	90	0.580	110	115.94
006	N/A	11	1	71	71	154	0.776	130	94.89
007	007.1	12	1	104	65	71	0.479	47	260.56
	007.2	13	1	80	75	68	0.408	88	260.56
	007.3	14	1	70	70	55	0.2695	222	260.56
	007.4	15	1	62	62	30	0.115	26	260.56
	007.3	16	1	60	40	53	0,1272	23	260.56
008	N/A	17	16	17	14	17	0.004	19.738	160.29
009	N/A	18	81	105	52	26	0.149	25	1,518.90
010	N/A	19	1	94	80	105	0.790	74	67.57
011	N/A	20	1	172	80	80	1.100	95	83.31
012	N/A	21	1	120	80	90	0.864	206	59.44
013	013.1	22	1	48	48	115	0.264	16	114.27
	013.1	23	3	47	40	43	0.0624	16	114.27
	013.2	24	1	65	44	37	0.105	16	114.27
014	N/A	25	1	122	102	94	1.160	104	242.33
015	N/A	26	1	120	80	123	1.180	366	269.93
016	016.1	27	1	280	60	80	1.344	280	266.29
	016.2	28	1	80	120	35	0.336	95	266.29
017	017.1	29	10	55	36	37	0.073	10	184.29
	017.2	30	2	60	41	35	0.086	30	184.29
018	N/A	31	6	80	40	30	0.096	70	103.23
019	N/A	32	6	80	40	30	0.096	87.5	179.79
020	020.1	33	3	138	92	91	1.155	105.3	805.95
	020.2	34	2	89	55	67	0.327	105.3	805.95
	020.3	35	2	74	51	51	0.192	105.3	805.95
	020.4	36	1	44	36	35	0.055	105.3	805.95
021	N/A	37	1	157	157	120	2.957	366	540.27
022	N/A	38	1	33	17	16	0.008	1	195.89
023	023.1	39	1	102	120	160	1.9584	500	1,146.32
	023.2	40	1	123	103	160	2.027	200	1,1464.32
024	N/A	41	1	120	80	75	0.720	196	121.14
025	025.1	42	1	145	38	51	0.281	27	128.69
	025.2	43	1	61	61	41	0.152	7	128.69
	025.3	44	1	36	36	20	0.025	152	128.69
026	N/A	45	1	120	80	112	1.075	393	81.93
027	N/A	46	1	120	50	42	1.492	68	165.63
028	028.1	47	1	71	56	53	0.210	121	214.9
	028.1	48	1	71	56	53	0.210	100	214.9
029	N/A	49	1	201	28	20	0.112	329	98.84
030	N/A	50	1	173	64	48	0.531	1	161.45
031	N/A	51	1	33	17	16	0.008	430.5	199.53
032	N/A	52	6	221	122	86	2.318	287	2,930.33
033	N/A	53	2	150	100	100	1.5	1	346.59
034	N/A	54	1	33	17	16	0.008	1	234.45
035	N/A	55	1	33	17	16	0.008	1	192.77
036	N/A	56	1	33	17	16	0.008	1	185.90
037	N/A	57	1	33	17	16	0.008	25	244.22
038	N/A	58	1	60	60	106	0.31	1	147.44
039	N/A	59	1	33	17	16	0.008	1	244.22
040	N/A	60	1	33	17	16	0.008	1	244.22
041	N/A	61	1	33	17	16	0.008	1	234.45
042	N/A	62	1	33	17	16	0.008	1	234.45
043	N/A	63	1	100	100	116	1.16	260	228.61
Total							**70.48**	**14,239.71**	**15,834.80**

Table 19: Booking data for the examined flight # 4.

D Results of the shipment dimensions forecasting model

Booking No.	**Part Shipments**	**Shipment Type No.**	$\bar{\mathbf{l}}_\mathbf{i}$ (cm)	$\bar{\mathbf{w}}_\mathbf{i}$ (cm)	$\bar{\mathbf{h}}_\mathbf{i}$ (cm)	$\sigma_{\mathbf{l_i}}$ (cm)	$\sigma_{\mathbf{w_i}}$ (cm)	$\sigma_{\mathbf{h_i}}$ (cm)
001	001.1	1	124.033	110.214	102.975	16.481	11.361	14.652
	001.2	2	116.641	108.457	94.515	16.399	11.445	14.887
002	N/A	3	121.277	90.699	76.374	16.331	11.168	14.485
003	N/A	4	98.140	67.475	66.965	17.615	11.481	15.888
004	N/A	5	118.476	95.274	74.853	16.310	11.244	14.439
005	005.1	6	102.756	69.141	43.839	19.786	11.854	15.290
	005.2	7	140.221	117.842	83.854	16.613	11.336	14.613
006	N/A	8	127.063	100.389	122.990	16.561	11.459	17.086
007	N/A	9	132.867	115.964	90.120	16.762	11.442	14.674
008	N/A	10	34.520	26.166	18.666	16.393	10.995	14.221
009	009.1	11	25.530	19.857	13.961	16.477	11.513	14.314
	009.2	12	42.929	33.176	25.399	16.360	10.889	14.171
	009.3	13	30.116	23.668	17.765	16.426	11.049	14.229
	009.4	14	115.964	96.478	70.637	16.444	12.154	14.837
	009.5	15	39.207	30.378	22.801	16.335	10.918	14.186
	009.6	16	92.997	58.208	42.951	16.358	10.975	14.257
010	N/A	17	50.700	36.180	30.295	16.424	10.908	14.144
011	N/A	18	119.200	80.104	71.879	16.328	10.944	14.272
012	N/A	19	78.581	59.125	33.723	16.223	10.865	14.258
013	N/A	20	88.306	68.906	54.695	16.649	11.195	14.407
014	N/A	21	55.476	41.383	36.035	16.212	10.838	14.082
015	N/A	22	110.727	79.858	49.732	16.569	11.024	14.531
016	N/A	23	117.549	80.520	52.538	16.396	10.951	14.373
017	N/A	24	116.638	80.598	49.273	16.436	10.991	10.476
018	018.1	25	119.128	80.127	68.485	16.313	10.990	14.650
	018.2	26	35.307	27.164	18.919	16.360	10.960	14.204
019	N/A	27	67.663	49.031	42.301	16.365	10.972	14.138
020	020.1	28	67.470	54.145	40.167	16.296	11.000	14.190
	020.2	29	158.854	45.446	37.513	16.207	10.913	14.091
	020.3	30	101.227	72.164	50.292	16.439	11.190	14.285

Table 20: Predicted Dimensions for the examined flight #1.

Booking No.	**Part Shipments**	**Shipment Type No.**	$\bar{\mathbf{l}}_\mathbf{i}$ (cm)	$\bar{\mathbf{w}}_\mathbf{i}$ (cm)	$\bar{\mathbf{h}}_\mathbf{i}$ (cm)	$\sigma_{\mathbf{l_i}}$ (cm)	$\sigma_{\mathbf{w_i}}$ (cm)	$\sigma_{\mathbf{h_i}}$ (cm)
001	001.1	1	119.690	80.734	59.060	16.488	10.954	14.080
	001.2	2	77.653	60.035	42.636	16.380	10.915	14.021
	001.3	3	57.919	44.403	38.383	16.350	10.862	13.805
	001.4	4	48.033	38.039	31.962	16.386	10.823	13.821
	001.5	5	119.541	80.759	57.456	16.498	10.952	14.070
	001.6	6	78.639	60.248	47.542	16.361	10.879	13.917
	001.7	7	98.809	80.603	71.900	16.518	10.970	14.156
	001.8	8	81.422	62.391	54.778	16.371	10.980	13.867
002	N/A	9	121.558	81.181	55.697	16.734	11.059	14.191
003	N/A	10	164.486	119.796	97.683	17.034	11.387	14.225
004	N/A	11	119.939	87.225	78.587	16.443	11.113	13.972
005	005.1	12	138.302	98.906	94.229	18.340	13.170	20.429
	005.2	13	116.335	77.234	62.559	16.517	11.000	14.320
	005.3	14	120.969	82.219	89.580	16.476	11.132	14.321
006	N/A	15	186.674	128.061	111.868	19.009	12.723	14.899
007	007.1	16	146.741	119.202	87.309	17.044	11.374	14.769
	007.2	17	138.709	118.773	81.158	16.664	11.398	14.281
008	N/A	18	119.675	101.340	78.997	16.443	11.352	14.009
009	N/A	19	233.480	172.138	153.924	23.674	15.930	17.466
010	N/A	20	65.661	46.778	37.371	16.455	10.956	13.856
011	N/A	21	118.055	95.955	64.398	16.469	11.422	14.215
012	N/A	22	80.790	58.228	50.493	16.359	10.855	13.942
013	N/A	23	64.013	46.086	40.801	16.356	10.848	13.814
014	N/A	24	81.932	118.947	53.372	16.556	11.009	14.164
015	N/A	25	79.669	60.893	50.012	16.365	10.918	13.895
016	016.1	26	81.483	120.149	96.513	16.454	10.969	14.205
	016.2	27	119.055	80.000	71.217	16.449	10.918	14.034
017	N/A	28	116.470	81.342	63.712	16.473	11.066	14.140
018	N/A	29	81.458	58.661	48.478	16.386	10.878	13.997
019	N/A	30	83.229	54.580	38.325	16.766	10.977	14.032
020	N/A	31	28.158	23.095	16.570	16.591	11.100	14.046
021	N/A	32	119.820	80.473	108.503	16.438	10.958	14.282
022	N/A	33	120.142	80.709	59.403	16.483	10.951	14.139
023	N/A	34	66.933	48.715	42.296	16.628	11.179	13.951
024	N/A	35	77.988	60.640	45.301	16.390	10.913	13.952
025	N/A	36	62.895	43.765	39.564	16.403	10.841	13.908

Table 21: Predicted dimensions for the examined flight # 2.

Booking No.	**Part Shipments**	**Shipment Type No.**	$\bar{\mathbf{l}}_\mathbf{i}$ (cm)	$\bar{\mathbf{w}}_\mathbf{i}$ (cm)	$\bar{\mathbf{h}}_\mathbf{i}$ (cm)	$\sigma_{\mathbf{l_i}}$ (cm)	$\sigma_{\mathbf{w_i}}$ (cm)	$\sigma_{\mathbf{h_i}}$ (cm)
001	N/A	1	119.865	81.102	108.295	16.445	11.089	14.398
002	N/A	2	80.397	52.908	50.565	17.196	11.203	14.287
003	003.1	3	141.228	92.217	58.368	18.066	13.271	16.180
	003.2	4	139.757	92.106	55.728	19.716	13.253	15.886
	003.3	5	138.952	91.320	56.472	18.007	13.423	16.071
004	N/A	6	110.878	96.254	71.301	16.742	11.652	14.264
005	N/A	7	119.328	82.149	84.647	16.445	11.053	14.357
006	006.1	8	119.799	80.147	73.679	16.445	10.917	14.027
	006.2	9	34.539	28.114	20.138	16.472	10.926	13.914
007	007.1	10	119.255	80.066	82.920	16.447	10.933	14.051
	007.2	11	28.120	19.338	14.030	16.535	11.117	13.989
008	N/A	12	118.758	80.756	74.394	16.455	10.944	14.038
009	N/A	13	119.897	80.512	105.753	16.441	10.977	14.278
010	010.1	14	80.391	58.521	53.611	16.364	10.854	13.925
	010.2	15	119.792	79.547	56.850	16.481	10.634	14.203
	010.3	16	119.356	79.957	74.239	16.451	10.919	14.017
	010.4	17	39.950	30.083	21.319	16.445	10.949	13.914
011	N/A	18	114.535	76.869	52.682	16.533	10.655	14.276
012	N/A	19	119.556	84.442	77.796	16.441	11.094	13.976
013	013.1	20	26.964	22.545	16.756	16.556	11.025	13.959
	013.2	21	71.690	56.462	42.965	16.403	10.917	13.928
014	N/A	22	119.715	80.551	108.905	16.434	10.977	14.310
015	015.1	23	19.451	18.424	11.600	16.715	11.227	14.158
	015.2	24	28.252	24.926	17.565	16.563	11.077	13.989
	015.3	25	17.097	16.632	9.994	16.818	11.340	14.235
016	016.1	26	119.317	80.027	58.462	16.480	10.939	14.227
	016.2	27	119.391	80.029	58.192	16.466	10.927	14.181
017	017.1	28	45.391	33.959	28.381	16.457	10.860	13.956
	017.2	29	40.907	31.113	25.696	16.447	10.887	13.903
018	N/A	30	54.124	37.199	33.500	16.461	10.871	13.964
019	N/A	31	195.210	112.689	109.864	18.079	11.541	16.602
020	020.1	32	121.626	89.311	95.557	16.471	12.045	16.003
	020.2	33	121.186	87.426	90.280	16.444	11.639	15.597
021	021.1	34	121.566	101.273	144.308	16.642	11.241	15.222
	021.2	35	119.614	98.335	136.057	16.504	11.252	14.772
	021.3	36	119.129	82.622	136.647	16.450	11.344	15.002
022	N/A	37	120.274	88.927	75.860	16.454	12.165	14.218
023	N/A	38	35.724	21.198	20.958	16.468	10.927	13.915
024	N/A	39	101.753	83.231	77.546	16.453	11.120	14.018
025	N/A	40	94.635	79.945	60.383	16.582	10.938	13.988
026	026.1	41	34.143	27.230	21.372	16.461	10.929	13.893
	026.2	42	26.779	22.085	16.873	16.526	11.007	13.940
	026.3	43	26.837	22.165	16.996	16.551	11.002	13.947
	026.4	44	34.123	27.249	21.426	16.449	10.996	13.791
	026.5	45	34.117	27.209	21.384	16.464	10.930	13.893
	026.6	46	34.150	27.271	21.360	16.454	10.923	13.889
027	N/A	47	122.915	95.386	81.295	16.504	11.278	14.154
028	028.1	48	118.444	83.159	91.781	16.471	11.089	14.414
	028.2	49	91.968	68.875	65.648	17.047	11.268	14.368
029	N/A	50	113.582	79.650	72.981	16.526	10.953	14.053

Table 22: Predicted dimensions for the examined flight # 3.

Booking	**Part**	**Shipment**	$\bar{\mathbf{l}}_\mathbf{i}$ (cm)	$\bar{\mathbf{w}}_\mathbf{i}$ (cm)	$\bar{\mathbf{h}}_\mathbf{i}$ (cm)	$\sigma_{\mathbf{l_i}}$ (cm)	$\sigma_{\mathbf{w_i}}$ (cm)	$\sigma_{\mathbf{h_i}}$ (cm)
001	001.1	1	131.446	119.031	81.583	16.625	11.482	14.360
	001.2	2	138.164	118.845	81.400	16.679	11.475	14.300
002	002.1	3	69.599	50.391	41.921	16.545	11.097	13.986
	002.2	4	88.084	64.451	58.215	17.161	11.413	14.433
	002.3	5	59.838	42.122	40.283	16.368	10.852	13.864
003	003.1	6	131.882	115.967	98.985	16.609	11.293	14.158
	003.1	7	142.474	117.996	100.529	16.674	11.312	14.160
	003.2	8	110.616	97.238	68.043	16.444	11.165	14.082
004	N/A	9	75.325	80.309	38.582	16.631	11.033	14.362
005	N/A	10	119.622	79.714	62.027	16.476	10.966	14.026
006	N/A	11	119.598	79.878	79.726	16.448	10.934	14.046
007	007.1	12	118.305	79.241	52.540	16.488	10.946	14.252
	007.2	13	105.189	73.082	54.894	17.090	11.262	14.744
	007.3	14	90.799	61.081	51.078	16.823	10.918	14.123
	007.4	15	64.795	42.746	40.044	16.852	10.945	13.953
	007.3	16	68.695	46.325	40.709	17.099	11.255	14.190
008	N/A	17	22.957	18.283	10.408	16.637	11.144	14.147
009	N/A	18	105.921	52.647	26.502	17.121	11.112	14.098
010	N/A	19	109.152	84.282	75.916	16.449	11.170	13.994
011	N/A	20	119.448	87.430	101.906	16.443	11.555	14.199
012	N/A	21	119.532	80.492	87.541	16.455	10.986	14.143
013	013.1	22	100.729	61.098	44.931	16.932	11.099	14.106
	013.1	23	57.486	38.199	29.851	16.788	10.842	13.835
	013.2	24	65.138	45.707	36.059	16.609	10.846	13.829
014	N/A	25	119.414	106.220	91.059	16.462	11.340	14.426
015	N/A	26	119.837	80.653	116.479	16.438	10.990	14.276
016	016.1	27	119.147	80.311	136.098	16.448	11.053	14.662
	016.2	28	81.053	60.037	72.997	16.646	11.069	14.587
017	017.1	29	56.245	39.418	33.532	16.356	10.822	13.869
	017.2	30	58.160	39.911	37.048	16.358	10.829	13.849
018	N/A	31	56.232	40.797	41.507	16.403	10.843	13.936
019	N/A	32	56.204	40.863	41.446	16.407	10.843	13.935
020	020.1	33	122.397	114.944	81.842	16.489	11.350	14.210
	020.2	34	91.913	66.113	54.704	16.697	11.322	14.034
	020.3	35	75.734	757.299	44.625	16.383	10.879	13.914
	020.4	36	49.040	37.535	30.644	16.397	10.839	13.822
021	N/A	37	153.449	119.053	153.486	17.908	11.686	16.931
022	N/A	38	30.032	17.693	16.795	16.527	11.235	13.971
023	023.1	39	154.528	119.691	102.346	16.709	11.323	14.264
	023.2	40	158.239	120.584	102.869	16.774	11.309	14.241
024	N/A	41	119.599	79.755	74.305	16.488	10.931	14.045
025	025.1	42	89.429	63.836	50.469	16.527	11.048	13.941
	025.2	43	66.702	49.777	42.727	16.675	11.129	13.929
	025.3	44	38.614	21.109	23.776	16.460	10.927	13.890
026	N/A	45	119.505	99.421	92.391	16.458	11.372	14.342
027	N/A	46	120.728	100.408	121.020	16.462	11.187	14.497
028	028.1	47	74.652	58.412	52.675	16.447	11.221	14.039
	028.1	48	74.700	58.378	52.538	16.437	11.231	14.042
029	N/A	49	62.481	40.816	40.936	16.483	10.992	13.891
030	N/A	50	108.049	79.340	60.628	16.587	10.974	14.134
031	N/A	51	30.074	17.823	16.847	16.530	11.235	13.962
032	N/A	52	210.646	115.602	89.791	21.376	12.280	15.210
033	N/A	53	99.047	119.264	129.936	16.971	11.335	14.270
034	N/A	54	29.969	17.660	16.723	16.534	11.231	13.971
035	N/A	55	30.015	17.707	16.846	16.527	11.200	13.967
036	N/A	56	30.051	17.795	16.832	16.526	11.232	13.955
037	N/A	57	29.964	17.582	16.748	16.524	11.221	13.946

038	N/A	58	83.235	63.571	56.306	16.548	11.017	13.919
039	N/A	59	30.124	17.848	16.862	16.527	11.226	13.965
040	N/A	60	30.097	17.748	16.804	16.522	11.208	13.957
041	N/A	61	30.235	17.810	16.961	16.519	11.206	13.951
042	N/A	62	29.986	17.721	16.749	16.525	11.219	13.965
043	N/A	63	121.082	101.851	90.846	16.449	11.139	14.175

Table 23: Predicted dimensions for the examined flight # 4.

II

Literature Study
previously graded under AE4020

1 Introduction

1.1. Background

During the recent years, with the advent of globalization, a significant development of the international air trade was experienced. Goods transported by air correspond to 35% of global trade by value, equating to a value of US$ 5.5 trillion and annual revenues of US$ 50 billions for IATA members [57]. As a consequence, air cargo generates substantial revenues for airlines.

Nevertheless, the lasting international trade tension between U.S. and China, as well as the uncertainty of a Brexit impact in the European trade, has caused cargo yields to move broadly sideways for the first quarter of 2019, while the industry expect yields to decrease further in the upcoming months [58]. Moreover, the huge structural overcapacity and the fierce competition in the air cargo market, result in low average load factors, leading many airlines to face constant drops in yields and profits.

In the light of this highly dynamic economic environment, airlines are challenged, perhaps more than ever, to efficiently handle air cargo operations through the development of strategic operation plans that capture the varying market demand and aim at increasing efficiency. In fact, the decision of selling the right capacity at the right customer at the right time is considered to be of key importance towards this end. This decision constitutes the essence of air cargo Revenue Management (RM) department, which is oriented around the optimal management of available capacity to generate the maximum revenue.

To achieve this goal, the air cargo RM integrates several disciplines such as forecasting, capacity plan and allocation, pricing, overbooking, and accept-or-reject policies [38, 116]. Forecasting, which can be regarded as the cornerstone of RM, focuses on predicting the booking requests, in terms of weight and volume, that can be potentially received during the booking period. Based on the results of the forecasting phase, in the capacity allocation stage, the available capacity is split into capacity dedicated for long-term contracts (allotments), capacity for passenger baggage (in case of passenger or combi aircraft) and capacity that is available for sale during the booking period. In parallel, the assignment of bookings to Unit Load Devices (ULDs) and how items will be arranged into ULDs is planned. According to capacity available for sale and the profitability of the shipment, the corresponding prices are set. To compensate for no-shows or short-term cancellations, the overbooking capacity is estimated, which involves accepting more bookings that can be physically loaded in the aircraft. Finally, the decision has to be made whether the incoming request will be accepted or rejected.

However, even though most modern airlines have highly sophisticated passenger revenue systems, the implementation of the aforementioned cargo Revenue Management tools is still in its infancy [106]. This is mostly due to the fact that the air cargo supply chain possesses more complex industry characteristics than passenger systems [60]. One fundamental difference is the fact that, while a passenger seat is a one-dimensional problem, in the case of cargo there is substantial variability due to volume, weight and shape of the shipment. Hence, air cargo can be considered a multi-dimensional problem. In addition, when considering passenger or combi aircraft for cargo transport, available cargo capacity is not fixed but stochastic, as it depends on several factors such as payload, belly space and the expected passenger baggage to accommodate in the specific flight.

What makes things even harder is the fact that shippers are not required to provide the exact shipment dimensions in advance, but only the volume of the booking. Hence, the true shipment dimensions are not known when operational planning is performed, but their realized values are learned shortly before the cargo shipment is loaded into the aircraft. This can further complicate the ULD loading strategy. For example, consider that case of a shipment with volume of $2m^3$, which could be represented by i) $1 \times 1 \times 2$m or ii) $0.5 \times 2 \times 2$m. The difference in the two shapes can severely impact the assignment of the specific booking in the ULD.

The simultaneous presence of all the aforementioned factors introduce a source of great uncertainty in the decision-making process of accepting or rejecting incoming bookings. Due to this uncertainty, there is either the risk of accepting bookings that cannot be loaded onto the aircraft, resulting in offloading and rerouting of cargo, or the risk of declining bookings that fit onto the aircraft, resulting in low average load factors. Both cases lead to profit loss for the airline.

1.2. Problem Statement

For the reasons outlined above, uncertainty of capacity and actual shipment dimensions makes decision-making in the air cargo domain rather complex and can have huge impact on the airline revenues. As stated previously, the majority of airlines have developed sophisticated business models for load forecasting and optimization. However, most forecasting techniques restrict themselves to nominal values by using metrics such as mean and standard deviation of simulation runs [48]. Consequently, revenue management teams focus mainly on the optimization of these expected values.

Generally, these methods rely on the assumption that the decision process is risk neutral. Nevertheless, human decision makers, especially those operating in revenue management teams, tend to seriously take into account the risks involved with every alternative. In fact, they attempt to balance the trade-off between profits and risks in order to prevent large losses. In other words, they prefer less risky decisions instead of risk neutral, especially when economic survival is determined by those decisions, i.e., they tend to adopt a *risk-averse* attitude [68].

Thus, maximizing the expected revenue or the number of shipments loaded is not the only concern of a revenue manager. He/she must also be able to control the impact or the variability of the losses [55]. In the light of this, the use of nominal values as basis for optimization is not justified. For example, standard deviation captures only the accuracy of the outcome with respect to the mean and does not reflect the revenue or the loading strategy outcome variability over a single simulation run.

Therefore, it can be suggested that there is a necessity for a model that provides a link between risk management and the decision-making process. Towards this end, it is essential that the forecasting model is not only restricted to predict shipment dimensions that are close to the actual values, but also includes a probability distribution, representing the uncertainty of the future values. Accordingly, this probability distribution should be integrated into the palletization model in the form of probabilistic (chance) constraints. The resulting chance-constrained model, would not have the the goal to find a palletization strategy that conforms to all possible outcomes, but instead, enforces that the probability of the palletization model to be implemented in practice is at least $1-\epsilon$, where $0 < \epsilon < 1$ is a risk rate defined by the user, in our case the revenue manager. This risk rate is introduced to show how the revenue manager can control the impact of prediction uncertainty in the resulting loading strategy.

1.3. Research Objective and Context

Goal of this research is to develop a model that incorporates in the air cargo decision-making process the risks associated with forecasting uncertainty. To pursue this goal, risk-averse metrics will be implemented into a palletization optimization framework. Therefore, the research objective can be defined as follows :

'Maximize the amount of loaded shipments by contributing to the development of a combined forecasting and risk-averse palletization model that would tackle the uncertainty of the forecast

The research objective can provide the guidelines for the desired key functionalities of the developed model, which can be summarized as follows :

- Forecast the available aircraft capacity and shipment dimensions while, simultaneously, generate the probability distribution regarding the uncertainty of predicted values.
- Using the results of the forecasting phase as input, implement a risk-averse loading strategy, such that the maximum number of shipments is loaded on the aircraft and the risk of this loading strategy not implemented is minimized.
- Explore different ULD configurations and propose a ULD re-configuration, if advantageous.

This study will be conducted in collaboration with Air France KLM Martinair Cargo (AFKLMP). The AFKLMP is part of Air France KLM Group and is specialized in managing air cargo operations, serving a network extended across 457 destinations around the world through Its two main hubs, Paris Charles De Gaulle Airport and Amsterdam Airport Schiphol.

AFKLMP is operating three types of aircraft to transport cargo, namely passenger, full freighter and combi aircraft. Full freighter aircraft, are dedicated to cargo transportation and they have the advantage of a fixed and very large capacity. On the other hand, in passenger aircraft, passengers are assigned the highest priority in terms of capacity, whereas cargo, is assigned the lowest priority behind fuel, crew and passenger bags. Their cargo capacity is significantly limited with respect to full freighter aircraft and is stochastic in nature, since it depends on the passenger bags. Nevertheless, these aircraft allow for greater flexibility and destination coverage, since they use the infrastructure of airlines' passenger network in terms of flight frequencies and destinations. Finally combi aircrafts, as their name suggests, are a combination of passenger and freighter aircrafts, meaning that still passenger bags have priority, but there is also more dedicated space for carrying cargo.

The context of this research is centered around Air France KLM Martinair Cargo (AFKLMP) passenger and combi aircraft and will therefore use the airlines' historic data for these type of aircraft to construct, test and finally validate the model. Nevertheless, the goal of this research is to provide a risk-averse cargo planning tool that can be used by revenue management departments of other airlines, as well as other industries, such as the shipping or rail industry.

1.4. Research Questions

The research goal along with the desired functionalities of the developed model can help us formulate the main research question. The main research question that needs to be addressed is the following :

How does an approach integrating forecasting uncertainty into a risk-averse palletization model can lead to improvements in airlines' revenue?

The main research question can be divided into several sub-questions that segment the overall research into different sequential steps. The research subquestions are as follows :

1. What methods can be used to forecast the available aircraft capacity?
    - What is the accuracy of the forecasted capacity?
    - What is the uncertainty related to this prediction?
2. What methods can be used to forecast the shipment dimensions?
    - What is the accuracy of the forecasted shipment dimensions?
    - What is the uncertainty related to this prediction?
3. How to optimally palletize shipments into ULDs in order to maximize a specific cost function?
4. What risk-averse modelling approaches can be combined with a palletization model?
    - What is the risk imposed to the loading strategy when deciding to accept a new shipment?
5. What is the ULD configuration that maximizes the specified cost function?
    - What is the number of ULD that should be used?

- What is the type of ULDs that should be used?

The aforementioned research questions can be grouped into two broader categories that will help define and segment the context for the literature study. More specifically, to answer RQ1 and RQ2 a study and evaluation of forecasting methods is required, whereas for RQ3-RQ5 the answers lie in the domain of Packing Models and Risk-Averse approaches. As such, the following literature study should be oriented around two key concepts:

- Analysis and evaluation of forecasting methods in the domain of revenue management
- Analysis and evaluation of risk-averse palletization models, which fall under the broader category of Packing Problems, as will be discussed in Chapter 2.

1.5. Report Structure

The remainder of this report is organized as follows. Chapter 2 provides an overview of the Air Cargo Loading Problem, and the related literature in order to shed light in the existing gaps this research will try to address. Chapter 3 provides an overview and critical analysis of forecasting models that are applicable to the predefined research questions. Chapter 4 provides a detailed insight into Packing Models, along with risk-averse approaches applied to decision-making processes and how these can be integrated into Bin Packing models.

2

Air cargo Load Planning Problem

In this section a basic introduction to the aspects of the air cargo load planning problem faced by the airlines will be provided, along with the technical terms that the reader should be familiar with. This would help us further clarify the scope and the contribution of this research to the field of air cargo revenue management. The analysis performed is partly driven by [18], which, to our knowledge, is the only consolidated approach of the air cargo loading planning problem and thus can provide the required theoretical grounds upon which we can start building our research. It is noted that this section will not focus on a specific airline, but will treat the air cargo problem from a more generic perspective. For the AFKLMP specific air cargo revenue management processes, we refer readers to [63].

2.1. Air cargo supply chain

The general workflow of an air cargo supply chain is presented in Fig. 2.1. The shipper is the entity from where the product flow originates. The product sold by the shipper must be delivered to the final customer or the consignee. This can be performed through two different supply chain concepts as depicted in Fig. 2.1. According to the concept depicted in the upper part, the forwarder is responsible for picking up the product from the shipper and booking the required capacity for the air transport. Next, the airline, either relying on a freighter or on a combination carrier, transports the product to the final destination. When the product arrives at the destination airport, the forwarder picks it up and delivers it to the final costumer. It is noted that this supply chain concept involves other stakeholders as well, such as handling operators, airport operators, or truck operators, which, for the purposes of this research, are not taken into account.

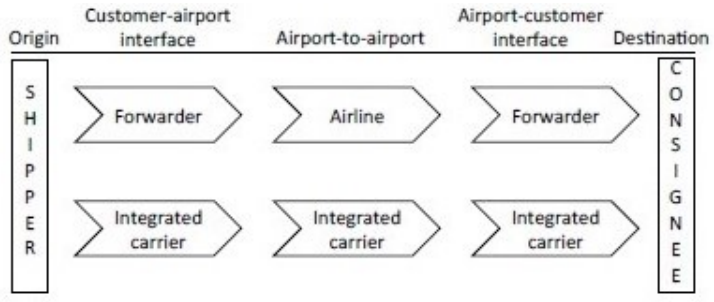

Figure 2.1: Air cargo supply chain [82]

A different supply chain concept is depicted in the lower part of Fig. 2.1, where only one integrated carrier exists. As its name suggests, an integrated carrier integrates the whole workflow of forwarder and airline and provides a door-to-door service from shippers to customers [82]. Examples of integrated carriers are DHL and FedEX. Nevertheless, as it has previously discussed, this study would be oriented around AFKLMP, meaning that the first supply chain concept is more relevant to this study, and more specifically, to the airline entity.

2.2. General characteristics of air cargo

Air freight is the most expensive mode used for goods transportation, and as such it is used for transportation of products that need fast and safe delivery. Usually, air transported goods fall under the following categories [18] :

- **Urgent** : Goods that need to be at a specific destination in a very short time. Typical examples are live animals or spare parts, that prevent production line stop at factories.
- **Perishable** : Goods that have a short economic lifecycle or need to be in a controlled environment in order not to lose their value. Typical examples include flowers, pharmaceutical products or fresh food. These items, especially those with a short economic lifecycle, will be treated in this research under the broader category of **must-fly** cargo.
- **Valuable** : Goods of high value, such as jewellery, banknotes or high-tech equipment, that need to be transported in a secure manner.
- **Dangerous** : Goods that potentially can harm the environment if not properly handled, such as radioactive material.

2.3. Air cargo packing and loading

To transport the aforementioned categories of goods, special containers or pallets covered with nets are used. These assemblies are generally called *Unit Load Devices* (ULDs), and they provide a standardized and fast way of loading passenger baggage or cargo [70]. These ULDs come into different shapes and sizes, some of which are shown in Fig. 2.2. For large shipments, pallets are assigned a highest preference, since they have an adjustable contour and thus they can be loaded easier in comparison with containers, where their contour is fixed. In any case, though, they have to be covered with nets and straps. Containers, on the other side, are most suitable for items of smaller size and passenger baggage and usually do not have to be covered with nets or straps.

Each ULD is loaded into a predefined special position on the aircraft equipped with latches and rollers. This means that ULDs cannot be placed in any position in the aircraft compartment, but rather, there are specific positions dedicated to a specific type of ULD. Each aircraft compartment has a number of distinct position slots.As a consequence, based on the number and the types of ULDs, different ULD configurations can be implemented [104]. These different configurations are subject to loading restrictions, which are more commonly referred as *weight and balance*. Weight and balance objective is to determine the loading configuration so that the Center of Gravity (CG) of the aircraft remains as close as possible to the position dictated by fuel and safety requirements [70].

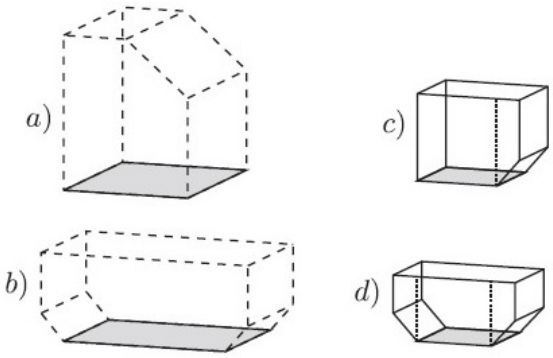

Figure 2.2: Different ULD Types [18]

2.4. Air cargo load planning

According to [18], for an airline to address the air cargo load planning problem, four type of decisions have to be taken:

1. **How many** and **what type** of ULDs should be loaded?
2. **When** should the ULDs be prepared for loading?
3. **How** to assign items inside the ULDs?
4. **How** to arrange the ULDs inside the aircraft?

Below, the parameters and complexities of each type of decision are analyzed, as well as the involved stakeholders, in order to assess how and whether these decisions are connected to the research goal and questions set in the previous chapter.

2.4.1. Number and type of ULDs to be loaded

This decision is the primary objective of the airlines' cargo revenue management department. It actually combines two nested problems. The outer problem is that of forecasting the available cargo capacity, in terms of weight and volume, as well as forecasting the must-fly cargo. The inner problem is a packing problem, i.e.,based on the results of the forecasting phase, the optimal configuration of ULDs, involving the number and type ULDs that fit into the aircraft, for each flight leg, needs to be determined. In any case, to fully solve this packing problem, the results from the palletization phase (subsection 2.4.3) need to be taken into account. The following Fig. 2.3 demonstrates several ULD configurations in the aircraft compartment. Both of the aforementioned problems will be addressed in RQ1, RQ2 and RQ5 of this study.

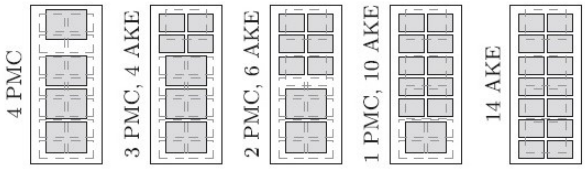

Figure 2.3: Several ULD configurations in an aircraft compartment [18]

Usually the type and number of ULDs are chosen so that the maximum available capacity is utilized and the maximum number of goods is loaded. In some cases, the required manpower and the handling efforts are taken into account [114], but these factors are beyond the scope of this research. Moreover, in real operations, this packing problem has to be run in parallel for all flight legs, while this specific research will focus on single flight legs.

Although both the forecasting and the packing problem are interrelated in the revenue management decision process, to our knowledge, there is no unified approach in the academic literature. In fact, they are treated as separate problems. Regarding the related literature on forecasting the available cargo capacity, the majority is focusing on overbooking, which is a widely used technique by the airlines to compensate for the risks of no-shows or cancellations. For this particular component of revenue management decision process, some useful insights are provided by [4, 93, 103]. Nevertheless, in this study the overbooking practice will not be considered. Instead, the available cargo capacity and the must-fly cargo volume will be forecasted using historical bookings data of AFKLMP by using one of the forecasting models that would be discussed in chapter 3. Moreover, the uncertainty related to this prediction will be addressed in terms of risk metrics applied to the subsequent packing phase.

With respect to the packing phase, i.e., selecting the number and the type of ULDs to be loaded on the aircraft, the majority of literature is oriented around selecting the appropriate ULD configuration in combination with weight and balance restrictions. This means that this decision usually is interrelated with the

decision of how to arrange the ULDs inside the aircraft. For example, [85] considers aircraft loading as two-dimensional bin packing problem and develops an advanced tabu search heuristic to assign ULDs into loading positions of military aircraft, while respecting weight and balance constraints. In [83], the optimization of aircraft container loading is addressed through the development of an off-the-shelf Mixed Integer Linear Programming (MILP) model, which maximizes the mass of products loaded into the aircraft, while balancing the load to satisfy weight and balance requirements. A similar model is proposed by [70], but instead of trying to minimize the deviation from the CG of the aircraft, the moment of inertia is minimized.

However, since this study focuses on the revenue management dimension, the objective of packing ULDs into the aircraft compartment and the alternative ULD configurations will be examined under the aspect of maximizing the number of the shipments loaded without taking into account any weight and balance restrictions.

2.4.2. Scheduling of ULD preparation

Scheduling of the ULD preparation for loading on the aircraft is one of the main objective of the handling department in the cargo terminal. It ensures that the ULDs are prepared in a timely manner before the departure of the aircraft. It also involves decisions on the manpower planning and scheduling, in order to smooth the workload throughout a day of operations and, at the same time, meet tight deadlines [38]. This component of the air cargo load planning problem is beyond the scope of this research.

2.4.3. Palletization of items inside the ULDs

The decision of how to assign shipments inside the ULD is one of the most prominent phases of air cargo load planning problem and one of the most challenging tasks of the revenue management department, since as discussed in chapter 1, shipment dimensions are learned shortly before the cargo is loaded onto the aircraft. The objective, as one could easily imagine, is to load as much cargo as possible. Taking into account the strong heterogeneity of transported goods and the weak heterogeneity of ULDs, this problem falls into the broad category of **Packing Problems**, using the typology of [111]. A detailed analysis of the Packing Problems in general will be performed in Chapter 4.

The majority of the literature addressing the Packing Problem in the air cargo context assumes that the exact shipment dimensions are already known. In [88], a mixed integer programming for solving a 3-D Bin Packing Problem (3DBPP) for air cargo is proposed, introducing constrains for fragility, weight distribution, and high vertical stability and orientation. However, this model managed to solve instances of only 8 or 12 boxes. The same model was extended in [89] by testing multiple heuristics such as Relax-and-Fix (R&F), Insert-and-Fix (I&F), and Fractional Relax-and-Fix (FRF) and showed that two of those heuristics (I&F and FRF) produced promising results for instances of up to 80 boxes, with computational time up to 35 minutes. Most recently, in [90] a tailored two-phase constructive heuristic for the 3-D Multiple Bin Size Bin Packing Problem (MBSBPP) is developed that manages to solve instances of up to 100 boxes, with the computational time not exceeding 12 seconds. The only model in the academic literature trying to integrate the forecasting shipment dimensions problem with that the optimal loading strategy is proposed in [63], where a Random Forest forecasting model combined with a reduced 2-D BPP formulation within a heuristic framework is developed.

However, the approach proposed in [63] considers that the decision process is risk neutral, i.e., it does not take into account the risks originating from the uncertainty of the forecast of shipment dimensions. In other words, it does not assess how "confident" is the forecasting model in its prediction and how the former can impact the palletization of items into the ULDs. This is exactly what is going to be addressed in this study through questions RQ3-RQ4. Moreover, through RQ5, it will be examined whether alternative ULD configurations can improve the amount of goods loaded.

2.4.4. Arrangement of ULDs inside the aircraft

The task of arranging ULDs inside the aircraft is the main objective of the aircraft operations department. It is treated under the previously discussed weight and balance restrictions, and is oriented towards the goal of loading all the prepared ULDs, and, in parallel, distributing them inside the aircraft compartment in such a way that fuel and safety requirements are satisfied. In this study, since we are focusing on the revenue management process, alternative ULD configurations will be evaluated in the light of maximizing of the amount

and commercial priority of the products loaded, and not under the aspect of minimizing deviations from the CG of the aircraft or the moment of inertia, as discussed in 2.4.1. Thus, addressing the weight and balance problem is beyond the scope of this research.

2.5. Contributions of this research to the air cargo load planning problem

Now that the decisions and the stakeholders involved in the air cargo load planning process have been analyzed, it is easier to identify the contribution of this research to this specific domain. First of all, decisions **2** and **4** of section 2.4 belong to the handling and aircraft operations department respectively, and will not be covered in this study. With respect to decisions **1** and **3**, these represent the main objectives of the revenue management department and the outcome of these decisions is what defines the accept-or-reject policy of the revenue manager and subsequently, the framework for this research.

Nevertheless, as previously stated, these particular decisions as well as the processes associated with them are treated as separate problems in the academic literature. To our knowledge, there is no unified approach, with the exemption of [63], that addresses all the previously analyzed steps of the decision making process of a revenue management department. Furthermore, there is no approach integrating risk metrics in such a unified air cargo decision-making framework, in order for the revenue manager to able to control and evaluate the impact of the forecasting uncertainty in the loading strategy.

All the above makes the contribution of this research to the revenue management field two-fold: firstly, a novel approach that combines the forecasting of available cargo capacity and shipment dimensions with the configuration of ULDs into the aircraft and palletization of items in the ULDs, will be developed. Secondly, this unified model will be enriched with risk-averse metrics so that the revenue manager is aware of the risks associated with the uncertainty of the forecasting model and make decisions accordingly. The next two chapters are devoted to providing a review of the two broad categories of models that will be used to achieve the research goal, namely the forecasting and the packing models.

3

Forecasting based on historical data

As it has been discussed in the previous chapter, the forecasting model shall have a dual functionality: forecast the available aircraft cargo capacity in combination with the must-fly cargo, and predict the shipment dimensions based on the incoming booking information. In this chapter a review of the most relevant forecasting methods that can be employed to solve this combined problem will be performed.

3.1. Overview of forecasting models

According to the existing literature, there are many data analysis models that have been developed to solve the forecasting problem. The forecasting models can be divided in two main categories, namely quantitative and qualitative [5]. Generally speaking, quantitative models rely on past data to predict the future values of interest, whereas qualitative models use other options, such as market research, executive or collaborative judgement, to make predictions. Since the forecasting method that will be applied on this research is based on historical bookings data, the literature review is focused in quantitative models. The most prominent quantitative forecasting models currently identified in the literature are the following :

- Statistical time series models, which can be used in forecasting aircraft cargo available capacity and must-fly cargo
- Statistical causal models, which can be used to forecast shipment dimensions
- Machine learning models, which can be used to forecast shipment dimensions, aircraft capacity available for cargo as well as must-fly cargo.

At this stage of the research process, all methods seem adequate to answer our needs when it comes to research questions RQ1 and RQ2. The first part of this research will shed light on what method(s) provided the best results.

3.2. Statistical time series models

Time series are sequences of values of a variable, ordered in constant time intervals. There are various example of time series such as the daily stock price, the daily consumption of electricity, or, as identified in this research, the daily available cargo capacity or the daily passenger baggage volume. Time series models use previously observed historical values of the variable of interest, in order to predict future values. They are mostly applicable for problems where there is sufficient amount of past data, and it is relatively safe to assume that whatever patterns were captured in the past data, similar patterns are expected to continue in the future.

Below, a review of the most popular time series forecasting models identified in the literature is performed.

3.2.1. Moving Averages and Single Exponential Smoothing

The most simple tools for forecasting time series are the *Moving Averages* (MA), and *Single Exponential Smoothing* (SES). These techniques are considered naive prediction methods [42]. In moving average method, each point in the predicted time series is the mean of a number of past consecutive points, where the number of past points is chosen so that the effect of irregularities or seasonalities is mitigated. The resulting equation of a moving average of order k can be written as:

$$F_{t+1} = \frac{1}{k} \sum_{i=t-k+1}^{k} y_i \tag{3.1}$$

As it is obvious, in simple MA the mean of k past observations is used to predict the future value, implying that each observation is assigned an equal weight. However, in most cases it is desired to value the most recent observations more than the older ones, as newer observations usually provide a better guide for the future. This can be achieved by exponentially decreasing, with the age of observation, weights, which is the concept of SES [56]. The simplest form is simple exponential smoothing, which is described in the following equation:

$$F_{t+1} = a(Y_t) + (1-a)F_t \tag{3.2}$$

where $0 \leq a \leq 1$ is the smoothing parameter. The forecast F_{t+1} is obtained by weighting the most recent observation Y_t and the and most recent forecast F_t [79].

3.2.2. Holt-Winters method

The aforementioned techniques are suitable for data with no trends or seasonal patterns. To deal with trend and seasonality, an extension of SES is used, namely the *Holt-Winters* method, which was introduced in [110]. Developed decades ago, it is still a very popular forecasting tool for data that contain seasonality and varying trends [42], similarly to the booking data that will be used in this research. To produce a forecast, the Holt-Winters method is using three smoothing equations to account for level, trend and seasonality respectively. Similarly to the SES, for each smoothing equation, there is a smoothing constant with values between 0 and 1. The basic equations of the Holt-Winters method can be written as follows:

$$\textbf{Level:} \quad L_t = a\frac{Y_t}{S_{t-s}} + (1-a)(L_{t-1} + b_{t-1}) \tag{3.3a}$$

$$\textbf{Trend:} \quad b_t = \beta(L_t - L_{t-1}) + (1-\beta)b_{t-1} \tag{3.3b}$$

$$\textbf{Seasonal:} \quad S_t = \gamma\frac{Y_t}{L_t} + (1-\gamma)S_{t-s} \tag{3.3c}$$

$$\textbf{Forecast:} \quad F_{t+m} = (L_t + b_t m)S_{t-s+m} \tag{3.3d}$$

where L_t is the level of series, b_t is the trend, S_t the seasonality, and F_{t+m} the forecast for m periods and a, β and γ the corresponding smoothing constants [79]. Since the forecasting of available cargo capacity is driven by passenger baggage, which is expected to contain seasonal patterns and trends, it can be assumed that Holt-Winters Method can provide a potential solution to this specific forecasting problem.

3.2.3. Autoregressive Moving Average (ARMA) and Autoregressive Integrated Moving Average (ARIMA)

A more sophisticated method for time series forecasting is the Autoregressive Moving Average (ARMA) and Autoregressive Integrated Moving Average (ARIMA). ARMA integrates AutoRegression (AR) and MA techniques into a single model and it is usually notated as ARMA(p,q), where p is defined as the autoregression parameter and q as the moving average parameter. AR(p) makes predictions on the future values of the variable of interest by taking into account linear combinations of past values of this variable. In other words, it is like multiple regression but with p lagged values of the variable of interest as predictors and can be written as:

$$X_t = \sum_{i=1}^{p} \phi_i X_{t-i} + w_t \tag{3.4}$$

where ϕ_i are the model parameters and w_t is a random error.

On the other hand, MA(q), rather than using the past values of the target variable as predictors, uses past forecast errors of order q to predict the variable of interest and it can be written as follows:

$$X_t = \sum_{j=1}^{q} \theta_j w_{t-j} + w_t \tag{3.5}$$

where θ_j are the model parameters and w_{t-j} the past forecasting errors. Combining eq. (3.4) and eq. (3.5) leads to the ARMA(p,q) model :

$$X_t = \sum_{j=1}^{q} \theta_j w_{t-j} + \sum_{i=1}^{p} \phi_i X_{t-i} + w_t \tag{3.6}$$

One essential limitation of ARMA models is that they suppose data stationarity, meaning that the time series data fluctuate around a mean, that remains constant independent of time, and the degree of fluctuation remains constant as well over the examined time interval [79]. As such, they do not account for seasonality or trends in the data, i.e., for non-stationarity. One potential solution is to convert the non-stationary data to stationary by computing the differences between consecutive values of observations. This procedure is known as *differencing* and it is the basis for the ARIMA model, which was popularized by Box and Jenkins in [17]. The Box-Jenkins ARIMA model is usually notated as ARIMA(p,d,q). The main difference with the ARMA model is the parameter d, which is called the integrated parameter, and corresponds to the degree of the first differencing. The equation for the simplest form of ARIMA, i.e., ARIMA(1,1,1) is:

$$(1-\phi_1 B)(1-B)X_t = c + (1-\theta_1 B)e_t \tag{3.7}$$

where c is a constant term, θ_1 is the moving average parameter, ϕ_1 is the autoregression parameter, e_t the error term at time t and B is the backshift operator which is used to take into account the data from the previous time period.

This model, sometimes with variations (e.g. SARIMA), is still a widely used statistical tool in many fields of business and especially in revenue management, as outlined in [45, 109]. Thus, it is a candidate solution to the problem of forecasting the available aircraft capacity.

3.3. Statistical causal models

In statistical causal models, the forecast model is expressed as a function of certain variables that influence the outcome. In its simplest form, a statistical causal model is defined as a *simple regression* model, which attempts to find an explanatory relationship between the dependent variable Y we wish to predict and only one independent variable X. However in the majority of cases, e.g., in the case of predicting shipment dimensions, there are multiple independent variables that control the dependent variable and the forecaster seeks to find a relationship between Y and all the independent variables $X_1 - X_n$. This is called *multiple regression* and has the general form:

$$Y = b_0 + b_1 X_1 + b_2 X_2 + \cdots + b_n X_n + \epsilon_i \tag{3.8}$$

where $b_0, b_1, ...b_n$ are fixed but unknown parameters, and ϵ_i is a random variable normally distributed with variance σ_ϵ.

The goal of multiple regression is to specify the unknown parameters of the model through the process of minimizing the difference between the predicted value $\hat{Y}$ and the actual value Y, i.e., the *residual*. The method of least squares is used in order find the minimum sum of the square errors, i.e., to find the $b_0, b_1, \cdots, b_n$ that minimize :

$$S = \sum_{i=1}^{n} (Y_i - \hat{Y}_i)^2 \tag{3.9}$$

Multiple regression can be used to solve the forecasting of shipment dimensions problem, however it has several limitations that need to be taken into account. First and foremost, there is an underlying assumption that a linear relationship between the independent and the dependent variables exists.. Moreover, no major correlation between the independent variables is assumed. These are assumptions that need to verified during the preprocessing phase of the booking data.

3.4. Machine learning techniques

In recent years, machine learning has become increasingly popular for building predictive data analytics models, i.e., models that make predictions based on historical patterns. Since in this study historical booking data will be used to predict the available aircraft capacity and shipment dimensions, machine learning techniques constitute a valuable tool worth exploring.

In each predictive analytics problem, there is a set of variables that are already measured, for example the historical booking data. Based on this historical data, the machine learning model automatically learns the correlation between a set of descriptive features (the independent variable) and the target feature (the dependent variable). Then it uses this relationship to make predictions in new instances of data. This procedure is called **supervised learning** [61].

Supervised learning can be used for classification or regression tasks. Since our research is centered around predicting real values, either that of the available aircraft capacity or shipment dimensions, the literature study will focus on supervised learning machine learning algorithms used for regression tasks. The most common machine learning models used for regression are the Random Forests (RF), Support Vector Regression (SVR) and Artificial Neural Networks (ANN).

3.4.1. Random Forests

Random forests are based on the concept of Classification and Regression Trees (CART) Models, also called decision trees. Decision trees are built by recursively partitioning the input dataset into regions. For each resulting region of the dataset, a local model (a leaf) is defined, which stores the distribution over class labels. The resulting model can be written in the following form:

$$f(x) = \mathbb{E}[y|x] = \sum_{m=1}^{M} w_m \phi(x, v_m) \tag{3.10}$$

where m is the number of the splitted region, w_m is the distribution over class labels in region m, and v_m represents the choice of the variable to split and the corresponding threshold on the path from the root to the $m-th$ leaf [84].

One problem of the decision trees is that they tend to be unstable, i.e., a very small variation of the input data can significantly alter the tree structure, leading to high variance of the estimates. One potential solution to reduce this variance is to average many estimates. For example, we can randomly choose different sets of data, train M different trees on them and then compute the ensemble. This process is known as bootstrap aggregating, or, as more commonly referred, **bagging**. In addition, to de-correlate the trees, additional randomness can be injected by choosing only a subset of features at each node split. The resulting model would be a collection of de-correlated trees, their predictions of which are averaged to obtain a final prediction with low variance. This model is known as **Random Forests** and was introduced in [19].

RF are good candidates to use when there is a high-dimensional dataset, with missing values and when this data suffers from multicollinearity. Moreover, according to [23], RF can achieve a relatively high predictive accuracy. In fact, RF was adopted by [63] to tackle the problem of predicting shipment dimensions and available cargo capacity with satisfactory results, and as such, it can provide a good benchmark for the results of the forecasting algorithm that would be implemented in this research.

3.4.2. Support Vector Regression

Support Vector Regression machines (SVR) are based on the concept of Support Vector Machines (SVM) to the regression problem, which is the focus of this research. SVMs were introduced in [105] and are another approach to machine learning predictive modelling implementing the error-based learning, by using kernel functions which map the inputs of the model to a high-dimensional feature space [29]. The intuition behind SVM is simple: the model seeks to find the best line (or **hyperplane**) that segments the data into classes. SVR maintains all the features of SVM used for classification, but instead of searching for the best separating hyperplane, it searches for the hyperplane that best fits the given points of the dataset. What separates them though from the simple regression problem is the fact that, while in simple regression we seek to minimize the error, in SVR we try to fit the error within a certain boundary.

To better understand the basic idea behind SVR, its simplest form will be discussed, as presented in [99]. Suppose a training set:

$$S = \{(x_k, y_k), x_k \epsilon R^n, y_k \epsilon R\} \tag{3.11}$$

where x_k is the input data and y_k is the target output data. The objective is to determine a function $f(x)$ which has at most ϵ deviation from the target variable y_k and in parallel be as flat as possible. The key concept is that errors in prediction are acceptable but in any case they should be less than ϵ. The fitting function $f(x)$, in its linear form, can be written as follows:

$$f(x) = \mathbf{w}^T \phi(x) + b \tag{3.12}$$

where w is the weight vector, b is the amount of deviation and $\phi(x)$ is the mapping function, which, as its name suggests, aims at mapping the inputs at to outputs. In case of a linear function $f(x)$, achieving flatness is equivalent to find the smallest value of w. Finding a small w can be achieved by minimizing the norm $||w^2||$, which turns our problem into a convex optimization problem:

$$\begin{aligned}
&\textbf{minimize} && \frac{1}{2}||w||^2 && \text{(3.13a)}\\
&\text{subject to :} && y_i - w\phi(x_i) - b \le \epsilon && \text{(3.13b)}\\
& && w\phi(x_i) + b - y_i \le \epsilon && \text{(3.13c)}
\end{aligned}$$

Behind this convex optimization problem, lies the assumption that a function $f(x)$ that approximates all pairs (x_k, y_k) actually exists, i.e., that the problem is feasible. Nevertheless, this may not always happen, or it may be as well the case that we would like to account for more error ϵ. To cope with this, slack variables ξ_i and ξ_i^* are introduced, leading to the formulation of [105] :

$$\begin{aligned}
&\textbf{minimize} && \frac{1}{2}||w||^2 + C\sum_{i=1}^{l}(\xi_i + \xi_i^*) && \text{(3.14a)}\\
&\text{subject to :} && y_i - w\phi(x_i) - b \le \epsilon + \xi_i && \text{(3.14b)}\\
& && w\phi(x_i) + b - y_i \le \epsilon + \xi_i^* && \text{(3.14c)}\\
& && \xi_i, \xi_i^* \ge 0 && \text{(3.14d)}
\end{aligned}$$

The constant C ($C \ge 0$) is called the *regularization constant* and it controls the trade-off between the flatness of $f(x)$ and the permitted error. The desired level of error is modelled by the ϵ-insensitive loss function $|\xi|_\epsilon$ [105]. Taking into account that we accept errors smaller than ϵ, the function has the following form:

$$|\xi|_\epsilon = \begin{cases} 0 & \text{if } |\xi|_\epsilon \le \epsilon \\ |\xi| - \epsilon & \text{otherwise} \end{cases} \tag{3.15}$$

The situation is depicted graphically in fig. 3.1. The cost is shaped only by the points outside the shaded region, since deviations are linearly penalized.

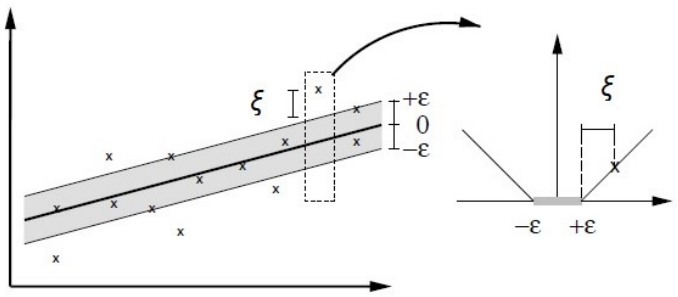

Figure 3.1: Margin loss for the linear function [99].

The problem is then transformed to a risk minimization problem, where the risk is the empirical error as modelled by the ϵ-insensitive function. It is noted that both C and ϵ are determined empirically by the user [22].

However, in the majority of cases, function $f(x)$ is not linear. In this case, transforming the original problem into its dual problem through the use of Lagrange multipliers and using Kernel functions that map lower dimensional data to higher dimensional data is the approach. By using kernel functions, a non-linear problem in the original space becomes linear in the new space, and from this point, we can model the dependencies between dependent and independent variables. For a detailed review on the solution of the non-linear problem, readers are referred to [99].

3.4.3. Artificial Neural Networks

Artificial Neural Networks are engineered systems that try to mimic the human brain, and more specifically the bioelectrical activity of the neurons in the brain. Similarly to the human brain, they have the ability to learn from experience (or past data), and use this acquired experience to generalize on new data. As forecasting is based on prediction of future outcomes based on past observations, ANNs have proven to be an attractive and valuable forecasting tool for researchers and practitioners in many different fields of science, industry and business [37]. Since the first part of this research is oriented towards forecasting, ANNs provide an attractive field for further exploration.

An ANN, in its simplest form, consists of three layers: the input layer, the hidden layer and the output layer. This type of neural network is called *single-layer feedforward neural network*. In fig. 3.2, a simple feed forward network with a three input nodes, a single hidden layer consisting of two nodes and a single output node is depicted:

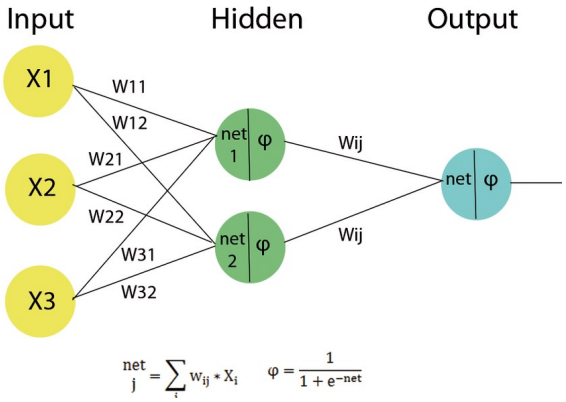

Figure 3.2: A feed forward neural network [44]

The input layer is the layer where the external information, i.e., our independent variables, are received. For forecasting problems, the number of the input nodes equals the number of the corresponding independent variables. The inputs are then passed to the nodes of hidden layer, through connections which are called *synapses* or *arcs*. Each arc is assigned a specific weight w_{ij}, where i is the input node and j is the hidden node. In each node of the hidden layer, two functions are implemented, namely the *integration* and the *activation* function.

The integration function is the weighted linear combination of the input vectors, i.e $net_j = \sum_{i=1}^{j}(w_i x_i)$, where j is the number of hidden nodes. The activation function is used to account for the non linear mappings between input and output data, since in the majority of problems we are dealing with high dimensional non-linear datasets. There are many types of activation functions but the most popular ones are the *Rectified Linear Unit*, the *Sigmoid* function and the *Hyperbolic Tangent* function [49]. In fig. 3.2, the Sigmoid activation function is used, which compresses the values of the integration function to a range between 0 and 1, where 1 declares a strong effect of the particular linear combination of the inputs to the output, whereas 0 declares a negligible effect. Generally speaking, the activation function is used to determine whether and to what extent each incoming signal, i.e., each different combination of the inputs, should progress through the network and affect the desired prediction.

The outputs of the hidden layer are passed through weighted arcs to the output layer, where the prediction is obtained, using again an integration and an activation function. Before any type of ANN can generate predictions, it must be trained. The key concept of training in ANN is the determination of the arc weights, as it is these linking arcs that determine the ability of the ANN to perform non linear mappings of inputs to outputs [100].

The arc weights are determined through a process called *backpropagation*. The backpropagation algorithm finds the weights that minimize the error between the actual values and the predicted values. The cost function that is used to define the observed error can be a general function that quantifies the total prediction error, such as the Sum of Squared Errors (SSE), the Mean Squared Errors (MSE) or the Exponential Log Likelihood. Training the neural network turns out to be an unconstrained non linear optimization problem, with the overarching goal of minimizing an error function. The most common optimization processes used for training an ANN are *gradient descent* based approaches [67]. Gradient descent involves using the chain rule to calculate the gradient of the error function with respect to the weights, and shifts the weights in the opposite direction of the partial derivatives by a predefined amount called *learning rate*. This procedure is performed recursively until the error reaches a minimum, which ensures the identification of the optimal weights [44] and concludes the training process.

The age of "Big Data" has simplified the application of ANNs, since the main burden of statistical estimation - generalizing well from a limited amount of data - has been removed [49]. However, the huge amount and the complexity of available data has risen the need for more complex ANNs than the one presented above, in order to model and learn increasingly complex relationships in real-world data and subsequently, to make accurate predictions. This can be achieved by adding more hidden layers and/or more neurons in each layer. Such neural Networks are called *Deep Neural Networks*. According to [66], deep learning models can provide better approximations to nonlinear functions than the models with a single hidden layer. The quintessential example of Deep Neural Networks is the MultiLayer Perceptron (MLP), which is a multi-layer feedforward neural network, based on the same principles as the one presented above, but with more than one hidden layers [49]. The fact that a large amount of high-dimensional booking data is going to be used in this research to predict shipment dimensions makes MLP an ideal candidate towards this purpose.

Moreover, since deep learning provides powerful tools for processing massive amounts of data and make accurate predictions, it would be interesting to explore one additional types of Deep Learning Networks, the *Long Short-Term Memory* (LSTM) network, that can be applied to the forecasting of available aircraft capacity or that of must-fly cargo.

Long Short-Term Memory (LSTM) Networks

LSTM networks are a variation of the Recurrent Neural Networks (RNNs). RNNs are used for modelling of sequential data and are designed for dealing with non-linear time varying problems [120]. Differently than conventional neural networks, where there are no connections between the nodes belonging to the same hidden layer, in RNNs the hidden nodes receive feedback from the previous state in order to compute the future state. This facilitates adjusting the weights by taking into account the residual in each subsequent time step and, as a result, the output of the model at time t is associated not only with the input at time t but also with recursive inputs at previous times [119]. They are called recurrent because this procedure is repeated for every element of the time sequence. The following Fig. 3.3 shows a simple RNN unfolded into a full network in two time steps:

Even though RNNs seem to be suitable for a time series forecasting problem like the forecasting of available aircraft cargo capacity, they suffer from the so-called *vanishing* or *exploding gradient* problem, which significantly limits their ability of capturing long-range dependencies [91], as it would be required in this research.

The response to the vanishing or exploding gradient problems of the RNNs was the design of the LSTM networks [53]. The key element of the LSTM networks is the memory cell, which is comprised of three gates: the input gate, the output gate and the forget gate. A LSTM network consists of a stack of LSTM memory cells as shown in the following Fig. 3.4:

The analysis performed is driven by [97]. First, the forget gate f_t determines which information from the previous step are going to pass to the cell state and which information are going to be discarded. A sigmoid function is used to control the activation of the forget which can be formulated as follows:

$$f_t = \sigma(x_t U^f + h_{t-1} W^f + b_f) \tag{3.16}$$

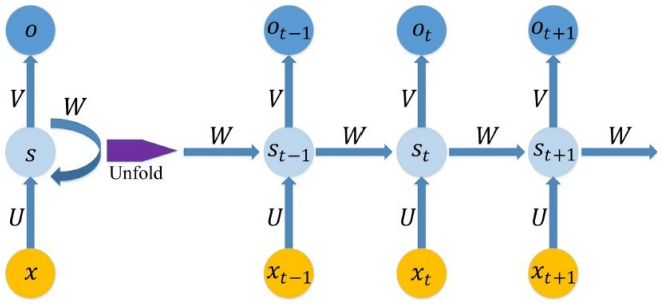

Figure 3.3: A Recurrent Neural Network . U, V and W are the corresponding weights of the input, hidden and output layer, x_t and o_t are the input and the output values at time t, and s_t is the hidden state at time t [8].

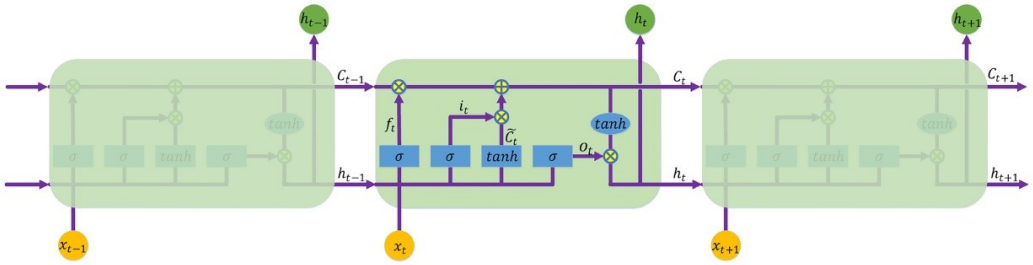

Figure 3.4: An LSTM Network.[8].

where σ corresponds to the sigmoid activation function, x_t is the input vector and h_{t-1} the value of the memory cell from the previous time step.

Next, it is determined which new information will be stored in the cell state. This is performed jointly in two steps. The sigmoid input layer i_t determines the values that will be updated ,whereas the $tanh$ layer creates the vector containing the candidate values that should be updated in the next state $\hat{C}_t$:

$$i_t = \sigma(x_t U^i + h_{t-1} W^i + b^i) \tag{3.17a}$$
$$\hat{C}_t = tanh(X_t U^c + h_{t-1} W^c + b^c) \tag{3.17b}$$

Then, the previous cell state C_{t-1} is updated into the new cell state C_t :

$$C_t = f_t * C_{t-1} + i_t * \hat{C}_t \tag{3.18}$$

where $f_t * C_{t-1}$ determines which information are going to be discarded from the old cell and $i_t * \hat{C}_t$ are the new candidate values.

Finally, a sigmoid function filters the cell state and then the filtered cell state o_t is passed through a $tanh$ function to determine which information are going to be produced as an output :

$$o_t = \sigma(x_t U^0 + h_{t-1} W^0 + b^0) \tag{3.19a}$$
$$h_t = o_t * tanh(C_t) \tag{3.19b}$$

The new cell state C_t and the hidden state h_t are passed to the next memory cell. This process is repeated until all weights and biases are adjusted so that the minimum error between the LSTM predictions and the actual training values is achieved.

4

Packing Problem

This section focuses on providing a literature background on the Packing Problem and relevant risk-averse approaches that can been applied to it, to shed light into models that can be used in order to address RQ3-RQ5.

4.1. Packing Problem Variants

Packing problems are complex combinatorial optimization problems with a variety of applications such as truck or aircraft container loading [90], cloud computing [101] or job scheduling [69]. As originally proposed by [32], they can be placed in the broader category of Cutting and Packing Problems (C&P). The reasoning behind this lies in the fact that packing small items, such as boxes, into larger objects, such as containers or bins, may be also interpreted as cutting the total empty space of the large objects into segments of empty space that can accommodated the small items. From this point on, and to be better aligned with the subject of the research, we will label the small items as *items*, boxes or shipments and the large items as *bins* or *containers*. The boxes and the bins may be identical or heterogeneous (strongly or weakly). In this research, boxes are considered to be strongly heterogeneous and the bins (i.e., the ULDs) are considered to be weakly heterogeneous, as they come in specific sizes and shapes, as discussed in chapter 2.

The most important characteristic of packing problems is dimensionality, which is used to specify the geometry of the problem. Under this aspect, one-dimensional, two-dimensional, three-dimensional and multi-dimensional packing problems (for example when time is also considered) can be formulated. For the purposes of this research we will focus only on the first three dimensions.

The common task of all packing problems is concentrated around the assignment of a set of boxes into a number of bins, subject to specific constraints, so that a given objective function is optimized. According to the typology introduced by [111], the objective of packing problems can have two basic formulations, either *input (value) minimization* or *output(value) maximization*. In the input (value) minimization, a given set of boxes has to be assigned to the minimum set of bins. All boxes will be packed and there is no selection process regarding the boxes. On the other hand, in output (value) maximization, a set of boxes has to be assigned to a given set of bins, in a way such that the value of bins is maximized. In this case, all bins must be used and there is no selection process regarding the bins. In most cases, the value that has to be minimized (or maximized) is directly proportional to the size of the boxes/bins and can be weight (for one-dimensional problems), area (for two-dimensional problems) or volume (for three-dimensional problems). In such cases, both type of problems can be translated into minimization of “wasted" space.

Following the typology from [111], the packing problems, based on the heterogeneity of the boxes and the formulation of the objective function can be categorized as shown in Fig. 4.1. The areas highlighted in circles are the problems that will be considered in this research, depending on the formulation of the objective function, namely the **Knapsack** problem and the **Bin Packing Problem**.

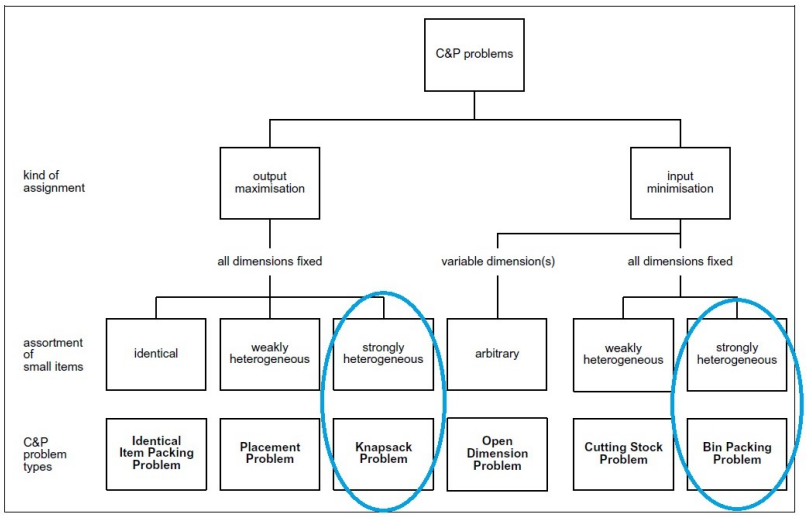

Figure 4.1: Basic types of Cutting and Packing Problems [111]

4.1.1. Knapsack problems

The simplest form of Knapsack problem is the *Classic (One-Dimensional) Single Knapsack Problem* or *0-1 Knapsack Problem*) (1DSKP), which has the objective of maximizing the value of the packed boxes that are placed into a single bin (knapsack) by choosing among a specific set of boxes with given weight and value [81]. Extensions of the Classic Knapsack problem are the *Two-Dimensional Single Knapsack* (2DSKP) [50] and the *Three-Dimensional Single Knapsack* (3DSKP) [92] in which boxes with rectangular shape have to be loaded into a single two- or three-dimensional container respectively. As previously discussed, if the value to be maximized is proportional to to the size of the boxes, then the maximization problem can be treated as a minimization problem of the unused space of the container.

A very interesting variation of the Single Knapsack problem, extended for multiple containers, that can be potentially be used to model the evaluation of different ULD configurations addressed in RQ5, is the Mutliple Heterogeneous Knapsack Problem (MHKP), where containers are weakly heterogeneous and the boxes are strongly heterogeneous [118].

4.1.2. Bin Packing Problem

The *Classic (One-Dimensional) Bin Packing Problem* (1DBPP), in its normalized version, can be informally stated as follows: A set of n boxes each of which has weight w_j ranges between 0 and 1, and a number of identical bins with unitary capacity c, is given. The goal is to load all the boxes into the minimum amount of bins, ensuring at the same time that the weight capacity of each bin is not exceeded [30]. The *Two-dimensional Bin Packing Problem* (2DBPP) involves loading a set of n rectangular boxes having width w_j and height h_j into a set of rectangular bins with width W and height H, where $w_j \leq W$ and $h_j \leq H$ [74]. Finally, the Three-dimensional Bin Packing Problem (3DBPP) involves loading a set of n rectangular boxes characterized by width w_j, height h_j and depth d_j into a set of rectangular bins with width W, height H and depth D, where $w_j \leq W$, $h_j \leq H$ and $d_j \leq D$ [81].

An extension of the BPP that can contribute towards the optimization of assignment of boxes into ULDs (RQ3) is the Multiple Bin Size Bin Packing Problem (MBSBPP), where containers are weakly heterogeneous and boxes are strongly heterogeneous, in accordance to the characteristics of air cargo addressed in this research [118].

4.1.3. Combination of Knapsack and Bin Packing Problems

In real life applications, the selection problem may exist for both the boxes and the bins. The same applies for this research since, as discussed in chapter 2, the number of the type of the ULDs (bins) has to be selected in combination with the boxes that will be assigned inside the ULDs. The former requires an extension of the objective function. An approach towards this direction, was proposed in [7], where a Generalized Bin Packing

Problem (GBPP) was studied. In this new type of BPP, a set of compulsory and non-compulsory shipments characterised by specific volume and profit, has to be packed into a set of containers with specified volume and cost. The developed algorithm tries to choose among the subset of non-compulsory shipments along with the compulsory ones to be packed into the selected bins, so that the total net cost is minimized. This model jointly considers the MBSBPP and MHKP and although it considers bin costs, which are not going to be taken into account into this research, it can provide guidelines for the packing model that will be developed.

4.2. Packing Problem Constraints

As previously discussed, the task of all packing problems is to optimize a given objective function, subject to specific constraints. According to [118], there are two types of constraints applied to the packing problems, the basic constraints, that are applied to all packing problems, and problem specific constraints, capturing a multitude of practical considerations applied to the specific type of problem. The basic constraints can be summarized as follows:

- Boxes should not overlap with each other
- The edges of the boxes must be placed parallel to the walls of the container.

In [15], the problem specific constraints are categorized to cargo, boxes, containers, loading and positioning constraints. In this study, we will briefly discuss some of these constraints, that are more relevant to our problem.

Weight Capacity and Distribution Constraints: The weight of the items packed may not exceed the weight capacity of the container. An indicative example of a model incorporating weight capacity constraints can be found in [31], where a multi-objective container loading problem is addressed. The objective is not only to utilize the maximum volume of the container, but also to load the maximum weight of items, that the container can carry. This is a very useful approach, that will be taken into account in this research since, apart from the loading space, weight capacity is also a binding constraint. Further examples of works accounting for weight capacity constraints can be found in [72, 88–90]. The weight distribution constraint (also called load balancing constraint) requires that boxes are placed inside the container in such way that the the weight is distributed as evenly as possible across the container's floor and the center of gravity is located as low as possible [16]. This constraints relates more to the handling operations and the general weight and balance problem and for the reasons discussed in chapter 2 will not be taken into account.

Orientation Constraints: Every box can be placed inside the container in six unique orientations. However, in practice the boxes may have to be placed inside the container into pre-determined orientations, as instructed by the shipper (For example, boxes labeled with “This way up" sign). To capture this type of constraints, each box is characterized by three parameters, l^+, w^+ and h^+ for length, width and height respectively. Depending on the orientation requirements of the box, parameters are set either to 1 or 0, allowing or not the rotation of the box in this particular dimension respectively. In [59], a mixed integer linear programming model for the container loading problem is developed, where only a single orientation is allowed. In [89], boxes can rotate orthogonally in the container. In any case, since the orientation of boxes can have a significant impact on the outcome of the loading strategy, the corresponding orientation constraints should be taken into account during the development of the palletization model of this study.

Stacking Constraints: Stacking constraints impose restrictions on the way the boxes can be placed on top each other inside the container. They are introduced to prevent damaging of the boxes based on the *load-bearing strength* of each box [13], i.e., the amount of pressure that can be applied to a box without damaging its context. In [59], the load bearing strength of each box is taken into account with the form of a fragility constraint, which can be interpreted as a trivial representation of the load-bearing strength. For the purposes of our research, since the items are labelled as “fragile" or “not fragile" a simpler case may be considered, in accordance with [39], where a fragility flag is used, being equal to 1 or 0, depending on whether the items are fragile or not respectively.

Load Stability Constraints: Load stability constraints ensure that the boxes are loaded in a stable manner and will not fall or slide during transport. Typically, there are two types of stability, vertical and horizontal stability [15]. Vertical stability ensures that the boxes will not fall onto the container floor during transport. According to [94], vertical stability can be achieved by following three approaches:

- *Full base support*, which requires that the base of each box is fully supported by the floor of the container or by the top of other boxes. Examples of full support requirements can be found in [46, 72, 90].
- *Partial base support*, which requires that the base of each box is either fully supported by the floor of the container, or a pre-specified percentage of the box area is supported by the top of other boxes. This pre-specified area percentage varies in the literature. For example in [52], it is assumed that a 70% percentage is enough for container loading, whereas in [39] a minimum of 80% is required. Interestingly, in [102], a minimum percentage of 85% is required for both the length and the width dimension of the box that is placed on top of other boxes.
- *Static mechanical equilibrium*, which requires that either the box is fully supported by the floor of the container, or the Center of Gravity of the box is located on the contact area of the supporting box. An example of this approach can be found in [71], however, as [94] argues, this approach by itself does not guarantee vertical stability.

Horizontal stability ensures that the items do not shift during the transport, i.e., the boxes withstand the inertia. This can be potentially achieved by ensuring that each item is adjacent to other items or the container wall. In [72], only one side of the box is required to be adjacent with another item or the container wall, whereas in [27] it is required that at least three sides of each box touch adjacent boxes or the container's wall.

In this research, both vertical and horizontal stability will be addressed, since a loading strategy that does not guarantee safe transport of items is not efficient in any case. Nevertheless, to increase the computational efficiency of the developed model, vertical stability may be considered as hard constraint, probably in the form of partial base support, whereas horizontal stability may be considered as a soft constraint.

Allocation constraints : Allocation constraints address requirements regarding the composition of shipments loaded into the containers. For example, some shipments must be in the same container if they are headed to the same destination (referred also as connectivity constraints in [72]) or due to shipment individual characteristics (for example food and radioactive material) they cannot be placed in the same container [34, 63]. In this specific research, allocation constraints will not be treated under the aspect of connectivity constraints, since a single flight leg will be assumed, but under the aspect of item characteristics.

Complete Shipment Constraints : Complete shipment constraints refer to cases where a shipment is composed of many individual boxes, that have to be delivered together in the final destination, such as in the case of furniture for example. In these cases, the requirement arises that when a box from this shipment is loaded, then all the boxes following this shipment should be loaded. This constraint is treated very rarely in the literature [34], and introduces an aspect that will be considered in this research.

Specific shape of ULDs: This is a constraint that applies specifically to air cargo, since ULDs come in different specific shapes to fit into the fuselage of the aircraft, meaning that they are not always rectangular. An approach accounting for the different shapes of ULDs was developed in [89], where a set of four possible cuts lying at each container's corner was assumed. Since in this research, specific ULDs used by AFKLMP are going to be taken into account, this type of constraint must be considered.

4.3. Packing Problem Heuristics

Packing Problems are considered to be combinatorial optimization problems that are NonDeterministic (NP) - Hard to solve. To address this NP-hardness, several heuristic algorithms have been developed. Although heuristics are not guaranteed to find always the optimal solution, their low computation time when solving large instances of NP-Hard problems, makes them an efficient solution strategy that can be used to find a satisfactory feasible solution [87]. These algorithms can be categorized into two broad categories, the **placement heuristics** and the **improvement heuristics** [113]. Below a brief review of those two categories will be performed. Readers are referred to [87, 118] for a detailed review of heuristics used in 2-D and 3-D packing problems.

4.3.1. Placement Heuristics

Placement heuristics (also called construction heuristics), provide a mechanism that is based on how the boxes are placed inside the container. Generally, the container is segmented into smaller areas and each area

is packed separately. In [118], placement heuristics are further categorized into **wall building**, **layer building**, **stack building** and **block building**.

In wall building, introduced in [43], the container is filled along a number of vertical strips (walls) across the depth of the container. The depth of each vertical strip is determined by the depth of the first box placed in the wall. Once this wall is full, the next wall is constructed next to the previous wall following the same logic until no walls can be added to the container. On the contrary, in layer building, first presented in [12], the container is filled along horizontal layers instead of walls. The first layer that is created is the layer located on the floor of the container. Once this layer is full, the same logic as in wall building is followed until the container is full. Layer building was developed in an attempt to tackle the stability issues resulting from large gaps existing between the walls in the wall building approach. The stack building approach, proposed in [40], consists of building stacks on a top of a base box located on the floor of the container. The stacks are then arranged such that the container floor is covered by solving a two-dimensional packing problem. Finally in the block building heuristic, used in [34], boxes are sorted by volume and then the most appropriate space for each box is chosen, so that the total volume of space where the remaining boxes cannot be placed is minimized. As it is evident there are many different approaches that can be used to create arrangements of boxes into the containers. In most of the cases, and most likely in this research as well, these approaches are combined with improvement heuristics that enhance their performance. These improvement heuristics will be discussed in the next section.

4.3.2. Improvement Heuristics

Improvement heuristics broaden the search space by using various neighbourhood structures and acceptance criteria. The most commonly used improvement heuristics is the **Genetic Algorithm** (GA), the **Tabu Search** (TS) and the **Simulated Annealing** (SA).

Genetic Algorithm

The concept of GA was firstly introduced in [54] and is based on the process of natural selection, by using techniques such as selection, crossover and mutation, which are generally called *genetic operators*. The process begins by generating an initial population of individuals, each of which is described by a set of parameters called genes. These genes form a unique string for each individual that is called a chromosome and encodes a potential solution to the problem. Next, a fitness function is defined for each individual which provides a fitness score for each individual, or equivalently, the quality of the solution. The highest the fitness score, the highest the probability the individual will be selected during the selection phase. During the selection phase, two pairs of individuals (parents) with the highest fitness scores are selected and pass their genes for reproduction. There is a variety of selection techniques, such as the Roulette Wheel selection, Rank Selection and Tournament Selection. For each selected pair of individuals, a crossover point is defined in the chromosome (usually randomly) and offsprings are created by exchanging genes between the pair of individuals until the crossover point is reached. The created offsprings are added to the population. Moreover, these new offsprings may be subject to mutation, meaning that some specific bits of the chromosome may change with low probability, in order to ensure population diversity and avoid being “trapped" in local minima. The same procedure repeats until the produced offsprings are not significantly different from the previously generated offsprings. In this case the population has converged and the algorithm has reached to a set of potential solutions.

One of the very first applications of GA in two-dimensional packing problems can be found in [40], where the stack building approach was used. In this case, a chromosome is defined by a placement vector that corresponds to a sequence of placement corners of the base box and two possible orientations of this box. Using the Rank Selection, i.e., by evaluating the ranking order of the fitness value of each box, each selected box is placed in the first available feasible placement corner. The procedure continues until all stacks are loaded. Another example of applying GA to solve a three-dimensional packing problem can be found in [112], where the chromosome contains two elements, the order of boxes that have to be packed and the possible rotations of the boxes. The initial population is formed by ordering the boxes based on their volume and by assigning a random rotation to each box. Roulette wheel selection is used to enable the better chromosomes to be copied to the next generation and mutation is applied to randomly alter the sequence of boxes and change their rotation so that the optimal solution is discovered.

Finally, a modified version of the GA, the Biased Random Key Genetic Algorithm (BRKGA) is used in [47] to solve 2D and 3D packing problems. The BRGKA is a variation of the Random Key Genetic Algorithm (RKGA) introduced in [9]. RKGA is considered ideal for problems where chromosomes have different parts, such as box sequence and box orientation. The BRGKA differs form RGKA in the way parents are selected. While in the RGKA, parents are chosen randomly from the population, in the BRGKA, each element consists of a parent chosen from the elite population and a parent selected from the rest of the population. The chromosomes, as in [112], consist of box packing sequence genes and box orientation genes. A fitness function defined as the *adjusted number of bins* is used to guide the evolutionary process, i.e., in case two solutions exist which use the same number of bins, then the bin with the least load factor is selected for potential improvement.

Tabu Search

The Tabu Search (TS) heuristics is considered to be one of the most popular techniques used in combinatorial optimization. It was firstly introduced in [35], and it is a local search method which avoids being “trapped" in local minima by restricting the feasible neighborhood using a “tabu" (forbidden) list. This list is actually the solution search history and contains moves that cannot be performed in reverse order in following iterations. Moreover, *aspiration criteria* can be defined that may allow accepting a move in case it improves all previous solutions, even though this move is restricted by the tabu list.

A very interesting approach using TS heuristics can be found in [115], where a three-dimensional bin packing problem is solved. The TS is used to assign items to bins without specifying their actual positions and then a placement heuristic is used to determine the actual assignment of boxes inside the container.

A modified approach is followed in [14], where a parallel tabu search algorithm is used to load weakly heterogeneous boxes in a single container. The TS algorithm covers the encoding of the packing sequence and the fillable packing spaces. Differently configured sequential TS algorithms work in parallel and use independent search paths. In each sequential TS algorithm, the search process is divided in several phases to ensure diversity. For each solution obtained by the sequential TS algorithm a basic heuristic is applied to generate the complete loading of the aircraft. Solutions are communicated between the independent sequential TS algorithms, thus providing an intensification of search in the region of the best results. As it was proved though, the quality of solution improved slightly in comparison with a single sequential TS algorithm.

Most recently, in [72], a hybrid tabu search heuristic is developed which uses TS and placement heuristics iteratively to address a container loading problem. An initial solution is obtained by using the placement heuristic. This solution is then transformed to a tabu list to be used by the TS algorithm. A number of feasible solutions is generated by the TS algorithm, which are translated to arrangement of boxes into the container through the use of the placement heuristic. By using evaluation criteria such as the weight limit and the weight distribution, the best solution is defined. With this best solution as initial solution, further feasible solutions are explored by the TS algorithm. The process continues until a termination criterion, which can be the number of iterations or the computational time, is satisfied. Based on the experimental results, this hybrid tabu search heuristic proved to achieve high volume utilization as well as high stability and outperformed the previously discussed approaches used in [14, 40].

Simulated Annealing

The Simulated Annealing (SA) algorithm is an optimization method inspired by annealing process used in metals. Annealing involves the physical process of cooling in metals after being placed in a heat bath, in order to reach their final structure and to retain their desired properties. The concept of annealing was firstly introduced to tackle combinatorial optimization problems in [62]. Actually, the SA algorithm is a local search algorithm that moves to an inferior solution according to an acceptance probability that decreases with the evolution of the search. This movement to inferior solution is performed to ensure that the algorithm escapes local optima. The decreasing probability relies on empirical evidence showing that in the beginning of the search, it is most possible for the algorithm to be “trapped" in local optima, and as the search progresses, this probability decreases. This acceptance probability is called the *temperature* variable, in accordance with the physical origin of the algorithm.

In [78], the parallel hybrid tabu search algorithm implemented in [14] is combined with SA to address a container loading problem. The concept is the same as in [14], with the difference that SA is used in the beginning to obtain a good starting solution for each independent sequential TS algorithm. The following

TS iterations are performed in order to achieve an even more intense examination of the area defined from the SA algorithm and obtain a better quality. This approach tries to exploit the advantages of both methods, while avoiding their weaknesses.

4.4. Packing Problems with Uncertainty

As discussed in chapter 2, a forecasting model would be developed such that the shipment dimensions are predicted. The predicted shipment dimensions would be fed into the palletization optimization model in terms of some of the constraints reviewed above. Nevertheless, there is no forecasting model that is 100% accurate, meaning that there would always be an uncertainty in the prediction of shipment dimensions. Disregarding this uncertainty when building the constraints of the palletization model and using nominal values for the shipment dimensions might provide a solution that violates the aforementioned constraints with an undesired probability. The violation of the constraints is translated to the risk of the loading strategy not implemented in practice. An indicative example that shows how small variations in the problem parameters can affect the optimal solution is presented in [11], where perturbations of 0.01% to problem parameters subject to uncertainty, caused violation of more than 50% of the constraints in 13 out of 90 NETLIB Linear Programming models. Therefore, since this research is treated using the revenue management perspective, it is considered essential to develop an optimization methodology that offers protection to the revenue manager from any risks arising from the uncertainty in the predictions of the forecasting model. This introduces the need for *chance constraints*.

Chance constraints can be used to guarantee a specified level of risk aversion, making them ideal candidates for controlling the impact of prediction uncertainty in the palletization model. Thus, optimal and reliable performance of the packing model can be achieved through the use of *Chance Constrained Optimization* (CCOPT), by requiring satisfaction of packing constraints within a pre-specified by the user probability. The CCOPT framework was originally developed in [24], with regard to financial planning problems. Since then, it has been widely used in many fields including, but not restricted, to production planning, optimization of power system management, supply chain management, financial risk management and portfolio optimization and optimal control of unmanned vehicles [41]. A generic formulation of the CCOPT can be stated as follows:

$$\textbf{min}\{f(x)\,|\mathbb{P}\{x \in P(\omega)\} \geq 1-\epsilon, \quad x \in X\} \tag{4.1}$$

, where $x \in \mathbb{R}^n$ is the vector of the decision variables that need to be selected in order for $f(x)$ to be minimized, ω is a random vector, $P(\omega) \subseteq \mathbb{R}^n$ is a region parametrized by ω and $X \subseteq \mathbb{R}^n$ is a set of deterministic constraints imposed on x [75]. In simple words, any event $x \notin P(\omega)$ is an undesirable outcome, and the probability of such outcome is restricted to $1-\epsilon$, where $\epsilon \in (0,1)$ and usually is chosen to have small values, e.g., 0.05 or 0.1. The term ϵ is called *risk tolerance* and it controls the trade-off between the solution of the cost function and the risk of violating the constraint. Usually in practice, and in this research subsequently, in order for the revenue manager to have an accurate idea of the solution in terms of cost and risk, a sensitivity analysis should be performed with varying risk levels ϵ. Readjusting the above formulation to better meet the requirements of packing problem constraints with n decision variables and m constraints results in the following general form:

$$\textbf{maximize} \quad \sum_{i \in N} \sum_{j \in N} p_{ij} \times V_i \tag{4.2a}$$

$$\text{subject to :} \quad \sum_{i \in N} p_{ij} \times V_i \leq V_j \tag{4.2b}$$

where $i = 1, \cdots, m$ and $j = 1, \cdots, n$, $\tilde{a}_{ij}$ a vector of random sizes with a joint probability distribution $\mathbb{P}$ on the left hand side (LHS) (for example the shipment dimensions) and $\tilde{b}_i$ the uncertain vector on the right hand side (RHS) (for example the ULD capacity). In this research ULD capacity is going to be fixed ($\tilde{b}_i = b$ deterministic), so we will deal only with LHS uncertainties.

Chance constrained problems can be categorized as individual chance constraint problems when $m = 1$ and as joint constraint problems when $m \geq 1$ [25]. In other words, a joint constraint problem imposes the requirement that a set of constraints must hold together in order to achieve a single goal, whereas in individual chance constraint problem, each constraint accounts for the probability of a single goal. As discussed in

[33], a joint chance constraint is deemed more suitable for problems where the individual chance constraints describe one single goal. On the other hand, if the individual chance constraints describe different goals, it is more appropriate to treat them separately, providing the flexibility to prioritize the set goals by defining varying reliability levels.

4.4.1. General Approximations to CCOPT

Chance constrained optimization problems are difficult to solve, mostly due to the following reasons :

1. Computing Equation 4.2b, i.e., checking the feasibility of the candidate solution x can be hard, because in multidimensional problems the calculation of a multidimensional integral is required, which cannot be computed with high accuracy [1].

2. The feasible region defined by the chance constraint imposed in Equation 4.2b is generally non-convex [86].

To deal with the above difficulties a number of CCOPT approaches has been developed.It is noted that a specific approach cannot be recommended at this phase of the study, since, as it will become evident, the approach that would be finally followed depends, among others, on the observed probability distribution of the uncertain parameters predicted in the forecasting phase.

First of all, promising results have been obtained by approaches addressing cases where the vector $\tilde{a}_{ij}$ follows a distribution that enables checking the feasibility and the feasible region is convex. Such cases exist when the $\tilde{a}_{ij}$ vector follows the normal distribution with mean a and correlation matrix Σ, the RHS vector $\tilde{b}_i = b$ is deterministic and $\epsilon \leq \frac{1}{2}$, Equation 4.2b can be reformulated as follows [117]:

$$ax_j + \Phi^{-1}(1-\epsilon)\sqrt{x_j^T \Sigma x_j} \leq b \tag{4.3}$$

where $\Phi^{-1}(\cdot)$ is the cumulative probability distribution of the Gaussian distribution. As discussed in [117], in this convex quadratic problem, feasible binary solutions to x_j can be obtained by using commercial solvers such as CPLEX. However it is not always the case that distributions are normal, meaning that this formulation is not always obtainable.

A number of approaches oriented around the common task of proposing convex approximations of non convex constraints and yielding feasible solutions to the original problem have been proposed in the literature. Approaches of this type are the **Bernstein** approximation developed in [86], and the **scenario** approximation methods studied in [20, 21]. The Bernstein approximation can be applied to cases where the components of $\tilde{a}_{ij}$ are independent and is based on setting upper bounds on the probability of the $\tilde{a}_{ij}$. The scenario approximation approach is developed under the concept of *robust optimization* [10], where the nominal problem is replaced by the worst-case problem and constraints need to be satisfied for every possible realization of $\tilde{a}_{ij}$, meaning that the risk level ϵ in Equation 4.2b is set to zero. Based on Monte Carlo Simulation, several scenarios are generated in order for the chance constraints to be discretized and convexity structures to be preserved. While this technique can be applied to any type of distribution, the requirement that all constraints need to be satisfied provides a very conservative solution and a deterioration of the objective function. Moreover, to approximate feasibility a very large number of scenarios is needed which can be computationally expensive [41].

A promising research stream that tackles the issue of providing a very conservative solution, is based on replacing the probability distribution of $\tilde{a}_{ij}$ with finite uniformly distributed deterministic samples. This leads to a **Sample Average Approximation** (SAA) of the CCOPT [76]. This approach is well known for being applicable to problems with expected value objectives and it uses as well the Monte Carlo Sampling approach. The key difference between this approach and the scenario approximation approach is that instead of requiring all constraints to be satisfied, a positive risk level ϵ is defined to allow for violation of constraints up to a pre-determined probability. In the setting of finite distribution of the uncertain parameters, the CCOPT problem is then formulated as a large scale deterministic MIP by introducing binary variables for each sample (scenario), and by adding a Big-M term for each inequality [3].

However, the fact that the Big-M reformulation suffers from weak linear programming relaxation, makes it inefficient to be solved by current programming solvers. To address this issue, several techniques have been developed, such as coefficient tightening, mixing inequalities, quantile cuts, Lagrange Relaxations and Progressive Hedging. These related MILP formulations have been extensively studied in the literature [3, 65, 75, 77, 108]. Readers are referred to [2] for a review of these relaxation techniques.

4.4.2. Risk-Averse approximations to CCOPT

Chance constraints provide a qualitative risk measure, i.e., they ensure that the quality of the solution remains feasible at a pre-determined high probability [73]. However, one potential drawback when using chance constraints is that they do not take into account the degree of danger resulting from violations above that level of probability. In other words, when Equation 4.2b is violated, and it would be violated with probability $1-\epsilon$, it should be determined whether this is simply creating an inconvenience or poses potential danger [95].

The key to address this issue is to condense the random vector $\tilde{a}_{ij}$ into a single value by quantifying the risk of loss, i.e the risk that constraint Equation 4.2b is violated, instead of quantifying the degree of uncertainty characterizing it. The most common method used in order to address this risk is to incorporate in the formulation of problem an additional term that quantifies the risk, defined in the literature as risk measure.

Risk measures were firstly introduced in [80], where variance was used as a risk measure to address the requirement to balance between risk and return. Apart from variance, other risk measures have been also recommended such as shortfall probability, expected shortage, value-at-risk (VaR) and conditional value-at-risk (CVaR) [26]. Among these measures VaR and CVaR are proven to be from the optimization portfolio theory the most efficient for risk management [64]. For a given confidence level $\alpha \in (0,1)$, VaR describes the expected maximum loss over a defined target horizon based on the α-quantile of the loss distribution [28] and can be formally stated as follows:

$$VaR_{\alpha}(W) = \inf\{t : \mathbb{P}\{W \leq t\} \geq \alpha\} \tag{4.4}$$

where W is a continuous random variable with distribution $\mathbb{P}$ and confidence level $\alpha \in (0,1)$. For example, if W is the value of a financial asset, the $VaR_{0.05}(W)$ for $\alpha = 0.05$ describes the risk of W as the amount that can be lost with probability of no more than 5%. However, even though VaR is considered to be a benchmark for risk management, it lacks convexity which limits significantly its use [106].

In [6], four requirements that a "good" risk function must possess, are determined. The risk measures that satisfy these four requirements are called *coherent* risk measures. The properties of the coherent risk measures are **Monotonocity**, **Convexity**, **Translation Invariance** and **Positive Homogeinety**. VaR is coherent only when the underlying loss distribution is normal. In any other case, it lacks the convexity property. Another disadvantage of VaR is the fact that it does not provide information regarding potential losses beyond the $1-a$ quantile.

The CVaR, introduced in [96], is a coherent risk measure suitable for optimization models. Its main advantage, when compared to VaR, is the fact that it can be used for any type of loss distribution and when the optimization problem is has more than one dimension. Moreover, it has the ability to quantify the right tails beyond the VaR, i.e it is the conditional mean of $(1-\alpha)100\%$ worst cases [36] and can be formally written as follows:

$$CVaR_{a}(W) = \mathbb{E}[W|W \geq VaR_{a}(W)] \tag{4.5}$$

Following the proof from [96], $CVaR_{a}(X)$ can be represented as follows:

$$CVaR_{a}(W) = \inf\{y + \frac{1}{1-a}\mathbb{E}[(W-y)_{+}]\} \tag{4.6}$$

It is easily obtainable that:

$$\mathbb{P}(W \leq 0) \geq a = CVar_{a}(W) \leq 0 \tag{4.7}$$

For example, a 95% confidence level determines the mean for the expected losses for loss values that exceed the 95% VaR. In other words, the key difference of VaR and CVaR is that VaR corresponds to the probability of loss excess whereas CVaR relates to the expected loss excess [51], and can be interpreted as shown in Fig. 4.2.

As it has become evident, the CVaR framework is theoretically preferable and can be potentially used in this research in order to build a risk-averse model. In the existing literature, there are two approaches that can be used to build risk-averse models, either by including a CVaR term in the objective function or by defining CVaR constraints.

In case a CVaR term is defined in the objective function, then Equation 4.2a can be informally rewritten as follows:

$$\textbf{min} \quad \lambda c^{'} x + (1-\lambda) CVaR_{a}(W(x)) \tag{4.8}$$

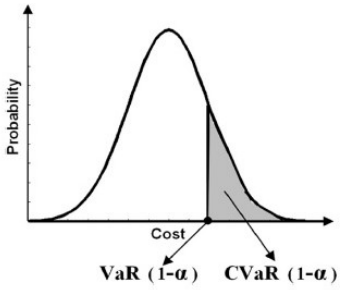

Figure 4.2: Definition of VaR and CVaR [51].

where the λ is a weighting factor that controls the trade-off between the cost and the risk measure. This is the factor that shows the importance of the risk concept for the revenue manager. When λ is set to 1, a risk neutral perspective is adopted. As λ approaches 0, a more risk-averse attitude is adopted. Generally, by varying λ different attitudes towards risk aversion can be formulated and different loading strategies may me implemented. The choice of λ as well as that of confidence or risk level α, is problem dependent. In [98], some general guidelines on how to choose λ and α parameters based on experiments on a hydrothermal scheduling problem are provided. An indicative example of a CVaR minimization problem developed for the air cargo domain can be found in [106], where risk neutral and risk-averse formulations were tested in order to determine the weight of items that should be assigned to long-term contracts and free reservations, considering demand, prices and show-up rates as variables with uncertainty.
In case, CVaR is applied to the chance constraints, then Equation 4.2b can be rewritten as follows:

$$P\{W(x) \leq 0\} \geq 1 - \epsilon \tag{4.9}$$

where $W(x) = ||\tilde{a}_{ij}x_j - \tilde{b}||_\infty$. Using Equation 4.6 and Equation 4.7, it can be shown that the chance constraint can be finally written as:

$$y + \frac{1}{\epsilon}[(||\tilde{a}_{ij}x_j - \tilde{b}_i||_\infty - y)_+] \leq 0 \tag{4.10}$$

The above represents a risk-averse approach to the chance constraint of Equation 4.2b and can be used in this research to constraint capacity CVaR to different risk levels ϵ. An example of a bin packing model that uses CVaR constraints can be found in [107], where the task of assigning surgery operations of random duration to hospital rooms was addressed. The algorithm developed in this study managed to solve problems of up to 1,000 scenarios in less than an hour.

5

Conclusions

This literature study provided an exhaustive overview of the tools required to address the complex task of air cargo load planning problem. The complexity of the air cargo load planning problem arises form the fact that many stakeholders are involved and a variety of decisions has to be taken. In this study, the air cargo problem is addressed under the revenue management perspective. More specifically, the objective is to provide the revenue manager with a tool that will facilitate the decision-making process of accepting or rejecting a shipment booking request. The decision making process combines two nested problems, namely the forecasting problem and the packing problem.

The forecasting problem involves the prediction of three quantities: the available aircraft capacity for cargo, the volume of must-fly cargo and shipment dimensions. Each one of these quantities represent inputs to the subsequent packing problem and will be determined using one of the models presented in chapter 3. The available aircraft capacity would be used to specify the number and the type of ULDs in which the individual shipment would be loaded. The volume of must-cargo and shipment dimensions would be used in order to optimally assign shipments inside the ULDs. Nevertheless, as discussed in chapter 4, there is no forecasting model that is 100% accurate, meaning that any uncertainty in the predicted valued is unavoidably transferred to the packing problem, posing risks to the successful implementation of the loading strategy.

As such, the packing problem should have a dual functionality: it should be able to optimally assign the shipments to the ULDs, and, at the same time, it should tackle the forecasting uncertainty by incorporating risk measures either in the objective function or in the corresponding packing constraints. The required framework for achieving this dual functionality, is provided by the concepts of packing problems and chance constrained optimization, which were reviewed in chapter 4. Moreover, the CVaR framework, widely used in portfolio optimization, provides an appropriate risk measure that can be used by the revenue manager to control the impact of uncertainties and adjust the loading strategy according to a selected risk profile.

The context of this research will be centered around Air France KLM Martinair Cargo (AFKLMP) and will therefore use the airlines' historic data for these type of aircraft to build, test and finally validate the model. Nevertheless, the goal of this research is to provide a risk-averse cargo planning tool that can be used by revenue management departments of other airlines, as well as other industries, such as the shipping or rail industry.

III

Supporting work

6

Experimental design of the 3D-MHKP model

In this section, two distinct design approaches of the 3D-MHKP are evaluated and compared, namely the **sequential** approach and the **parallel** approach. According to the sequential approach, the 3D-MHKP is solved sequentially for each ULD of the determined ULD configuration, i.e., the EP heuristic is applied to the first ULD until is filled and the offloaded shipments (if any) are considered for placement in the next ULD. The same procedure continues until there are no offloaded shipments or no ULDs left, whatever happens first. In the parallel approach, the EP heuristic searches for suitable EPs by exploring the residual space in all ULDs in parallel. The flowcharts for both approaches are depicted in the following figures :

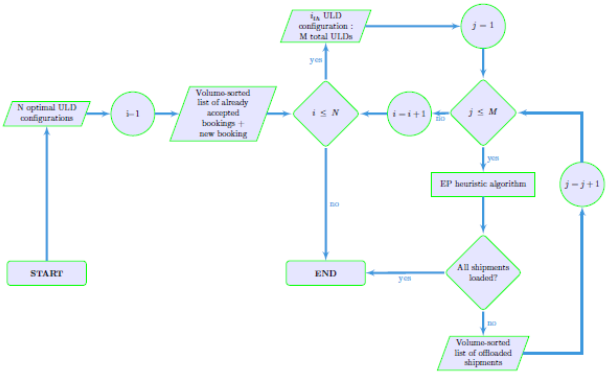

Figure 6.1: Sequential approach

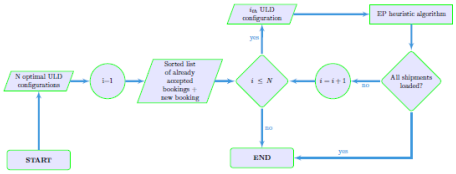

Figure 6.2: Parallel approach

The performance of both approaches will be evaluated in terms of loaded volume for four flights with real booking data, provided by our partner airline. Moreover, the achieved Shipment Contribution (SCb) will be noted, but for reference purposes only, as it is not included in the objective function. The corresponding flight and booking characteristics as provided by the airline can be found in table Table 6.1.

Flight #	**Cargo capacity** (m^3)	**ULD configuration**	**Volume of booking requests** (m^3)	**SCb of booking requests**
Flight #1	74	7 LDPs - 1 LD-3	71.232	45,554.81
Flight #2	77	6 LDPs - 3 LD-3	72.651	18,413.13
Flight #3	96	8 LDPS - 4 LD-3	89.49	55,182.34
Flight #4	78	7 LDPs - 1 LD-3	70.480	15,834.80

Table 6.1: Flight and booking information.

6.1. Comparative sensitivity analysis for predicted cargo capacity

The first step of the comparative sensitivity analysis consists of generating the probability distribution of the predicted cargo capacity, passing as inputs to the LSTM network the capacity data of the previous sixty (60) days for the corresponding flight. Every design approach of the 3D-MHKP was run for different confidence levels of the predicted cargo capacity, using as inputs the booking dimensions as provided by the partner airline . The computational time required by every approach to solve the complete set of booking is presented in Table 6.2.

		Computational time(sec)	
Flight #	**No. of individual shipments**	**Sequential**	**Parallel**
Flight #1	97	5	12
Flight #2	91	5	12
Flight #3	122	7	19
Flight #4	194	89	174

Table 6.2: Flight and booking information.

As it can be observed, the parallel approach is slower than the sequential approach, with respect to computational efficiency. The sharp increase noted for flight #4 for both approaches is related to the increased number of the considered shipments.

Next,the performance of each approach per flight in terms of loaded volume and shipment contribution is evaluated and the results are summarized in Figure 6.3. As it is evident,for specific confidence levels, the parallel approach slightly outperforms the sequential approach in flights #1 and #2. For flight 4, for confidence level $\alpha - 0.99$, the sequential approach loads approximately 10 m^3 more than the parallel approach, whereas for flight #3 and for confidence levels $\alpha = 0.8$ and $\alpha = 0.9$, the parallel approach loads approximately 10 m^3 more than the sequential approach.

Overall, both approaches provide better results in terms loaded volume of shipment contribution in comparison with the partner airline, with the exception of flight #1 for confidence level $\alpha = 0.99$ (both approaches) and flight #3 for confidence level $\alpha = 0.99$ (parallel approach only).

6.2. Comparative sensitivity analysis for predicted shipment dimensions

The next step of the comparative sensitivity analysis consists of evaluating how each approach performs with varying confidence levels of the predicted shipment dimensions distributions. Using the MLP network, we generate the corresponding shipment dimensions distribution per flight and apply both approaches to each flight.

The computational time for both approaches remained the same as in Table 6.2, since the same flights and booking requests were considered. The results regarding the loading performance in terms of loaded volume and shipment contribution are presented in Figure 6.4. As it is depicted, there is no dominant approach for flight #1. The sequential approach slightly outperforms the parallel approach for specific confidence levels in flights #3 and #4, whereas the parallel approach provides slightly better results than the sequential approach in flight #2.

Overall, from the performed comparative analysis it can be concluded that there is no clear winning approach in terms of loaded volume and shipment contribution results. However, the fact that the sequential approach in all cases is faster than the parallel approach in combination with the real-time requirements of a RM environment, supports the choice of sequential over parallel approach as the main design approach that will be used in this work.

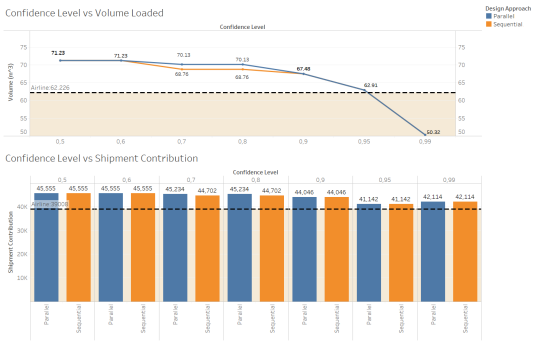

(a) Flight #1

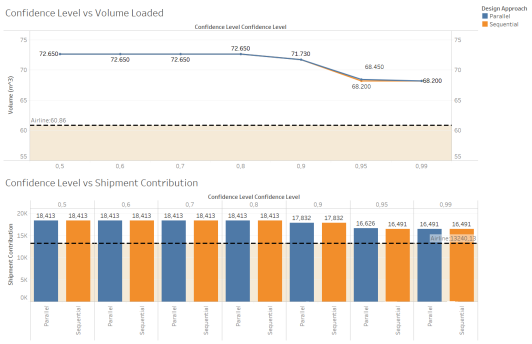

(b) Flight #2

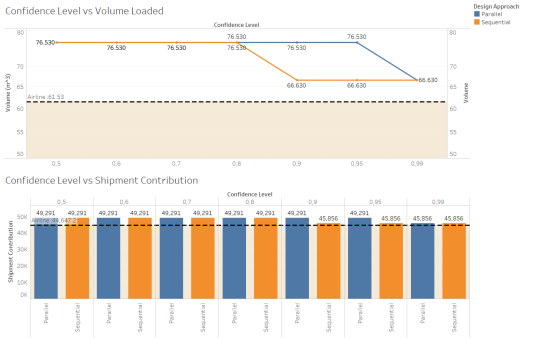

(c) Flight #3

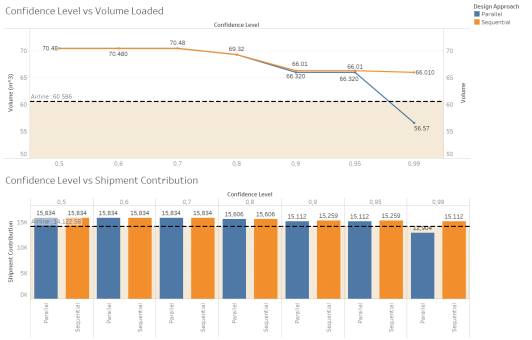

(d) Flight #4

Figure 6.3: Comparative sensitivity analysis of design approaches for predicted cargo capacity

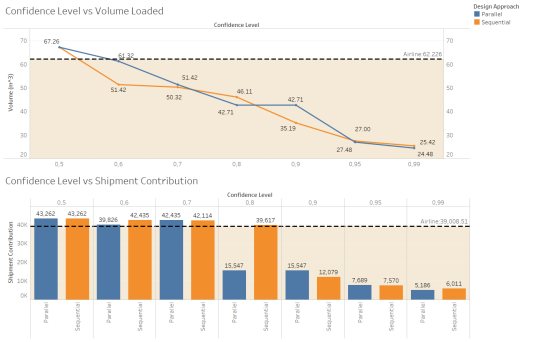

(a) Flight #1

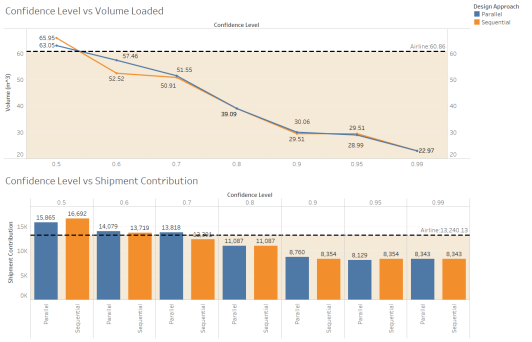

(b) Flight #2

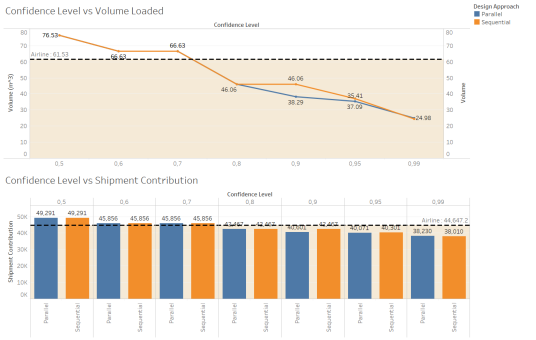

(c) Flight #3

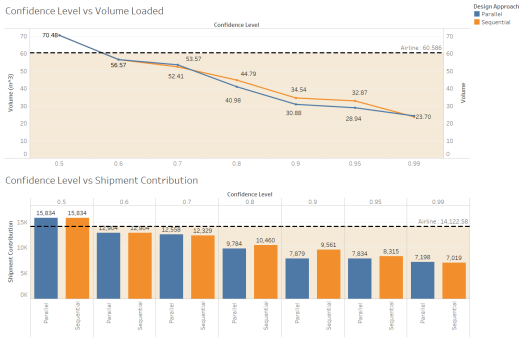

(d) Flight #4

Figure 6.4: Comparative sensitivity analysis of design approaches for predicted shipment dimensions

Bibliography

[1] S. Ahmed and A. Shapiro. Solving chance-constrained stochastic programs via sampling and integer programming. *Tutorials in Operations Research*, 10:261–269, 2008.

[2] S. Ahmed and W. Xie. Relaxations and approximations of chance constraints under finite distributions. *Mathematical Programming*, 170:43–65, 2018.

[3] S. Ahmed, J. Luedtke, Y. Song, and W. Xie. Nonanticipative duality, relaxations, and formulations for chance-constrained stochastic programs. *Mathematical Programming*, 162:51–81, 2017.

[4] K. Amaruchkul and P. Sae-Lim. Airline overbooking models with misspecification. *Journal of Air Transport Management*, 17:143–147, 2011.

[5] J.S. Armstrong. *Principles of forecasting: A handbook for researches and practicioners*. Kluwer Academic Publishers, 2001.

[6] P. Artzner, F. Delbaen, J.M Eber, and D. Heath. Coherent measures of risk. *Mathematical Finance*, 9: 203–228, 1999.

[7] M.M Baldi, T.G Crainic, G. Perboli, and Tadei.R. The generalized bin packing problem. *Transportation Research Part E*, 48:1205–1220, 2012.

[8] W. Bao, J. Yue, and Y. Rao. A deep learning framework for financial time series using stacked autoencoders and long-short term memory. *PLoS ONE*, 2017.

[9] J.C Bean. Genetic algorithms and random keys for sequencing and optimization. *ORSA Journal of Computing*, 6:154–160, 1995.

[10] A. Ben-Tal and A. Nemirovski. Robust convex optimization. *Mathematical Operations Research*, 23: 769–805, 1998.

[11] A. Ben-Tal and A. Nemirovski. Robust solutions of linear programming problemscontaminated with uncertain data. *Mathematical Programming*, 88:421–444, 2000. doi: 10.1007/s101070000163.

[12] E.E Bischoff and M.S.W Ratcliff. Issues in the development of approaches to container loading. *Omega*, 23:377–390, 1995.

[13] E.E. Bischoff, F. Janetz, and M.S.W. Ratcliff. Loading pallets with non-identical items. *European Journal of Operational Research*, 84:681–692, 1995.

[14] A. Bordfelt, H. Gehring, and D. Mack. A parallel tabu search algorithm for solving the container loading problem. *Journal of Parallel Computing*, 29:641–662, 2003.

[15] A. Bortfeldt. Constraints in container loading - a state-of-the-art review. *European Journal of Operational Research*, 229:1–20, 2013.

[16] A. Bortfeldt and H. Gehring. A hybrid genetic algorithm for the container loading problem. european. *Journal of Operational Research*, 131:143–161, 2001.

[17] G.E.P Box and J.M Jenkins. Time series analysis : Forecasting and control. 1970.

[18] F. Brandt and S. Nickel. The air cargo load planning problem - a consolidated problem definition and literature review on related problems. *European Journal of Operational Research*, 275:399–410, 2018.

[19] L. Breiman. Random forests. *Machine Learning*, 45, 2001.

[20] G. Calafiore and M. Campi. Uncertain convex programs: randomized solutions and confidence levels. *Mathematical Programming*, 102:25–46, 2005.

[21] G. Calafiore and M. Campi. The scenario approach to robust control design. *IEEE Transactions in Automated Control*, 51:742–753, 2006.

[22] E.H.F Cao, L.J. Tay. Support vector machine with adaptive parameters in financial time series forecasting. *IEEE Transactions on Neural Networs*, 14:1506–1518, 2003.

[23] R. Caruana and Niculescu-Mizil. An empirical comparison of supervised learning algorithms. *International Conference in Machine Learning*, 2006.

[24] A. Charnes and William W. Cooper. Chance constrained programming. *Management Sciences*, 6:73–79, 1959.

[25] W. Chen, M. Sim, J. Sun, and C. Teo. From cvar to uncertainty set: implications in joint chance-constrained optimization. *Operational Research*, 58:470–485, 2010.

[26] A. Conejo, M. Carrion, and J.M Morales. Decision making under uncertainty in electricity markets. 2010.

[27] M.D.G Costa and M.E Captivo. Weight distribution in container loading: a case study. *International Transactions in Operational Research*, 23:239–263, 2016. doi: 10.1111/itor.12145.

[28] R. Dahlgren, C.C. Liu, and J. Lawarree. Risk assessment in energy trading. *IEEE Transactions on Power Systems*, 18:503–511, 2003.

[29] D.C.Patranabis D.Basak, S.Pal. Support vector regression. *Neural Information Processing Systems*, 9: 203–224, 2007.

[30] M. Delorme, M. Iori, and S. Martello. Bin packing and cutting stock problems: Mathematical models and exact algorithms. *European Journal of Operational Research*, 255:1–20, 2016.

[31] Z.T Dereli and G.S Das. A hybrid simulated annealing algorithm for solving multi-objective container-loading problems. *Applied Artificial Intelligence*, 23:463–486, 2010.

[32] H. Dyckhoff. A typology of cutting and packing problems. *European Journal of Operational Research*, 44:145–159, 1990.

[33] O. Elci, N. Noyan, and K. Bulbul. Chance-constrained stochastic programming under variable reliability levels with an application to humanitarian relief network design. *Computers and Operations Research*, 96:91–107, 2018.

[34] M. Eley. A bottleneck assignment approach to the multiple container loading problem. *Operations Research Spectrum*, 25:45–60, 2003.

[35] Glover F. Future paths in integer programming and artificial intelligence. *Computers and Operational Research*, 13:533–549, 1986.

[36] CI. Fabian. Handling cvar objectives and constraints in two-stage stochastic models. *European Journal of Operational Research*, 191:888–911, 2008.

[37] K. Fatemi Ghomi, S.M.T Forghani. Airline passenger forecasting using neural networks and box jenkins. *12th International Conference on Industrial Engineering*, 2016.

[38] L. Feng, B. Yanzhi and Zuo Jun Max Shen. Air cargo operations : Literature review and comparison with practices. *Transportation Research part C : Emerging Technologies*, 56:263–280, 2015. doi: https://doi.org/10.1016/j.trc.2015.03.028.

[39] G. Fuellerer, K. Doerner, R.F Hartl, and M. Iori. Metaheuristics for vehicle routing problems with three-dimensional loading constraints. *European Journal of Operational Research*, 201:751–759, 2010.

[40] H. Gehring and Bordfelt A. A genetic algorithm for solving the container loading problem. *International Transactions in Operational Research*, 4:401–418, 1997.

[41] A. Geletu, M. Kloppel, H. Zhang, and P. Li. Advances and applications of chance-constrained approaches to systems optimisation under uncertainty. *International Journal of Systems Science*, 44:1209–1232, 2012. doi: https://doi.org/10.1080/00207721.2012.670310.

[42] R. Gelper, S. Fried and C. Croux. Robust forecasting with exponential and holt-winters smoothing. *Journal of Forecasting*, 29, 2010.

[43] J.A George and D.F Robinson. A heuristic for packing boxes into container. *Computers and Operations Research*, 7:147–156, 1980.

[44] Lars Gerlitz, Olaf Conrad, and Jürgen Böhner. Large-scale atmospheric forcing and topographic modification of precipitation rates over high asia - a neural-network-based approach. *Earth System Dynamics*, 6:61–81, 03 2015. doi: 10.5194/eds-6-61-2015.

[45] I. Ghalehkhondabi, E. Ardjman, W. Young, and G. Weckman. A review of demand forecasting models and methodological developments within tourism and passenger transportation industry. *Journal of Tourism Futures*, 5:75–93, 2019.

[46] J.F Goncalves and M.G.C Resende. A parallel multi-population biased random- key genetic algorithm for a container loading problem. *Computers and Operations Research*, 39:179–190, 2012.

[47] J.F Goncalves and M.G.C Resende. A biased random key genetic algorithm for 2d and 3d bin packing problems. *International Journal of Production Economics*, 145:500–510, 2013.

[48] J. Gonsch. A survey or risk averse and robust revenue management. *European Journal of Operational Research*, 263:337–348, 2017.

[49] Y. Courville A. Goodfellow, I. Bengio. *Deep Learning*. The MIT Press, 2015.

[50] P. Healy and R. Moll. A local optimization-based solution to the rectangle layout problem. *Journal of the Operational Research Society*, 47:523–537, 1996.

[51] R. Hemmati, H. Saboori, and S. Saboori. Stochastic risk-averse coordinated scheduling of grid integrated energy storage units in transmission constrained wind-thermal systems within a conditional value-at-risk framework. *Journal of Energy*, 113:762–775, 2016.

[52] J. Hemminki, T. Leipala, and O. Nevalainen. On-line packing with boxes of different size. *International Journal of Production Research*, 36:2225–2245, 1998.

[53] S. Hochreiter and J. SchmidHuber. Long short-term memory. *Neural Computations*, 8:1735–1780, 1997.

[54] J.H. Holland. Adaption in natural and artificial systems. 1970.

[55] Douglas Hubbard. *The failure of Risk Management*. John Wiley & Sons, 2009.

[56] R. Hyndman and G. Athanasopoulos. *Forecasting:Principles and Practices*. OTexts, 2013.

[57] IATA. Cargo strategy report. 2018.

[58] IATA. Cargo chartbook. 2019.

[59] L. Junqueira, R. Morabito, and D.S. Yamashita. Three-dimensional container loading models with cargo stability and load bearing constraints. *Computers and Operations Research*, 39:74–85, 2012.

[60] R.G. Kasilingam. Air cargo revenue management : Characteristics and complexities. *European Journal of Operations Research*, 96:36–44, 1996. doi: 10.1109/ICSSSM.2010.5530228.

[61] B. Kelleher, J. MacNamee and A. D'Arcy. *Fundamentals of Machine Learning for Predictive Data analytics*. The MIT Press, 2015.

[62] S. Kirkpatrick, C.D Gellat, and M.P. Vechi. Optimization by simulated annealing. *Journal of Science*, 220:671–680, 1983.

[63] M.R Koch, Alessandro Bombelli, and Bruno Santos. An optimisation and forecast framework for uld packing in the air cargo supply chain. *Master Thesis, TU Delft*, 2019.

[64] P. Krokhmal, M. Zabarankin, and S. Uryasev. Modelling and optimization of risk. *Surveys in Operation Research and Management Science*, 16:49–66, 2011.

[65] S. Kucukyavuz. On mixing sets arising in chance-constrained programming. *Mathematical Programming*, 132:31–56, 2013.

[66] Nicolas Le Roux and Y Bengio. Deep belief networks are compact universal approximators. *Neural Computation*, 8:2192–2207, 2010.

[67] Y. Lecoun, L. Bottou, G.B. Orr, and K.R Muller. *Neural Networks : Tricks of the trade*. Springer, 2012.

[68] J. Lei, L. Zhou and H. Wang. Air cargo overbooking model with stochastic capacity and penalty cost under cvar framework. *2009 IEEE International Conference on Grey Systems and Intelligent Services (GSIS 2009)*, 2009. doi: 10.1109/GSIS.2009.5408101.

[69] W. Leiberger, G. Karypis, and V. Kumar. Multi-capacity bin packing algorithms with applications to job scheduling under multiple constraints. *Proceedings of the 1999 International Conference on Parallel Processing*, 1999.

[70] S. Limburg, M. Schyns, and G. Laporte. Automatic aircraft cargo planning. *Journal of the Operational Research Society*, 63:1271–1283, 2012.

[71] J.L Lin, C.H Chang, and J.Y. Yang. A study of optimal system for multiple- constraint multiple-container packing problems. *Advances in Applied Artificial Intelligence*, pages 1200–1210, 2006.

[72] J. Liu, Y. Yue, Z. Dong, C. Maple, and M. Keech. A novel hybrid tabu search approach to container loading. *Computers and Operations Research*, 4:797–807, 2011.

[73] X. Liu. Integer programming approaches to risk-averse optimization. *PHD Thesis*, 2016.

[74] A. Lodi, S. Martello, and M. Monaci. Two-dimensional packing problems: A survey. *European Journal of Operational Research*, 141:241–252, 2002.

[75] J. Luedtke. A branch-and-cut decomposition algorithm for solving chance-constrained mathematical programs with finite support. *Mathematical Programming*, 146:219–244, 2014. doi: 10.1007/s10107-013-0684-6.

[76] J. Luedtke and S. Ahmed. A sample approximation approach for optimization with probabilistic constraints. *SIAM Journal On Optimization*, 19:674–699, 2008.

[77] J. Luedtke, S. Ahmed, and G.L Nemhauser. An integer programming approach for linear programs with probabilistic constraints. *Mathematical Programming*, 122:242–272, 2010.

[78] D. Mack, A. Bordfelt, and H. Gehring. A parallel hybrid local search algorithm for the container loading problem. *International Transactions in Operational Research*, 11:511–533, 2004.

[79] S. Hyndman R. Makridakis, S. Wheelright. *Forecasting Methods and Applications*. Jonh Wiley Sons, 2008.

[80] H. Markowitz. Portfolio selection. *Journal of Finance*, 7:77–91, 1952.

[81] S. Martello, D. Pisinger, and D. Vigo. The three-dimensional bin packing problem. *Journal of Operational Research*, 48:256–267, 2000.

[82] MergeGLobal. End of an era? *American Shipper*, 50:32–47, 2008.

[83] C. Mongeau, M.and Bes. Optimization of aircraft container loading. *IEEE transactions on Aerospace and Electronic Systems*, 39:140–150, 2003.

[84] K.P. Murphy. *Machine Learning: A probabilistic perspective*. The MIT Press, 2012.

[85] R.L Nance, A.G Roesener, and J.T Moore. An advanced tabu search for solving the mixed payload airlift loading problem. *Journal of the Operational Research Society*, 62:337–347, 2011.

[86] A. Nemirovski and A. Shapiro. Convex approximation of chance constrained programs. *SIAM Journal on Optimization*, 17:969–996, 2006. doi: 10.1137/050622328.

[87] J.F Oliveira, A.N Junior, E. Silva, and M.A Carravilla. A survey on heuristics on the two dimensional rectangular strip packing problem. *Brazilian Operations Research Society*, 36:197–226, 2016.

[88] C. Paquay, M. Schyns, and S. Limburg. A mixed integer programming formulation for the three-dimensional bin packing problem deriving from an air cargo application. *International Transactions In Operational Research*, 23:187–213, 2014. doi: 10.1111/itor.12111.

[89] C. Paquay, M. Schyns, S. Limburg, and J.F Oliveira. Mip-based constructive heuristics for the three-dimensional bin packing problem with transportation constraints. *International Journal of Production Research*, pages 1–12, 2017. doi: 10.1080/00207543.2017.1355577.

[90] C. Paquay, M. Schyns, and S. Limburg. A tailored two-phase constructive heuristic for the three-dimensional multiple bin size bin packing problem with transportation constraints. *European Journal of Operational Research*, 267:1–12, 2018. doi: 10.1080/00207543.2017.1355577.

[91] Pascanu, Razvan, T. Mikolov, and Y. Bengio. On the difficulty of training recurrent neural networks. *Proceedings of the 30th International Conference on Machine Learning*, 28:1310–1318, 2013.

[92] D. Pisinger. Heuristics for the container loading problem. *European Journal of Operational Research*, 141:382–392, 1996.

[93] C.R Qin, L. Luo, Y. You, and Y.X Xiao. An optimization model of the single-leg air cargo space control based on markov decision process. *Journal of Applied Math*, 2012. doi: https://doi.org/10.1155/2012/235706.

[94] G.A. RAmos, J.F Oliveira, J.F. Goncalves, and M.P Lopes. A container loading algorithm with static mechanical equilibrium stability constraints. *Transportation Research*, 91:565–581, 2016.

[95] T. Rockafellar. Coherent approaches to risk in optimization under uncertainty. *Tutorials in Operational Research*, pages 38–61, 2007.

[96] T. Rockafellar and S. Uryasev. Optimization of conditional value-at-risk. *Journal of risk*, 2:21–42, 2000.

[97] A. Sagheer and M. Kotb. Time series forecasting of petroleum production using deep lstm recurrent networks. *Neurocomputing*, 323:203–213, 2018.

[98] A. Shapiro, F. Cabral, and J. Costa. Guidelines for choosing parameters λ and α for the risk averse approach. *Report, Georgia Institute of Technology and ONS*, 2015.

[99] B. Smola, A. Scholkopf. A tutorial on support vector regression. *Statistics and Computing*, 14:199–222, 2004.

[100] G. Soa, E. Patuwo, and M.Y Hu. Forecasting with artificial neural networks : The state of the art. *International Journal of Forecasting*, 14:35–62, 1998.

[101] W. Song, Z. Xiao, Q. Chen, and H. Luo. Adaptive resource provisioning for the cloud using online bin packing. *IEEE transactions on Computers*, 63:2647–2660, 2014.

[102] A. Techanitisawad and P. Tangwiwatwong. A ga-based heuristic for the interrelated container selection loading problems. *Industrial Engineering and Management Systems*, 3:22–37, 2004.

[103] R. Totaname, A. Dasgupta, and S. Rao. Air cargo demand modellling and prediction. *IEEE Systems Journal*, 8:52–60, 2014.

[104] W. Vancroonenburg, J. Verstichel, K. Tavernier, and G.V Berghe. Automatic air cargo selection and weight balancing: A mixed integer programming approach. *Journal of Transportation Research*, 65: 70–83, 2014. doi: https://doi.org/10.1016/j.tre.2013.12.013.

[105] S. Vapnik, V. Golowich and A. Smola. Support vector method for function approximation, regression estimation, and signal processing. *Neural Information Processing Systems*, 9, 1997.

[106] F. Wada, M. Delgado and Pagnoncelli B. A risk averse approach to the capacity allocation problem in the airline cargo industry. *Journal of the Operations Research Society*, 68:643–651, 2017. doi: 10.1057/s41274-016-0135-x.

[107] S. Wang, J. Li, and Sanjay Mehrotra. Chance-constrained bin packing problem with an application to operating room planning. *optimization-online.org*, 2019.

[108] J.P Watson, R.J. Wets, and D.L Woodruf. Scalable heuristics for a class of chance-constrained stochastic programs. *INFORMS Journal on Computing*, 22:543–554, 2010.

[109] L. Weatherford. The history of forecasting models in revenue management. *Journal of Revenue and Pricing Management*, 15, 2016.

[110] P. Winters. Forecasting sales by exponentially weighted moving averages. *Management Sciences*, 6: 324–342, 1960.

[111] G. Wscher, H. HauSSner, and H. Schumann. An improved typology of cutting and packing problem. *European Journal of Operational Research*, 183:1109–1130, 2007.

[112] Y. Wu, W. Li, M. Goh, and R. de Souza. Three-dimensional bin packing problem with variable bin height. *European Journal of Operational Research*, 202:347–355, 2010.

[113] X. Xiang, C. Yu, H. Xu, and S. Zhu. Optimization of heterogeneous container loading problem with adaptive genetic algorithm. *Complexity*, 2018. doi: 10.1155/2018/2024184.

[114] Yan, Shangyao, Chen, and Chung-Kai. Short-term shift setting and manpower supplying under stochastic demands for air cargo terminals. *Journal of Transportation*, 33:425–444, 2008. doi: https://doi.org/10.1155/2012/235706.

[115] Jin Z., T Ito., and K Ohno. The three-dimensional bin packing problem and its practical algorithm. *JSME International Journal Series C Mechanical Systems, Machine Elements and Manufacturing*, 46: 60–66, 2003.

[116] Cunlu Zhang, Ruibin Luo, and Zhixin Chen. An optimization model of cargo space allocation for air cargo agent. *2010 7th International Conference on Service Systems and Service Management, Proceedings of ICSSSM' 10*, 06 2010. doi: 10.1109/ICSSSM.2010.5530228.

[117] Y. Zhang, R. Jiang, and Shen S. Ambiguous chance constrained binary programs under mean-covariance information. *SIAM Journal on Optimization*, 28:2922–2944, 2018. doi: 10.1137/17M1158707.

[118] X. Zhao, J.A Benell, T. Bektas, and K. Dowsland. a comparative review of 3d container loading algoriths. *International Transactions in Operational Research*, 23:287–320, 2016.

[119] Z. Zhao, W. Chen, X. Wu, P.C.Y Chen, and J. Liu. Lstm network: a deep learning approach for short-term traffic forecast. *IET Intelligent Transport Systems*, 11(2):68–75, 2017. doi: 10.1049/iet-its.2016.0208.

[120] H. Zheng, J. Yuan, and L. Chen. Short-term load forecasting using emd-lstm neural networks with a xgboost algorithm for feature importance evaluation. 2017.